The Role of H1 Linker Histone Variants in Ovarian Cancer

A Dissertation
Presented to
The Academic Faculty

by

Magdalena Medrzycki

In Partial Fulfillment
Of the Requirements for the Degree
Doctor of Philosophy in Biology

Georgia Institute of Technology

August 2013

The Role of H1 Linker Histone Variants in Ovarian Cancer

Approved by:

Dr. Yuhong Fan, Advisor
School of Biology
Georgia Institute of Technology

Dr. John F McDonald
School of Biology
Georgia Institute of Technology

Dr. Marion B. Sewer
Skaggs School of Pharmacy and Pharmaceutical Sciences
University of California, San Diego

Dr. Francesca Storici
School of Biology
Georgia Institute of Technology

Dr. Melissa Lambeth Kemp
Wallace H. Coulter Dept. of Biomedical Engineering
Georgia Institute of Technology

Date Approved: June 24th, 2013

ACKNOWLEDMENTS

I would like to express my great appreciation to my thesis advisor, Dr. Yuhong Fan, for her professional and personal support, never-ending encouragement, and faith in my strength and determination. Without her inspiring mentorship and guidance over my graduate career, I would have never become a scientist capable to perform independent research and think critically over future projects.

I would also like to thank the members of my thesis committee. First, I thank my co-advisor, Dr. John McDonald, for giving me the opportunity to study ovarian cancer. I am truly grateful to the remaining members of my committee, Dr. Marion Sewer, Dr. Francesca Storici and Dr. Melissa Kemp for their advice, guidance and encouragement throughout my graduate studies.

I would like to thank all the members of the Fan Lab, past and present, for their friendship and support. Especially, I thank Yunzhe Zhang, Kaixiang Cao, Chenyi Pan and Po-Yi Ho for their support, critical discussions, sharing ideas and reagents, and above all, for their friendship.

Last but not least, I would like to thank my dearest husband, son, and wonderful family for their unconditional love, support, faith, and endless patience that I was blessed with throughout my graduate study. I could not have accomplished this work without them.

TABLE OF CONTENTS

LIST OF TABLES

LIST OF FIGURES

LIST OF SYMBOLS AND ABBREVIATIONS

AR - androgen receptor

BAF - barrier-to-auto integration factor

bFGF - basic fibroblast growth factor

bp - base pair

BRCA1 - breast cancer susceptibility gene 1

BRCA2 - breast cancer susceptibility gene 2

cDNA – complementary DNA

CT - computed tomography

Ct – threshold of cycle

Da - Dalton

ddH_2O – double-distilled water

DNA – deoxyribonucleic acid

dsDNA – double-stranded DNA

EMT - epithelial-to-mesenchymal transition

ESC - embryonic stem cell

EtOH - ethanol

FIGO - International Federation of Gynecology and Obstetrics system

FRAP - fluorescence recovery after photobleaching

FSH - follicle-stimulating hormone

GAPDH - glyceraldehyde 3-phosphate dehydrogenase

GFP - green fluorescence protein

H_2SO_4 – sulfuric acid

HAT - histone acetyltransferase

HBOC - hereditary breast-ovarian cancer syndrome

HDAC - histone deacetylase

HIF - hypoxia-inducing factor

HNPCC - hereditary non-polyposis colorectal cancer

HP1 - heterochromatin protein 1

i.p. - intraperitoneal

i.v. - intravenous

IGF - induction growth factor

IL - interleukine

LH - luteinizing hormone

mAU - milli-absorbancy unit

mESC – mouse embryonic stem cell

$MgCl_2$ – magnesium chloride

MMP - matrix metalloproteinase

mRNA – messenger ribonucleic acid

MSH1 - DNA mismatch repair gene 1

MSH2 - DNA mismatch repair gene 2

Mu - mucin

MW - molecular weight

MyoD - myogenic determination factor

OSE - ovarian surface epithelium

PBS – phosphate buffered saline

PCR – polymerase chain reaction

PMS1 - postmeiotic segregation increased 1 gene

PMS2 - postmeiotic segregation increased 2 gene

PMSF - phenylmethanesulfonyl fluoride

qRT-PCR – quantitative reverse transcriptase polymerase chain reaction

RFP - red fluorescence protein

RISC - RNA-induced silencing complex

RNA – ribonucleic acid

RP-HPLC - reverse phase high performance liquid chromatography

RT – real-time

RT-PCR – real-time polymerase chain reaction

SDS-PAGE - sodium dodecyl sulfate polyacrylamide gel electrophoresis

TFA - trifluoroacetic acid

TGF - tumor growth factor

Tm – melting temperature

Tris - tris(Hydroxymethyl)aminomethane

TSS - transcription starting site

UTR – untranslated region

UTR - untranslated terminal region

VEGF - vascular endothelial growth factor

WHO - World Health Organization

SUMMARY

Linker histone H1 associates with nucleosomes, facilitating folding and packaging of DNA into higher order chromatin structure. With 11 variants in mammals, histone H1 is the most divergent histone class. Histone H1 variants are differentially expressed during development and cellular differentiation, and regulate specific gene expression *in vivo*. Ample studies have established the role of linker histone H1 in chromatin compaction and gene expression regulation; however, its role in diseases, such as cancer, remain understudied.

In this study, we explore the role of H1 in ovarian cancer, one of the most devastating gynecological cancers due to its poor prognosis and difficulty in early diagnosis. Although mutations of genes responsible for cell proliferation, differentiation and survival have been found in ovarian cancers, ample evidence also suggests an important role of epigenetic changes in the disease occurrence and progression. Because epigenetic changes do not alter DNA sequence and can be reversed or reprogrammed, they offer an attractive avenue for therapeutic intervention in cancer treatment.

Using quantitative RT-PCR assays, we systematically examined the expression of 7 H1 genes in 33 human epithelial ovarian tumors. By clustering analysis, we found that ovarian malignant adenocarcinomas and benign adenomas exhibited characteristic expression patterns. We demonstrated that expression profiling of 7 H1 genes in tumor samples discriminates adenocarcinomas vs. adenomas with high accuracy. These findings indicate that the expression of H1 variants is exquisitely regulated and may serve as potential epigenetic biomarkers for ovarian cancer.

To further investigate the role of H1 subtypes in ovarian cancer cells, we employed an over-expression approach to test the function of H1 subtypes in an ovarian cancer cell line, OVCAR-3. We found that histone H1.3 over-expression significantly

suppresses the growth and colony formation of OVCAR-3 cells. Gene expression arrays identified many genes affected by H1.3 over-expression, and oncogene H19 was among the genes most dramatically repressed by H1.3 over-expression. Over-expression of several other H1 subtypes did not lead to significant reduction of H19 expression, suggesting a specific effect by H1.3. Consistently, knockdown of H1.3 increased H19 expression. Furthermore, increased expression of H1.3 led to accumulation of H1.3 as well as increased DNA methylation at the regulatory regions of H19. Finally, we identified a synergistic effect of H1.3 over-expression and H19 knockdown on inhibition of ovarian cancer cell growth. These results establish oncogene H19 as a direct target of histone H1.3, identify a novel role of H1 variants in ovarian cancer mediated through regulating oncogene H19 expression, and may offer new approaches for ovarian cancer therapeutics.

CHAPTER 1: Introduction

1.1. Role of linker histone in chromatin structure and dynamics

1.1.1. Chromatin structure and nucleosome particles

The human genome contains 3 billion base pairs (bp) accommodated in less than 10 micrometers of cell nucleus. To accomplish this task, DNA must be efficiently packaged. At first, 146 bp of double-stranded DNA are wrapped around a histone octamer consisting of two molecules of each H2A, H2B, H3 and H4 core histones. Together, they form a nucleosome, a fundamental repetitive unit of chromatin that can be further folded into high-ordered chromatin structures [1-3]. The DNA fragment between nucleosomes, called linker DNA, is bound by linker histone H1 that stabilizes higher order chromatin folding. Histone H1 binds at the entry and exit of nucleosomal DNA and linker DNA, forming a chromatosome. The formation of chromatosome by nucleosome and linker histone H1 plays an essential role in folding a transcriptionally active “beads-on-a-string” structure into a 30 nanometer (nm) chromatin fiber [4]. Further compaction in the nucleus includes 100 to 400 nm interphase fibers and an even more condensed metaphase chromosome structure.

1.1.2. Core histones

Core histones are small evolutionarily conserved proteins that assemble into an octamer and form the nucleosome core [5]. Each core histone protein consists of a globular domain interacting with neighboring histones and an amino terminal tail that extends from the nucleosome surface. It was demonstrated that core histone tails are fundamental elements required for nucleosomal structure formation [6].

Posttranslational modifications, such as acetylation, phosphorylation, methylation, ubiquitylation, sumoylation, and ribosylation, frequently occur on lysines

(K), arginines (R), serines (S) and threonines (T) of core histone tails. It has been proposed that a combination of different posttranslational modification serves as a code for regulating biological functions [7,8]. For instance, in higher Eukaryotes, transcriptional repression correlates with tri-methylation of histone H3K9 and a simultaneous lack of acetylation on H3 and H4 [9]. By facilitating the recruitment of chromatin remodeling complexes and modifying activities, histone marks participate and influence the dynamics of transcription and gene expression.

1.1.3. Linker histone H1

1.1.3.1. Histone H1 protein family and its variants

Linker histone H1 interacts with linker DNA at the dyad axis of the nucleosome at the entry and exit sites of the nucleosomal DNA. Its extended structural functions include stabilization, folding and condensation of chromatin into the 30 nm chromatin fiber, as well as positioning and spacing between nucleosomes [10-12]. Numerous studies have also shown that the linker histone H1 participates in multiple cellular processes occurring on the chromatin template, such as gene expression and DNA replication and repair [11,13-19].

Histone H1 belongs to a winged-helix family of DNA-binding proteins. The ratio of histone H1 per nucleosome varies between 0.5 in embryonic stem cells (ESC) to 1 or more in differentiated tissues [10]. *Saccharomyces cerevisiae*, *Tetrahymena thermophile* or *Ascobolus immerses*, contain only one variant of linker histone [20-22], and deletion of histone H1 leads to up- and down-regulation of specific genes and even growth arrest in *Ascobolus* [18,23,24]. The number of different H1 subtypes increases in higher Eukaryotes, with five H1 isoforms in *Xenopus laevis* and as many as 11 variants in mammals [25].

Histone H1 is a lysine-rich protein, consisting of a short basic N-terminal tail, a highly conserved globular domain, and a long, positively charged C-terminal tail

(Figure 1.1A). The central globular domain contains α–helix and β–sheet structures (Figure 1.1B). H1 proteins, especially the tails, are post-translationally modified, mostly by phosphorylation, but also by acetylation, methylation, sumoylation, and ubiquitination [11,26-28]. Those modifications can often modulate the interactions of H1 with chromatin and other proteins. For instance, histone lysine methyltransferase Ezh2, a component of Polycomb Complex 2 complex, methylates histone H1.4 at Lys26 [29,30]. Once methylated at K26, H1.4 is specifically recognized by chromodomain of HP1, the major heterochromatin protein, which further leads to transcriptional repression. In contrast, simultaneous phosphorylation of the neighboring Ser27 by cyclin-dependent kinase 2 (CDK2) prevents interaction with HP1 [31,32].

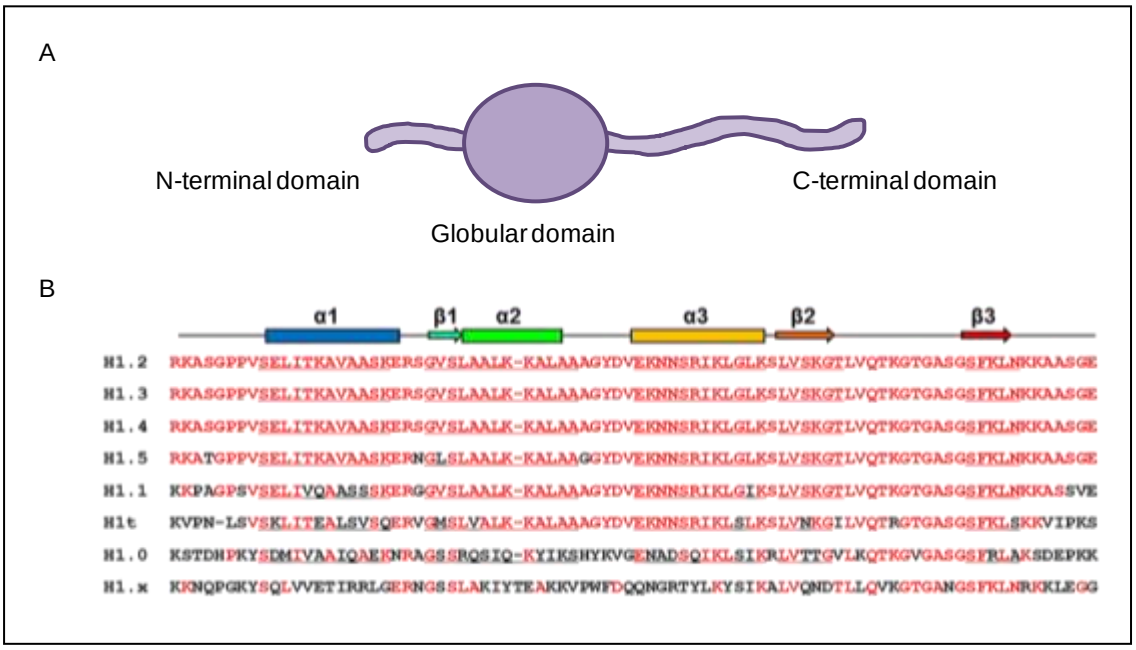

Figure 1.1: Linker histone H1 structure. A. Schematic representation of histone H1. B. Amino acid sequence comparison of histone H1 subtype globular domain. α1-3 represent three helices, β1-3 show beta-sheets.

In mammals, there are five major somatic H1 subtypes (H1.1, H1.2, H1.3, H1.4 and H1.5) differentially expressed in dividing and non-dividing cells [33-35]. For instance, expression of histones H1.1 and H1.5 are low in most of tissue and cell types, except in the thymus, spleen and lymphocytes, and further decreases in quiescent or differentiated cells [36-38]. Histones H1.2, H1.3 and H1.4 are ubiquitously expressed, suggesting their critical role in maintaining cellular functions. H1.2 and H1.4 often increases in expression during cell differentiation or quiescence [22,33,36,37,39,40]. The replacement subtype H1.0 accumulates in terminally differentiated cells. Tissue specific H1 subtypes include testis-specific subtypes such as H1t, H1T2, HILS1, oocyte-specific subtype H1oo, and the recently-discovered H1x [32,33,41-44].

The nomenclature of histone H1 subtypes has changed over time and may bring confusion; Table 1.1 lists the different names used by scientists for human H1 subtypes. Most histone H1 subtypes are intronless genes that lack poly-A tails, but are terminated by palindromic termination elements. H1oo is the only H1 subtype that contains introns and its alternative splicing results in two mRNA forms (alpha and beta) [45]. A large cluster of histone H1 is located in chromosome 6 of the human genome, and others reside in chromosome 22 (H1.0), chromosome 3 (H1x, H1oo), chromosome 12 (H1t2) and chromosome 17 (HILS) (Table 1.1).

Table 1.1. Overview of common nomenclatures of human linker histone subtypes.

	Official Symbol	Full official name	Albig& Doenecke	Ohe& Iwai	Also known as	Accession number	Average MW (DA)	AA	Chr.
Replication-dependent	**HIST1H1A**	Histone cluster 1, H1a	**H1.1**	hH1e	H1A H1F1 H1a	NM_ 005325	21710	214	6
	HIST1H1C*	Histone cluster 1, H1c	**H1.2**	hH1d	H1C H1F2 H1s-1	NM_ 005319	21233	212	6
	HIST1H1D	Histone cluster 1, H1d	**H1.3**	hH1c	H1D H1F3 H1s-2	NM_ 005320	22218	220	6
	HIST1H1E	Histone cluster 1, H1e	**H1.4**	hH1b	H1E H1F4 H1s-4	NM_ 005321	21734	218	6
	HIST1H1B	Histone cluster 1, H1b	**H1.5**	hH1a	H1B H1F5 H1s-3	NM_ 005322	22580	225	6
	HIST1H1T	H1 histone family member O oocyte-specific	**H1t**		H1Ft	NM_ 005323	22066	207	6
Replication-independent	**H1FO**	H1 histone family member O	**H10**		H1FV	NM_ 005318	20731	193	22
	H1FOO	H1 histone family member O	**H1oo**		osH1	NM_ 153833	35875	346	3
	H1FX	H1 histone family member X	**H1x**			NM_ 006026	22355	212	3
	H1FNT	H1 histone family member N, testis-specific	**H1t2**			NM_ 181788	28116	255	12
	HILS1	H1 histone family,spermatid –specific 1, pseudogene				NM_ 024193	27950	260	17

*Histone H1.2 (HISTH1C) expresses both DNA-replication dependent and independent (poly A^+) mRNAs, Chr. - chromosome, AA - amino acids.

Transcription of linker histone subtypes can occur during replication dependent or independent processes. All somatic H1s and testis-specific H1t are transcribed during early or middle S-phase, and sustain their high levels until the end of DNA replication process. Histone H1.3 has one of the highest expression levels in mRNA

during S-phase although its protein amount drastically differs from the respective RNA levels [46]. Replication-dependent histone genes encode most linker histone proteins [47,48]. Instead of poly-A tails, mRNAs of most linker histones contain 3' stem-loop sequences. Among the replication dependent H1s, histone H1.2 is the only somatic H1 gene whose mRNA also possesses a poly-A tail for 3' processing signals [49].

Four regulatory mechanisms control the proper amount of histone protein accumulation during cell cycle: transcription of histone genes, pre-mRNA processing efficiency, half-life of mRNA, and degradation of excessive histone proteins. Replication-dependent histones are the most highly cell-cycle-regulated proteins in mammalian cells. Replication-independent histone H1 subtypes containing polyadenylation signals, such as H1.0, H1x, H1t and H1oo, are not strictly limited to particular cell cycle phase (reviewed in [50]).

Histone H1 variants differ in timing of expression, extent of phosphorylation, turnover rate, and chromatin binding affinity [51-57]. Histone H1 proteins are thought to be continuously exchanged at chromatin binding sites after being dissociated from another binding site. Fluorescence recovery after photobleaching (FRAP) enabled the analysis of many linker histone properties in living cells, such as binding dynamics to chromatin, exchange rate and recovery time [58,59]. Such studies indicated that histone H1 mobility is less rapid than other chromatin binding proteins. However, their exchange rate is much higher than core histones [60]. The amount of time histone H1 resides at the chromatin binding site depends on the posttranslational modifications on its terminal domains and other nuclear proteins that compete for particular binding sites [58,61].

Many studies have been dedicated to classifying H1 subtypes according to their affinity to chromatin and condensation abilities; however, the conclusion remains controversial due to discrepancies among different experiment approaches [46,56,62-65]. Nevertheless, most studies suggest that H1.4 has the strongest affinity

among all subtypes; H1.3 can be classified as of intermediate affinity, whereas histones H1.1 and H1.2 bind chromatin with low affinity.

The linker histone heterogeneity is conserved among species, suggesting that the individual variants may have unique properties and functions [66]. In addition, H1 variants have differential subnuclear distribution, indicating their specific roles in nucleus [56]. For example, over-expression of GFP-tagged proteins suggests that euchromatin is commonly enriched in histone subtypes H1.0, H1.1, H1.2 and H1.3, whereas H1.4 and H1.5 frequently accumulate within the heterochromatin region.

1.1.3.2. Role of histone H1 in gene expression

Several studies indicate that linker histone H1 subtypes interact with other transcription factors and agglomerate into large complexes that regulate the expression levels of specific target genes. For instance, histone H1.1 was shown to specifically interact with Barrier-to-autointegration factor (BAF), giving BAF access to chromatin and facilitating the higher order chromatin structure [67]. Also, histone H1.4 was found to play an important role in heterochromatization processes that leads to gene silencing through the recruitment of Polycomb complexes and heterochromatin protein 1 (HP1) [29,30,32].

Interestingly, histone H1.5 was found to selectively interact with Ω promoter element controlling the expression of histone H3.2. The greatly elevated binding affinity was not observed on closely related H3.3 Ω promoter element, which indicates H1.5 high specificity towards H3.2 regulation [68]. Histone H1.5 also participates in expression regulation of myogenic determination factor (MyoD), by interacting with Msx1 (key regulatory element of MyoD). This cooperation leads to MyoD gene repression and inhibition of muscle differentiation [69]. On the other hand, H1.2 has been also shown to complex with P53 to repress its target genes [70].

1.1.3.3 Manipulations of H1 subtypes in cell lines and animal models

Although previous *in vitro* studies indicated histone H1 as a general repressor for gene expression, depletion of H1s *in vivo* suggests more specific effects of H1 in different organisms. RNAi silencing of H1.1 in nematode *Caenorhabditis elegans* causes the loss of gene silencing in the germline cells and blockade of germline development. Silencing H1 in *Arabidopsis* leads to pleiotropic developmental abnormalities and alterations in the DNA methylation patterns [71]. Although mice lacking one or two H1 variants have a normal total H1 levels and no apparent phenotypes, suggesting compensation among H1 variants [72], mice with knock-out of H1.2, H1.3 and H1.4, die by mid-gestation with a broad spectrum of defects and the remaining subtypes were unable to fully compensate for the loss of three H1 subtypes [73]. This result establishes that H1 is essential for mammalian development.

Mice with testis specific H1t deletion do not exhibit any phenotype or any defects in spermatogenesis [74]. Lack of histone H1t does not lead to its replacement by H1.1 or H1.2 during spermatogenesis, suggesting great diversity between somatic and testis-specific subtypes [75]. Oocytes microinjection with antisense oligonucleotides against H1oo reveals an essential role of this subtype in germinal oocytes maturation [76].

Knockdown or over-expression of individual H1 subtypes in cell culture shows that different H1 subtypes have specific effects on cell growth probably by either activating or repressing expression of specific genes. For example, in breast epithelial cell line studies, depletion of histone H1.2 leads to G1 arrest and an increase in apoptotic events [77]. In contrast, the over-expression of H1.2 in 3T3 cells had no obvious effect on cell cycle but causes increased expression of some genes, such as c-myc and cyclophilin [78,79]. Knockout of histone H1.0 did not

produce any obvious phenotype in mouse model [80], but proper terminal differentiation in dendritic cells was not possible without H1.0 [81]. In comparison, over-expressed H1.0 in 3T3 cells significantly delayed the cell cycle progression by arresting in G1 and S phase and inhibited the expression of a number of genes responsible for cell cycle control.

1.1.3.4. The effect of histone H1 on tumor growth and metastatic progress of cancer cells

For decades, researchers interested in linker histone H1 and its influence on cancer progression have been trying to comprehend its cytotoxic effect on tumor growth. It was found that histone H1 significantly inhibited growth of cancer cell lines, suggesting an anti-proliferating effect against leukemia and breast cancers [82,83]. Gine et al. showed that H1.2 is responsible for apoptosis induction in chronic lymphocytic leukemia, especially in patients with abnormal p53 functions [84]. The cytotoxic effect of H1 has been attributed to its structural homology with proteins secreted by activated macrophages and tufstin, a tetrapeptide stimulating macrophages migration, and their phagocytic and tumoricidal activity [85,86]. Since cationic amino acid sequence of linker histone acts like natural antibiotic peptide, it interacts with anionic phospholipid to disrupt negatively charged membranes leading to apoptosis [87].

These experiments show that the scientists tried different approaches to verify histone H1 as a target gene or potential therapeutic agent. Although it is evident that linker histone variants have unique properties and play specific roles in eukaryotic cells, the literature still lacks the fundamental answers regarding the molecular mechanisms and pathways that are regulated by particular subtypes.

1.2. Ovarian cancer

1.2.1. Introduction and etiology

Ovarian cancer is the ninth most common and the fifth most deadly cancer in women with a predicted 22,240 new diagnosed patients and 14,030 deaths in the United States in 2013 [88]. It is estimated that 1 in 81 American women will develop this type of cancer by the age of 85. According to these statistics, ovarian cancer was identified as the gynecological malignancy with the highest case-to-fatality ratio [89].

The ovary is a paired female reproductive organ with main function to generate a fertilizable oocyte and to secrete steroid hormones responsible for preparation of the reproductive tract for fertilization. Single layer of surface epithelial cells covers the external surface of the ovary, and dense stromal tissue constitutes the internal scaffold. Other specialized cells essential for ovary functions include: germ cells (oocytes), granulosa cells, theca cells, and hilus cells (specialized in hormone production) (reviewed in [90,91]).

More than 90% of malignant ovarian tumors are believed to arise from the ovarian surface epithelium (OSE), a specialized coelomic mesothelial layer of cells covering and protecting the ovary. The other malignancies derive from germ cells or supporting cells [92-94].

The ovarian surface epithelium undergoes repetitive disruption and repair during the ovulation cycles, and is constantly stimulated to proliferate during the repair processes. Most ovarian cancers develop from the surface epithelium or postovulatory inclusion cysts situated in the ovarian stroma [95-98]. When trapped within inclusion cysts, epithelial cells are exposed to a unique microenvironment in which mutation accumulation may occur more favorably [96,97,99]. In fact, the “incessant ovulation” theory states that the cyclic disruption and repair of OSE may lead to accumulation of mutations in genes essential for cellular survival, leading to

ovarian cancer [100,101]. Contributing factors to increased risk of malignancy of ovarian epithelium may also include the stimulatory effect of Follicle-stimulating hormone (FSH), Luteinizing hormone (LH) and androgens on growth and cell division, as well as inflammation occurring during ovarian surface epithelium damage [102-105].

A number of studies indicate that OSE cells can undergo epithelial-mesenchymal transition (EMT) in response to regenerative stimuli which may increase cell motility, proliferation and extracellular matrix modifications [106], and may acquire high metastatic potential after malignant transformation.

Although ovarian cancer incidents are not associated with one particular cause and occur sporadically in population, there are several well-defined factors that increase the risk of developing ovarian carcinomas. For instance, women at older age and first or second degree relatives with the disease and women with infertility or endometriosis have an increased risk of developing this type of cancer [107-109]. Also women carrying the mutations in breast cancer susceptibility gene 1 and 2 (BRCA1 and BRCA2) are at higher risk to develop both ovarian and breast cancer often at an earlier age than the general population [110,111]. These mutations are found in 5-13% of all ovarian cancer cases [69,112]. Another factor that significantly increases the risk of developing ovarian carcinoma is a family history of hereditary nonpolyposis colorectal cancer (HNPCC, known as Lynch syndrome) associated with mutations in the DNA mismatch repair genes hMSH1, hMSH2, hPMS1 and hPMS2, or hereditary breast-ovarian cancer syndrome (HBOC) in which BRCA1 and BRCA2 genes are involved [113,114]. Both syndromes increase ovarian cancer risk to around 50%. In addition, extensive pharmacological studies suggest that consumption of certain drugs increases the risk of ovarian cancer incidence in women. The list includes: hormone replacement therapy (especially received for more than 10 years) and long-term use of fertility drugs, such as clomiphene citrate or gonadotropins [115-120].

Early stages of ovarian cancer are usually asymptomatic or characterized by non-specific symptoms until the disease reaches more advanced stages. Due to difficulties in correlating these subtle signs with developing ovarian cancer, patients are rarely diagnosed and treated at early stages, such as stage I/II [121]. Typical symptoms include: pelvic and abdominal pain, bloating, urinary disorders, vaginal bleeding, appetite loss, and back pain, all of which could have been over-looked as symptoms of menstrual irregularities, menopause, or other non-serious conditions. The accumulation of ascites in the abdominal cavity increases patients' discomfort and intensifies pain in late stages [122].

Ovarian cancer can be detected by physical and pelvic examination, transvaginal ultrasound, computed tomography scan (CT), biopsis and biomarker tests. Unfortunately, none of these techniques is reliable enough for detection of the early stages of ovarian cancer. In order to improve assay sensitivity and specificity, several biomarkers are simultaneously analyzed [123,124]. Recently developed multiplex assay combining six serum markers: leptin, prolactin, osteopontin, insulin-like growth factor II (IGF2), macrophage inhibitory factor (MIF) and CA-125, is thought to increase the test sensitivity to 95.3% and specificity to 99.4% [125].

Histological grading (Grade 0 to 3) describes the malignancy of the tumor and indicates the probability of the cancer cells to metastasize to other tissues. Grade 0 indicates non-invasive, borderline, or low malignancy potential tumors, Grade 1 describes well-differentiated, low-grade tumors, with the cell morphology similar to normal cells, (good prognosis), Grade 2 depicts moderately differentiated tumors, and Grade 3 - poorly differentiated tumors with abnormal cell morphology (bad prognosis).

In 1973 the World Health Organization (WHO) published the *Classification of Ovarian Tumors* providing a standardized reference tool reflecting the variation of the disease. The document was updated in 1999 and approved by the International Society of Gynecological Pathologists (reviewed in [91,126,127]). Stage of the

ovarian surface epithelial tumors can be evaluated according to the TNM system established by the American Joint Committee on Cancer or the International Federation of Gynecology and Obstetrics system (FIGO).

1.2.2. Prognosis and treatment

Inefficient screening methods and detection of tumors in late stages correlate with poor recovery prognoses for ovarian cancer patients. 61% women already experience the advanced stages (III-IV) of cancer at the time of diagnosis and their five-year survival rate decreases drastically to 26.9% [128]. At these stages, cancer cells shed into the abdominal cavity fluids and metastasize to peritoneal organs as well as to lymph nodes and distant organs. Additional complications include: accumulation of ascites in the abdominal cavity, intestinal obstruction, loss of function of various organs.

The most common treatment in ovarian malignancies is a combination of surgical intervention and chemotherapy. Current surgical strategy for advanced stages is cytoreduction, which often involves resection of tumors, reproductive organs, and sigmoid colon [129]. Additionally, women with stage III/IV cancer receive chemotherapy with platin (Cisplatin, apoptosis inducer) or taxane (Paclitaxel, mitotic inhibitor) through intraperitoneal (i.p.) or intravenous (i.v.) injection [130]. Studies in which those two administration techniques were compared, suggested that IP cisplatin and IP paclitaxel result in a longer disease progression-free survival and overall survival [130-132]. A combination chemotherapy regimen improved the median survival of patients with advanced ovarian cancer from 5-10% to 20-25% [133]. Despite this improvement, the majority of patients with ovarian malignancies still die of the disease and new treatment approaches are needed.

1.2.3. Prevention and epidemiology

Ovarian cancer occurs sporadically in the population with no known effective prevention practice. The disease is more prevalent in developed countries that in third world countries and mostly affects women between 55 and 74 years old. Less that 1% of epithelial ovarian cancers are detected in women younger than 30 years old and those malignancies are most probably germ cell tumors [134,135].

Nevertheless, several studies suggested factors that may have protective effects and may reduce the risk of ovarian cancer. For instance, oral hormonal contraception received for more than 10 years, was found to decrease the lifetime risk of developing ovarian cancer from 1.8% to 0.6% [136-138]. Multiple pregnancies and breastfeeding seem to have similar protective effect on women's health [139-141]. Lastly, some surgical procedures, such as tubal ligation and hysterectomy, were associated with reduced risk of ovarian cancer incidences even in patients carrying BRCA1 mutation [142].

1.2.4. Molecular mechanisms of ovarian cancer progression

Many studies indicate that steroid hormones play an important role in ovarian cancer etiology and progression. Hormonal shift from estrogens to androgens after menopause resulting in high androgen serum levels is believed to elevate the risk of ovarian cancer. Androgen receptor (AR) is expressed in OSE and is also found in 95% of ovarian cancer cells suggesting its importance in ovarian cancer progression [143,144]. Several studies indicated that androgens treatment induces cellular proliferation and decreases cell death [145,146]. These physiological changes may be the results of repressing effect of androgens on TGFβ receptors (TβR-I and TβR-II) expression, abrogating the normal growth inhibition signaling induced by TGFβ [147].

Before ovarian cancer cells metastasize from the primary tumor, they need to undergo an epithelial-to-mesenchymal (EMT) transition resulting in decreased

attachment to basement membrane and adhesion between other cells [148]. This transition correlates with Mullerian differentiation during which the shape of the cells is altered and accumulation of E-cadherin, junctional complexes, and mucins (including MUC16 – CA125) are observed [149-151]. One of the most important molecules responsible for epithelial cell adhesion is E-cadherin. This membrane glycoprotein located at cell adherens junctions anchors epithelial cells to each other [152,153]. Downregulation of E-cadherin in cancer cells is caused by up-regulation and transcriptional repression by Sip1/ZEB2, Snail and Slug [154]. Shedding and survival of the cancer cells in detached form is also enhanced by upregulation of collagen-binding integrins and matrix metalloproteinase MMP-9 [155,156]. As a result, ovarian cancer cells can passively spread to peritoneum and omentum, carried by physiological movement of peritoneal fluids [157].

Accumulation of ascites is a very common symptom of advanced stage of ovarian cancer. Ascites formation occurs when cancer cells obstruct subperitoneal lymphatic channels and prevent physiologically produced fluid from absorption. Additionally, secretion of vascular endothelial growth factor (VEGF) by cancer cells increases vascular permeability and promotes ascites production [158,159]. VEGF is an angiogenic protein remarkably upregulated in majority of ovarian cancer cells and its expression positively correlates with the degree of tumor malignancy [160,161]. A long list of VEGF inducers include: Hypoxia-Inducing Factor (HIF), Interleukins (IL-1β, IL-6), Induction Growth Factor (IGF-1), Transformation Growth Factor (TGF-α, TGF-β), Basic Fibroblast Growth Factor (bFGF), and others [162-164]. Once the ovarian cancer tumor reaches a certain size, the diffusion can no longer provide a sufficient amount of nutrients required for its growth. In this case, VEGF stimulates vascular and lymphatic endothelium to form new blood vessels [165]. High expression of VEGF in tumors and its presence in serum and ascites indicates cancer progression and poor prognosis [166,167]. It was recently found that neovascularization process regulated by VEGF in ovarian carcinoma models can be

inhibited by specific anti-VEGF monoclonal antibodies and once this treatment is combined with Taxol therapy, significant improvement in tumors and ascites regression is observed [168].

Oncogene disregulation and tumor suppressor inactivation are commonly found in ovarian cancer cells, which facilitate tumor progression at different stages. Among the activated oncogenes, HER family of tyrosine kinase receptors draws particular attention of researchers. One of the family members, HER-2, is over-expressed in 15% ovarian cancer tumors and associated with a poor prognosis [169,170]. Also, the PI3 kinase signaling pathway components, such as PI3, AKT, PTEN, are amplified, over-expressed or activated in more than 70% of ovarian cancers [171-173]. As it is found in other malignancies, TP53 gene is also mutated in more than 50% of ovarian carcinomas, especially in high-grade tumors [174-176].

1.2.5. Epigenetics in ovarian cancer

The epigenetic alterations have been observed in early and late stage ovarian cancers. Epigenetic changes, such as DNA methylation, histone modifications, and micro-RNA disregulation, have been noted in ovarian cancers and are subjected to intense investigations in recent years [177-180].

In mammals, DNA methylation occurs predominantly in cytosines located at the side of guanines, frequently called CpG site (CpG dinucleotides) [181]. DNA methylation patterns are tissue and cell type-specific and disruption of DNA methylation may lead to tumor development [182]. Hypermethylation of gene promoters typically leads to gene silencing, and reduction of methyl groups in CpGs may increase transcription [183]. Tumor suppressor genes frequently reported as hypermethylated in ovarian cancer, such as BRCA1, hMLH1, hMLH2, ICAM-1, GATA4, estrogen receptor, p16 and SURVIVIN [184-190], whereas DNA hypomethylation was found in SERPINB5, Claudin4, HoxA10 [191-193].

Posttranslational histone modifications are also important mechanisms of epigenetic gene regulation. Acetylation, deacetylation, methylation, demethylation, phosphorylation, ubiquitination, ADP-ribosylation and sumoylation alter the biochemical properties of histones [194-198]. In general, loss of histone acetylation is associated with more compact chromatin conformation and decreased transcriptional activity. Histone acetylation is controlled by histone acetyltransferases (HATs), which add acetyl groups to specific lysine residues, and histone deacetylases (HDACs), which catalyze their removal. HDACs are frequently over-expressed in ovarian cancer tissues and play a significant role in ovarian carcinogenesis [70].

Similarly, the accumulation of H3K9 trimethylation leads to chromatin compaction and gene silencing [199,200]. Interestingly, histone H3/lysine K4 methylation is associated with active genes which bring increasing complexity of histone code [201,202].

microRNAs, small non-protein-coding RNA molecules, were recently introduced as epigenetic components of posttranscriptional gene downregulation [203]. They effectively inhibit the translation of their target genes by binding to their 3' UTR region and creating the RNA-induced silencing complex (RISC) with Argonaute proteins and Dicer [204]. MicroRNA regulation is also altered in ovarian cancer tumors. For instance, miR-200a, miR-141, miR-200c and miR-200b are found over-expressed, but miR-199a, miR-140, miR-145 and miR-125b1 are downregulated [205]. microRNAs play key roles in both normal and pathologic ovarian activities by targeting the expression of specific genes.

Although the impact of aberrant epigenetic regulations on ovarian cancers is gaining increasing appreciations, the role of linker histones in this disease has not been studied.

1.2.6. Potential histone H1 targets in ovarian cancer

As mentioned above, linker histone H1 was previously analyzed in the context of breast cancer cell lines. Various subtypes were found to inhibit cell growth, induce apoptotic events, and even stimulate cytotoxicity in cancer cells. However, to date not much attention was paid to the putative linker histone H1 effects on ovarian cancer progression.

Previous studies indicate that linker histone H1 subtypes specifically modulate the expression of target genes in direct or indirect manners in various contexts ([40,206] ,unpublished observation). Here we demonstrate that individual H1 variants have distinct expression patterns in malignant ovarian adenocarcinomas compared with benign adenomas. Through modulating H1 variants levels in ovarian cancer cell line, we have identified H19 as a direct target of H1.3 in OVCAR-3 cells. H19 is non-protein coding gene and an ovarian cancer biomarker. H19 is a well-known oncofetal gene frequently over-expressed in ovarian cancer as well as in other solid tumors. Its expression is regulated by epigenetic mechanisms, and recent studies showed that the level of linker histone H1 influence the amount of H19 in mouse embryonic stem cells [73,207]. Our studies here establish a mechanism by which a specific H1 variant, H1.3, suppresses ovarian cancer growth by inhibiting H19 oncogene.

CHAPTER 2: Profiling of linker histone variants in ovarian cancer

This chapter was published under the same name in the following article: Frontiers in bioscience, 2012 Jan 1;17:396-406.

Magdalena Medrzycki[1,2], Yunzhe Zhang[1,2], John F. McDonald[1,2,3], Yuhong Fan[1,2,3]

[1]School of Biology, Georgia Institute of Technology, 310 Ferst Drive, Atlanta, GA, 30332, USA, [2]The Petit Institute for Bioengineering and Bioscience, Georgia Institute of Technology, 315 Ferst Drive, Atlanta, GA, 30332, USA, [3]Ovarian Cancer Institute, Georgia Institute of Technology, 315 Ferst Drive, Atlanta, GA, 30332, USA

2.1. Abstract

H1 linker histones play a key role in facilitating higher order chromatin folding. Emerging evidence suggests that H1 and its multiple variants are important epigenetic factors in modulating chromatin function and gene expression. Ovarian cancer is a devastating disease, ranking the fifth leading cause of all women cancer death due to its poor prognosis and difficulty in early diagnosis. Although epigenetic alterations in ovarian cancers are being appreciated in general, the role of H1 has not been explored. Here, using quantitative RT-PCR assays, we systematically examined the expression of 7 H1 genes in 33 human epithelial ovarian tumors. Whereas the expression of H1.3 was markedly increased, the expression of H1.0, H1.1, H1.4 and H1x were significantly reduced in malignant adenocarcinomas compared with benign adenomas. Strikingly, ovarian adenocarcinomas and adenomas exhibited characteristic expression patterns, and expression profiling of 7 H1 genes in tumor samples discriminated adenocarcinomas vs. adenomas with high accuracy. These findings indicate that the expression of H1 variants is exquisitely regulated and may serve as potential epigenetic biomarkers for ovarian cancer.

2.2. Introduction

Ovarian cancer has the highest mortality rate among gynecological malignancies and ranks as the fourth most common cancer in women. Each year more than 21,000 women are diagnosed with ovarian cancers and about 15,000 women die of the disease [208,209]. Due to the lack of effective screening methods and asymptomatic nature of ovarian cancers at early stages and during relapse, most women have advanced stage ovarian cancers at the time of diagnosis and the 5-year survival rate is only 25-50%. The etiology of ovarian cancers involves both genetic and epigenetic alterations. Unlike genetic mutations, epigenetic changes, such as alterations in DNA methylation and histone modifications, are reversible, thus offering

an attractive avenue for therapeutic interventions. Better understanding of epigenetic changes associated with ovarian neoplasia will facilitate designing new strategies for early detection and effective therapy of ovarian cancers.

Aberrant epigenetic regulations contribute significantly to ovarian cancer development and progression [177,210]. Accumulating evidence shows that alterations in DNA methylation and/or core histone modifications are responsible for silencing of tumor suppressor genes or upregulation of cancer-promoting genes in ovarian cancers [177,211,212]. Ovarian tumors also display genome-wide DNA hypomethylation and differential expression patterns of genes encoding histone modifying activities [210,213]. Such global changes in DNA methylation and histone modifications suggest that ovarian cancer cells adopt drastically different chromatin structure, because both DNA methylation and core histone post-translational modifications can profoundly impact on chromatin folding. However, the role of linker histones, the key factors in mediating higher order chromatin structure has not been explored in ovarian cancer. Here we take the first step to investigate a potential connection between specific linker histone variants with ovarian cancer through expression profiling of various H1 subtypes.

Linker histone H1 binds to the nucleosome core particle, the basic repeating unit of chromatin consisting of an octamer of two molecules of each of the four core histones (H2A, H2B, H3 and H4) wrapped by 146 bp of DNA, and the linker DNA between nucleosomes to mediate higher order chromatin folding into a 30-nm fiber [10,214]. Consistent with its role in chromatin condensation and limiting genome accessibility, H1 acts as a general transcription repressor, repressing transcription by all three types of RNA polymerases in *in vitro* studies (reviewed in [214,215]). However, recent work using *in vivo* systems demonstrated a rather selective role of H1 in gene regulation, such that H1 can either activate or repress specific gene transcription under various physiological contexts [22,23,73,216-222].

The H1 histone family is the most divergent and heterogeneous group of histones among the highly conserved histone protein families. All metazoan H1s share the same tripartite domain structure with a central globular domain flanked by N-terminal and C-terminal tail regions. The globular domain is evolutionally conserved from yeast to humans. Different H1 subtypes exhibit significant sequence divergence from one another, yet H1 subtypes are highly conserved during evolution in mammals, suggesting distinct functions for these subtypes. There are 11 H1 subtypes (H1.0, H1.1, H1.2, H1.3, H1.4, H1.5, H1oo, H1t, H1x, H1t2 and H1LS1) identified in mammals that are differentially regulated during development and cellular differentiation [25]. H1.1 through H1.5 are somatic H1s that are ubiquitously expressed in all cell types and tissues. The synthesis of these 5 somatic H1s is cell-cycle dependent and tightly regulated during development, such that each tissue has a characteristic composition of somatic H1 subtypes [36,223]. Although individual somatic H1 subtypes appear to be dispensable for normal mouse development, loss of three somatic H1 subtypes (H1.2, H1.3 and H1.4) by sequential gene targeting leads to embryonic lethality at mid-gestation, demonstrating that linker histones are required for mammalian development [72,224-228]. H1x is a more distantly related H1 variant whose RNA messages are present in many somatic tissues [43,229]. H1x proteins are found to accumulate in nucleoli in G1 phase and at chromosome periphery during mitosis in cultured cells, but its total protein level remains unchanged throughout cell cycle [230,231]. H1x is highly expressed in neuroendocrine cells and its expression is increased in neuroendocrine tumors [232]. The replacement H1 variant, H1.0, is expressed mainly in differentiated and non-dividing cells [233]. H1oo and H1t are oocyte- and testis- specific variants, respectively [42,234]. H1T2 and H1LS1 are two distantly related H1t-like proteins that are specifically expressed in spermatids [41,235]. Different H1 subtypes exhibit distinct *in vivo* binding dynamics in oocytes and during embryonic stem (ES) cell nuclear transfer [236]. These properties of H1 subtypes suggest that exquisite

regulation of high order chromatin compaction in various cellular processes may be achieved with different complements of H1 subtypes.

In this study, we analyzed the expression pattern of H1 subtypes as a means to probe the specific chromatin status associated with malignant ovarian cancer. The vast majority of malignant ovarian tumors are epithelial ovarian adenocarcinomas, which are derived from the ovarian surface epithelium [96]. While also derived from ovarian surface epithelium, ovarian adenomas are generally benign and do not have aggressive growth, nor do they metastasize to adjacent tissues. Here, we first systematically screened 14 malignant ovarian adenocarcinomas and 11 benign ovarian adenomas of the mRNA levels of all somatic and replacement H1 subtypes by quantitative reverse transcription-polymerase chain reaction (qRT-PCR) assays. We found that several H1 subtypes displayed drastically different expression patterns in malignant ovarian cancers compared with benign adenomas. Furthermore, profiling and hierarchical clustering analysis of the expression levels of H1 subtypes can accurately discriminate between benign adenomas and malignant adenocarcinomas of all 25 samples, and correctly segregate ovarian adenomas from adenocarcinomas in a second set (blind test) of 8 tumor samples with 87.5% accuracy, suggesting a potential use of specific H1 subtypes as ovarian cancer biomarkers.

2.3. Materials and methods

2.3.1. Tumor samples

A total of 33 tumor samples with an initial set of 25 tumors and a second set of 8 tumors, including 18 benign serous cystadenomas and 17 malignant adenocarcinomas (Stages III and IV), were obtained from the Ovarian Cancer Institute (Atlanta, USA). Primary tumor tissues were collected from patients who underwent surgery for removal of ovarian tumors at Northside Hospital (Atlanta,

USA) according to procedures approved by the Institutional Review Boards of Georgia Institute of Technology and Northside Hospital. Patients had not been pretreated with chemotherapy at the time of surgery and the tumor tissues were snap frozen in liquid nitrogen immediately at the time of surgical removal.

2.3.2. RNA isolation

Tissue samples (75-100 mg) were ground with a PowerGen 125 homogenizer (Fisher Scientific) on ice in the presence of Trizol (Invitrogen, Carlsbad, CA) for 3 times with 15 seconds each time to obtain crude homogenates. RNAs were subsequently extracted from the crude homogenates with Trizol according to the manufacturer's instructions. RNA samples were subsequently cleaned and concentrated using RNeasy Mini kit (Qiagen, Valencia, CA). The concentration and quality of RNA were measured and verified with a Nanodrop ND1000 Spectrophotometer (Nanodrop, Wilmington, DE) and gel electrophoresis.

2.3.3. Real-time quantitative RT-PCR (qRT-PCR)

2.5 μg of total RNAs extracted from ovarian tumors were reverse transcribed into cDNAs using Superscript III kit (Invitrogen, Carlsbad, CA) according to the manufacturer's manual. Since most histone RNAs do not have long poly-A tails, random hexamers (instead of oligo-dT) were used as primers in the reverse transcription reactions. cDNAs were subsequently analyzed by real-time PCR analysis to quantitatively measure the expression levels of H1 subtype genes and house-keeping genes, e.g. glyceraldehyde-3-phosphate dehydrogenase (GAPDH) gene, which served as normalization controls. Real-time quantitative PCR analysis with an RNA template was performed as RT(-) reactions to control for potential genomic DNA contamination. In all of the reactions, the amount of PCR product produced from RT(-) reactions was less than 1% of that from RT(+) samples,

indicating that genomic DNA contamination, if any, was minimal. Primers used for the real-time quantitative PCR analysis of H1 genes are listed in Table 2.1.

The amount of cDNAs or DNA fragments was quantified and analyzed by real-time PCR using iQ SYBR green PCR Supermix kit (Bio-Rad Laboratories, Hercules, CA) in a MyIQ Single Color real-time PCR Detection System (Bio-Rad). Each primer pair was tested by a standard curve method using serial dilutions of DNA template and the dissociation curve was measured to assure that only the expected PCR product was produced. All samples were typically analyzed in duplicate in at least 3 independent runs. Real-time data were recorded and quantified using iQ5 software provided by the manufacturer and expression values of H1 genes were normalized against that of GAPDH. The genes for somatic H1s (H1.1-H1.5), H1.0, and H1x do not have introns. In order to cross-compare the relative mRNA message abundance within a tumor sample, the mRNA amount was normalized by the primer coefficiency determined by qPCR using genomic DNA as template by standard curve method. The following program was applied for the experiment: 95^0C for 3 min., 95^0C for 10 sec., 60^0C for 20 sec., 72^0C for 30 sec., 95^0C for 1 min. in 40 cycles.

2.3.4. Statistical analysis

Statistical analysis and p values of the differences between the median of H1 expression levels in ovarian adenomas and adenocarcinomas were calculated by Mann-Whitney unpaired two-tailed test. A p value of less than 0.05 was considered to be statistically significant.

2.3.5. Immunoblotting

Tumor samples were homogenized with a PowerGen125 homogenizer (Fisher Scientific) in Lysis buffer (30 mM Tris pH 8.0, 150 mM NaCl, 0.1% SDS, 0.5% Na-deoxycholate, 0.1% NP-40, Proteinase Inhibitor tablet). Protein concentrations of the

cell lysates were determined by Bradford Protein Assay (Bio-Rad). 20 µg of cell lysates were boiled for 5 minutes in Loading Buffer (2% SDS, 10% Glycerol, 50 mM Tris pH 7.0, 100 mM DTT, 0.1% bromophenol blue) before subject to 12% SDS-PAGE. Proteins were subsequently transferred to a nitrocellulose membrane (Bio-Rad) and blotted with a monoclonal antibody against H1.0 (Santa Cruz, sc-56695) [237], or GAPDH (Ambion, AM4300) as a loading control, followed by a Fluor® 680 goat anti-mouse IgG secondary antibody (Invitrogen A21058). The protein bands were visualized and quantified using the Odyssey Infrared Imaging System (LI-COR Biosciences).

2.3.6. Cluster analysis

Hierarchical clustering analysis was performed using the cluster 3.0 software from open source clustering software (http://bonsai.hgc.jp/~mdehoon/software/cluster/software.htm#ctv) and visualized using Treeview, which was developed based on program Cluster/Treeview [238].

2.4. Results

2.4.1. Analysis of the expression patterns of histone H1 subtypes using qRT-PCR

We developed a set of real-time RT-PCR assays to quantitatively measure the mRNA levels of individual H1 variants. Because mRNAs of most H1 genes contain a stem-loop structure at their 3' untranslated regions (UTR) and lack the long poly-A tails normally present in most other cellular mRNAs, we prepared cDNAs from total

Table 2.1: List of primers used for qRT-PCR analysis of human variant H1 genes and housekeeping genes

Gene name	Accession number	Sequence	Product size (bp)	Annealing temperature
H1.1	HIST1H1A: NM_005325	F' - CTCCTCTAAGGAGCGTGGTG - 5' R' - GAGGACGCCTTCTTGTTGAG - 5'	192	57^{o}C
H1.2	HIST1H1C: NM_005319	F' - ACACCGAAGAAAGCGAAGAA - 5' R' - GCTTGACAACCTTGGGCTTA - 5'	154	57^{o}C
H1.3	HIST1H1D: NM_005320	F' - GGAGACTGCTCCACTTGCTC - 5' R' - GCCTTCTTCGCCTTTTTCTT - 5'	75	57^{o}C
H1.4	HIST1H1E: NM_005321	F' - GTCGGGTTCCTTCAAACTCA - 5' R' - GCCTTCTTTGGGGTCTTCTT - 5'	171	57^{o}C
H1.5	HIST1H1B: NM_005322	F' -GTCAAAAAGGTGGCGAAGAG - 5' R' - CTTGGCCTTTGCAGCTTTAG - 5'	159	57^{o}C
H1.0	H1F0: NM_005318	F' - CTCGCAGATCAAGTTGTCCA - 5' R' - GAAGGCCACTGACTTCTTGG - 5'	127	57^{o}C
H1x	H1FX: NM_006026	F' - GTGGTTCGACCAGCAGAATG - 5' R' - GAGCTTGAAGGAACCGTTGG - 5'	115	57^{o}C
GAPDH	GAPDH:NM_002046	F' -GAGTCAACGGATTTGGTCGT - 5' R' - GACAAGCTTCCCGTTCTCAG - 5'	185	57^{o}C
ß-actin	ACTB: NM_001101	F' - CTCTTCCAGCCTTCCTTCCT - 5' R' - AGCACTGTGTTGGCGTACAG - 5'	116	57^{o}C

RNAs using random-primer based reverse transcription. By this means, we analyzed mRNA expression of all H1 subtypes, except those of the four germ cell specific H1s.

The H1 genes measured include the 5 somatic H1s (H1.1-H1.5), H1.0 and H1x. Table 2.1 lists RT-PCR primers utilized in these assays.

2.4.2. Differential expression of the histone H1 subtype genes in ovarian tumors

To test if any of the H1 genes are differentially expressed during ovarian carcinogenesis, we measured the mRNA levels of 7 H1 genes in 11 benign ovarian adenomas and 15 malignant ovarian adenocarcinomas of stage III/IV using qRT-PCR assays. The mRNA levels of GAPDH and beta-actin remained constant across all tumor samples, indicating little variations in sample preparation and qRT-PCR analysis. Each sample was analyzed in at least three independent experiments and the expression levels of H1 subtypes were normalized by the expression level of GAPDH. Since all 7 H1s measured here are intronless, we normalized the relative primer efficiency for individual H1 subtypes by performing PCR reactions using the genomic DNA templates. After adjusting for the relative efficiency of individual PCR reactions, we quantified relative mRNA expression levels of individual H1 subtypes (Figure 2.1) as well as the total H1 mRNA levels (Figure 2.2).

Among the 7 H1 genes, H1.1, H1.4, H1.0, and H1x mRNA levels were significantly reduced in ovarian malignant adenocarcinomas compared with benign adenomas. The reduction in expression values was highly statistically significant, with P values less than 0.0001 for H1.0, and equal to 0.006, 0.014, 0.003 for H1.1, H1.4 and H1x, respectively. In contrast, H1.3 was increased 2.5-fold in malignant tumors ($p=0.0029$) (Figure 2.1). The average expression levels of H1.2 and H1.5 did not appear to be statistically different between adenomas and adenocarcinomas ($p >0.05$). Quantitation of total mRNA levels from all 7 H1 subtypes showed that, on average, the sum of total H1 mRNAs declined 40% in adenocarcinomas ($p=0.0007$) (Figure 2.2A).

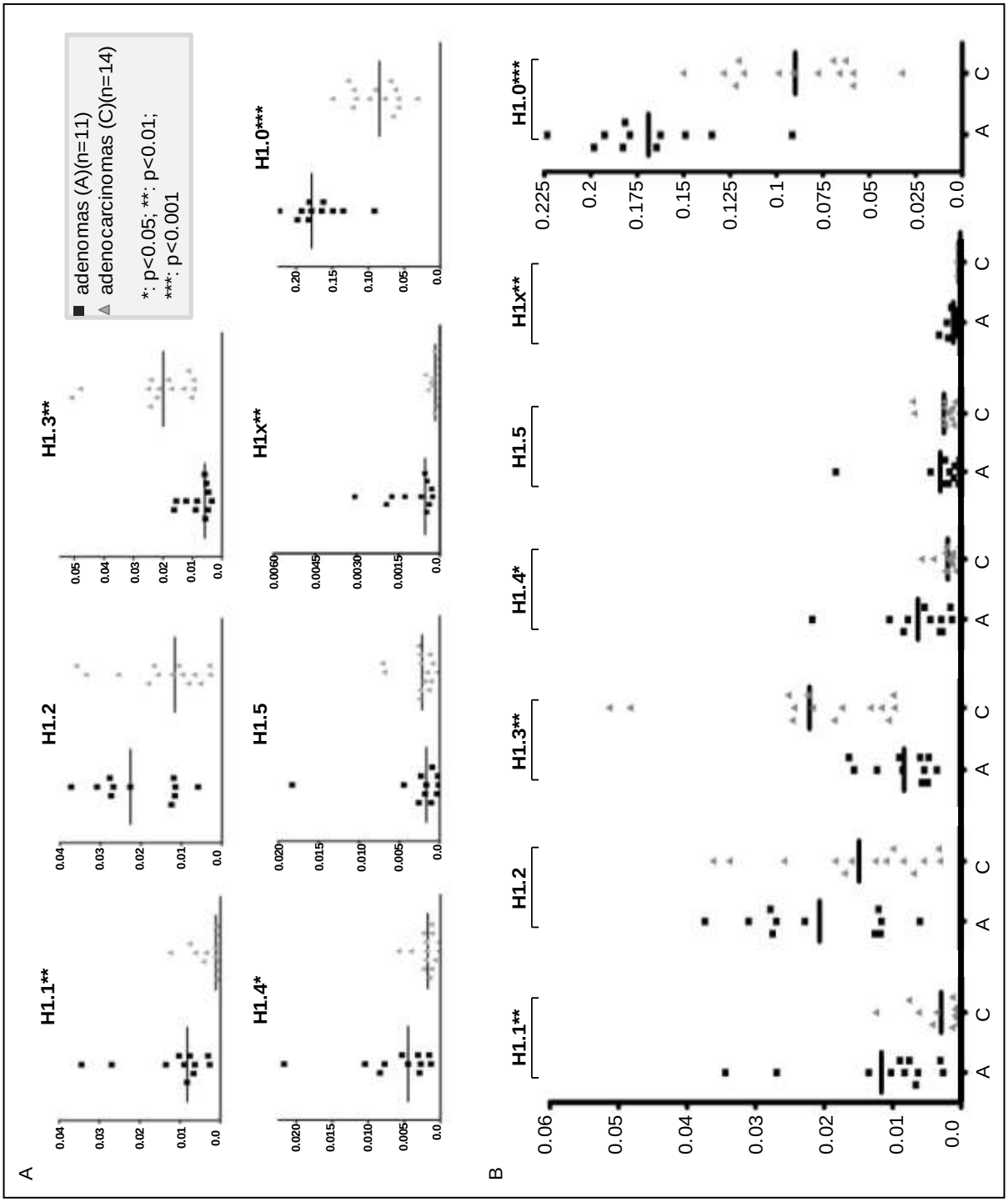

Figure 2.1. qRT-PCR analysis of mRNA levels of linker histone variants in ovarian tumors. Normalized mRNA expression levels of H1 subtypes are presented individually (A) and as a group (B). Y axis represents relative expression units. Each dot represents average expression values obtained from three independent measurements from one tumor sample. Data were normalized with the expression level of GAPDH and primer efficiency factor. *: p<0.05; **: p<0.01; ***: p<0.001.

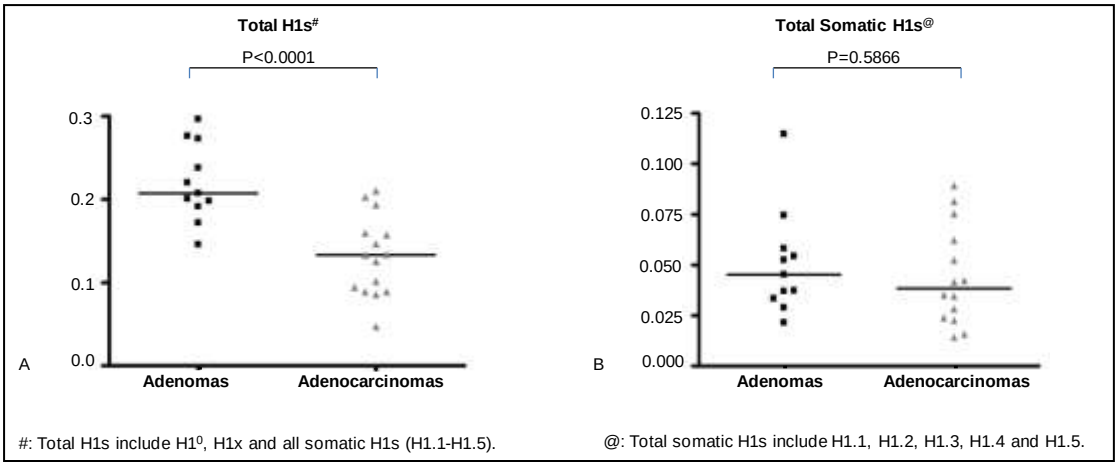

Figure 2.2. Quantification of mRNA levels of total H1s and total somatic H1s. A: Total relative expression units for all H1s. B: Total relative expression units for all somatic H1s (H1.1-H1.5). Y axis represents relative expression units. Each dot represents the average value of the relative expression units obtained from three independent measurements of one tumor sample. Data were normalized with expression of GAPDH and primer efficiency factor. *: $p<0.05$; **: $p<0.01$; ***: $p<0.001$.

This decrease in total H1 mRNA messages is mainly due to the reduction of H1.0 mRNA levels because the total levels for S-phase dependent, stem-loop ended somatic H1 mRNAs (H1.1-H1.5 mRNAs) were similar between these two tumor types (Figure 2.2B), and the mRNA levels of H1x were negligible compared with other H1 subtype mRNAs (Figure 2.1). H1.0 mRNA, however, is polyadenylated, produced throughout cell cycle and processed differently than somatic H1 (H1.1-H1.5) mRNAs [223,239,240]. Interestingly, although ovarian adenomas and adenocarcinomas have similar levels of total S-phase dependent somatic H1 mRNAs (H1.1-H1.5) (Figure 2.2B), the relative proportions of mRNAs expressed from different somatic H1 genes are drastically different (Figure 2.1). This result suggests that individual somatic H1 subtypes are transcriptionally differentially regulated in benign adenomas vs. malignant adenocarcinomas.

We next determined if the drastic differences in H1.0 mRNA levels in adenomas vs. adenocarcinomas resulted in changes in H1.0 protein levels in these two types of tumors. We analyzed H1.0 protein levels in two adenocarcinomas (c647 and c756) and two adenomas (a564, a670), which contained H1.0 mRNA levels 3-fold of that

from c647 and c756 (Figure 2.3A). The two adenomas had significantly higher levels of H1.0 proteins than the two adenocarcinomas (Figure 2.3B), and quantitation of the protein band signals showed a 4-fold increase of H1.0 protein in the two adenomas.

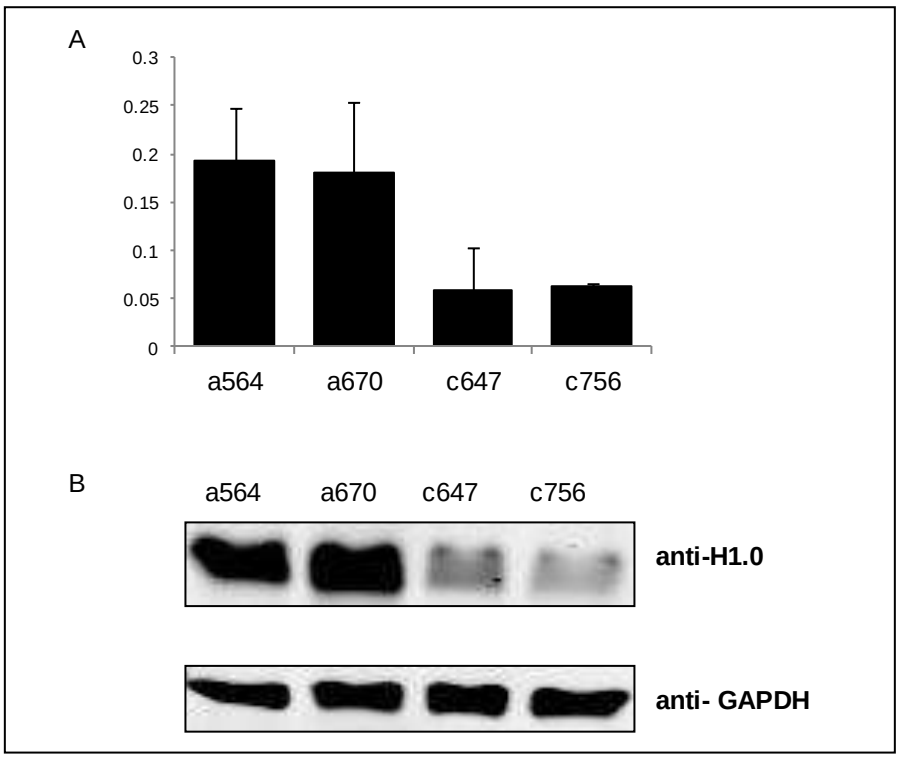

Figure 2.3. Reduced H1.0 expression in ovarian adenocarcinomas. A: qRT-PCR analysis of H1.0 mRNA messages. Y axis: relative expression units of H1.0. Expression values were normalized by the expression level of GAPDH. B: Western blot analysis of H1.0 protein levels. GAPDH served as a loading control.

Immunostaining of the sections of these 4 tumors indicated that H1.0 proteins were ubiquitously present in all cells, and that the two adenomas displayed stronger signals for H1.0 than adenocarcinomas (data not shown). These results suggest that a higher level of H1.0 mRNA leads to a corresponding increase in H1.0 protein in adenomas.

2.4.3. Expression patterns of histone H1 subtypes discriminate ovarian adenomas from adenocarcinomas

Expression profiling of H1 subtypes demonstrated that multiple H1 genes exhibit differential expression levels in adenocarcinomas compared with adenomas (Figure 2.1), suggesting characteristic H1 expression signatures associated with carcinogenesis.

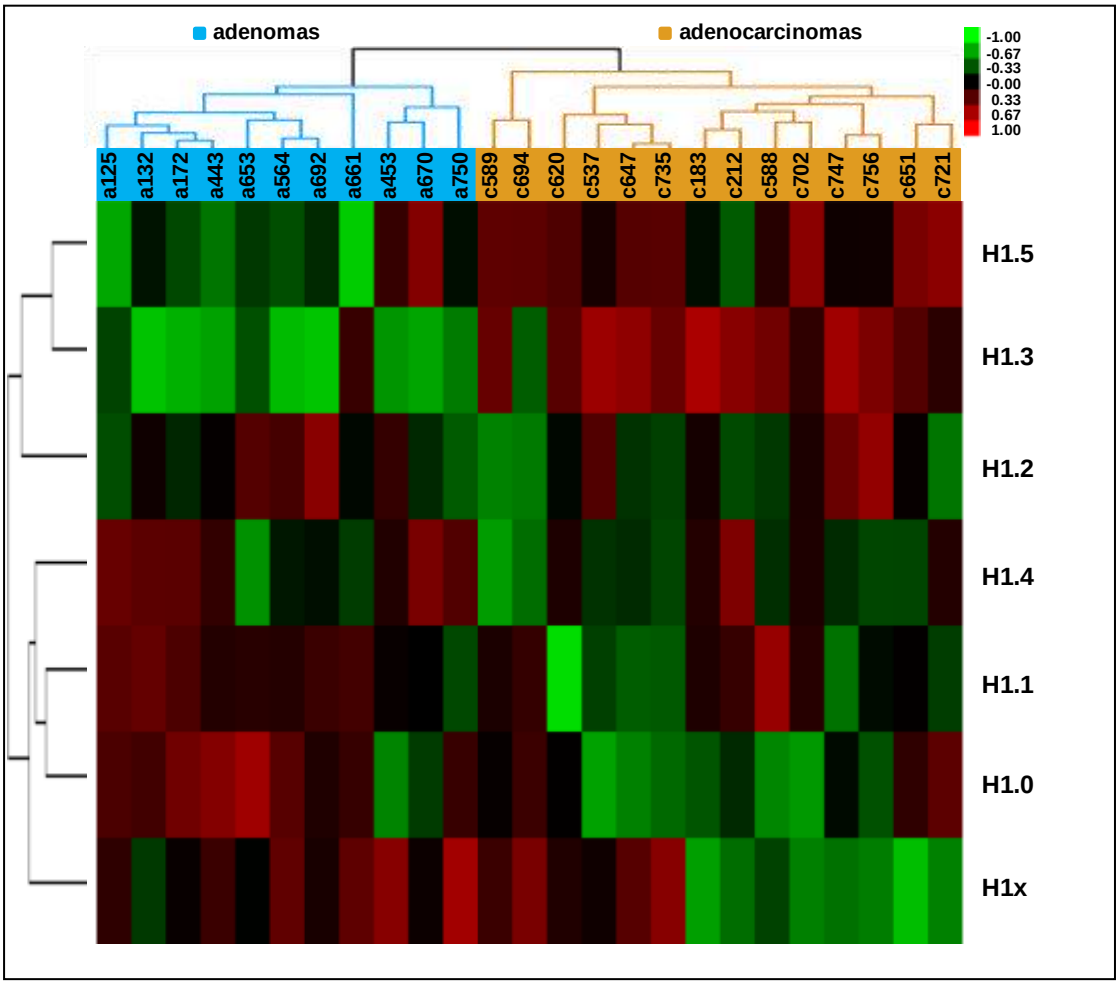

Figure 2.4. Hierarchical clustering diagram of differential expression data of 7 H1 subtypes in ovarian adenomas and adenocarcinomas. Red, green or black colors represent higher, lower, or no change in relative expression compared with the median expression level across all tumor samples, respectively. The dendrograms at the top and on the left show the clusters defined by similarities in expression patterns across the samples and genes. All adenocarcinoma samples cluster separately from adenomas.

To determine whether H1 variant genes can serve as transcriptional classifier genes to discriminate ovarian adenomas from malignant adenocarcinomas, we

performed hierarchical clustering analysis of expression patterns of the H1 genes for these 25 ovarian tumors.

Figure 2.4 shows that the clustering algorithm segregated all 25 samples into adenomas and adenocarcinomas accurately based on the similarities of H1 subtype expression patterns in these samples. Expression patterns of H1 genes of all 11 adenomas were more closely related to each other, forming a group separately from that of adenocarcinomas, which also clustered in a group.

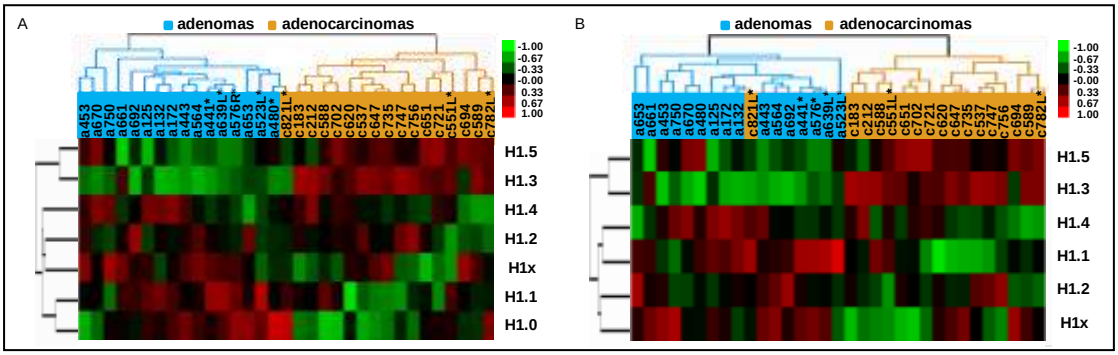

Figure 2.5. Validation of discriminating expression patterns of H1 subtypes in ovarian adenomas and adenocarcinomas. Hierarchical clustering diagrams of expression profile of all 7 H1 genes (A), or leaving out H1.0 (B), of all 33 samples were shown. Samples include 8 blind test samples (marked with *) and 25 tumors from the initial batch. Both (A) and (B) show correct segregation of all but one (c821L) samples into ovarian adenomas vs. adenocarcinomas.

To further test if analysis of mRNA expression patterns of H1 genes can predict ovarian adenomas vs. adenocarcinomas using these 25 tumor samples as templates, we obtained 8 additional tumor samples as a blind test set. We analyzed H1 expression levels by qRT-PCR, and performed hierarchical clustering analysis of these 8 samples together with the initial set of 25 samples. We clustered each blind test sample together with the 25 samples, and such analyses correctly clustered all but 1 (c821L) blind test samples into their corresponding tumor groups, representing an accuracy of 87.5% (7 out of 8) in discriminating adenomas vs. adenocarcinomas within this blind test set. Figure 2.5A shows a clustering diagram of all of the 33 samples analyzed, suggesting an overall accuracy of 97% (32 out of 33) in

segregation of these two types of tumors. These results suggest that expression profiles of H1 variants can potentially serve as biomarkers to differentiate ovarian adenocarcinomas from adenomas. To identify the minimum number of H1 genes whose expression levels contribute to accurate prediction of clustering of tumor types, we re-clustered all of the 33 samples using expression patterns from any combinations of 6 H1 genes (leaving out one H1 gene at a time). Interestingly, as with clustering using all 7 H1 genes, leaving out H1.0 did not affect the correct discrimination of all samples but c821L (Figure 2.5B), whereas leaving out any of the 5 somatic H1s and H1x resulted in disruption of correct segregation of two or more tumor samples (data not shown).

2.5. Discussion

Numerous gene expression microarray analyses show that malignant tumors exhibit distinct expression fingerprints compared to normal tissues or benign tumors [74,241,242]. Changes in global and/or local chromatin structure contribute to the acquisition or maintenance of malignancy. Indeed, increased nuclear staining and nuclear size are often early cytological abnormalities found with dysplasia [243]. The presence of multiple H1 histone variants provides an additional level of regulation in modulating chromatin folding, so it is likely that malignant transformation is associated with changes in the expression of various H1 subtypes. However, expression changes in mRNAs of histone genes are often missed from microarray profiling studies. This is because histone mRNAs, including that of most H1 genes, contain a stem-loop structure at their 3' untranslated region (UTR) and lack a long poly-A tail, and are thus not selected when oligo-dT based reverse transcription assays are adopted.

In the present study, we designed a set of qRT-PCR assays, coupling random primer based reverse transcription with real-time PCR, to quantitatively measure the expression of all H1 genes that are expressed in ovarian tumors. Using this set of assays, we initially analyzed a total of 25 ovarian tumors (11 adenomas and 14 adenocarcinomas),

and found that benign ovarian adenomas and malignant adenocarcinomas have distinct expression patterns of several H1 genes. Specifically H1.0, H1.1, H1.4 and H1x are significantly reduced in expression, whereas H1.3 has drastically increased expression in ovarian adenocarcinomas compared with adenomas. Furthermore, clustering analysis of gene expression of these 7 H1 genes or 6 H1 genes (leaving out H1.0) segregates adenomas from adenocarcinomas with an overall accuracy of 97% for all 33 tumor samples (including 25 tumors of the initial batch and 8 samples of the blind test batch). These results suggest that H1 subtype genes display discriminative expression signatures which may serve as biomarkers and classifier genes to differentiate ovarian adenomas from adenocarcinomas. These highly sensitive and quantitative real-time RT-PCR assays can be attractive alternative or auxiliary diagnostic tools to current pathological analysis. This possibility can be further investigated using a larger set of ovarian tumor samples. With a larger set of ovarian tumor samples, it will also be possible to examine if subgroups from clustering analysis correlate with tumor progression stages and/or patient prognosis.

Synthesis of somatic H1 subtypes (H1.1-H1.5) is primarily S-phase dependent, and the expression of H1 genes can be regulated at transcriptional level, post-transcriptional mRNA processing and stability, as well as protein degradation [223]. Cell cycle arrest or terminal differentiation in cell culture causes a reduction in H1.1, H1.3, H1.5 mRNAs and a slight decrease of H1.2 and H1.4 mRNAs [223], thus, we surmise that an increased proliferation rate in malignant tumors may lead to a reduction of the total levels of somatic H1 mRNAs in these cells. Interestingly, careful quantification shows no difference in the combined levels of somatic H1 mRNAs (Figure 2.2B), instead, a change in the proportions of mRNAs from individual somatic H1 subtypes was observed in malignant adenocarcinomas compared with benign adenomas (Figure 2.1). Although the relative proportions of protein levels for individual H1s do not recapitulate their relative proportions of mRNA levels due to different mRNA processing efficiencies [244] and varied turn-over rate of H1 subtypes [36,223,245], for a specific H1 subtype, the

increase or decrease in mRNA levels often leads to a corresponding change in its protein level [36,223], as is the case for H1.0 shown in this study (Figure 2.3). We have previously observed similar fold increases in the levels of mRNAs and proteins of H1.0 and H1.5, in H1.2/H1.3/H1.4 triple null mouse ES cells and embryos ([73], and Zhang and Fan, unpublished observation). These studies suggest that changes in H1 subtype protein levels are likely to occur during ovarian tumor progression, and the trend of changes will probably follow the changes in the mRNA levels for a given H1 subtype. Individual somatic H1 subtypes have different DNA binding affinities and varying degrees of chromatin compacting ability [56,62,64,65], and they can be grouped into the strong condensers (H1.4 and H1.5), the intermediate condenser (H1.3) and the weak condensers (H1.1 and H1.2) in compacting minichromosomes [46]. Thus, changes in the protein levels of individual somatic H1s are likely to cause alterations in chromatin folding and compaction, modulating chromatin accessibility and function.

It is noteworthy that clustering analysis using the expression levels of only 5 somatic H1 genes can segregate 23 of the initial 25 tumor samples correctly (92% accuracy) into adenomas vs. adenocarcinomas (data not shown), suggesting that the distinctive expression patterns of the somatic H1s (H1.1-H1.5) alone can discriminate ovarian adenocarcinomas from adenomas with high confidence. It will be interesting to investigate how these changes in the expression of specific H1 subtypes are brought about in malignant ovarian adenocarcinomas. Interestingly, leaving out H1.2 and H1.5, whose expression levels do not differ significantly in the two types to tumors, leads to incorrect segregation of more tumor samples by unsupervised clustering analysis (data not shown), significantly dampening the discriminative power of H1 profiling in classifying adenomas vs. adenocarcinomas. We postulate that there may be cross-regulation among the somatic H1 subtypes, and the mRNA levels of H1.2 and H1.5 are probably connected to the expression levels of the other H1 subtypes.

H1.0 mRNAs and proteins are significantly reduced in adenocarcinomas (Figure 2.1, Figure 2.3). H1.0 is considered to be a differentiation specific H1, as it accumulates in

terminally differentiated and non-dividing cells (reviewed in [233]). H1.0 expression is low or undetectable in rapidly dividing cells or tissues, but is induced or upregulated during differentiation and senescence [36,81,233,246]. The significantly lower expression of H1.0 in ovarian adenocarcinomas is consistent with the higher proliferation rate of ovarian malignant adenocarcinomas compared with ovarian benign adenomas. As the smallest subtype with the highest percentage of positively charged amino acids among the H1 family proteins, H1.0 has high affinity for DNA and can strongly compact minichromosomes *in vitro* [46,247]. Thus, accumulation of H1.0 proteins would be consistent with an increased level of chromatin compaction and heterochromatin found in terminally differentiated cells [248]. The reduction of H1.0 expression in ovarian adenocarcinomas observed in this study may indicate a reduced level of chromatin compaction in these malignant tumor cells.

Besides the potential of serving as biomarkers for discriminating ovarian adenocarcinomas vs. adenomas, the distinctive expression patterns of histone H1 subtypes may contribute to the causes for carcinogenesis of ovarian cancer. Alterations of H1 levels and chromatin compaction impact on a variety of cellular properties. Modulating levels of specific H1 subtypes can lead to changes in cell cycle and proliferation rate in a cell type specific and H1 subtype dependent manner [77,79]. Depletion of H1.2 in human breast cancer cell line T47D by inducible shRNA causes cell cycle arrest at G1-phase, although knockdown of other somatic H1 variants in T47D does not show similar effects on cell cycle [77]. Interestingly, over-expression of H1.0, but not H1.2, in mouse 3T3 cells, leads to a transient delay in S-phase entry [79] . Although deletion of three somatic H1s, H1.2, H1.3 and H1.4, does not appear to affect cell growth rate in mouse ES cells [73], deletion of all 6 H1 genes in chicken B lymphocyte cell line DT40 significantly impairs cell growth and causes elongation of all stages of the cell cycle [249]. Reduced expression of strong condensers, such as H1.0 and H1.4, combined with a marked increase of intermediate condenser (H1.3), may result in a more open and accessible chromatin conformation in ovarian

adenocarcinomas. This is likely to cause expression changes of specific genes, which may contribute to carcinogenesis. On the other hand, it has been shown that degrees of global chromatin condensation per se impact on DNA damage response, cell migration and invasiveness [250-252]. Global chromatin de-condensation, either by depletion of H1.2/H1.3/H1.4 in mouse ES cells or induced by treatment with histone deacetylase inhibitors (HDACi) in human breast cancer cell line MCF7, results in increased DNA damage response [250]. Migration signals cause an increase in heterochromatin, and induction of chromatin de-condensation by HDACi in mouse melanoma cell line B16-F1 inhibits cell migration [252]. Taken together, these studies indicate that the effects of H1 subtypes as well as the role of overall H1 levels and general chromatin condensation on cancer cell properties are multifaceted and context dependent. Our findings that distinctive expression patterns of H1 subtypes discriminate ovarian adenomas from adenocarcinomas extend the roles of H1 variants into ovarian cancer, and suggest that a further investigation of the functional roles of specific H1 subtypes in ovarian cancer cells is warranted.

2.6. Acknowledgements

This work is supported by Georgia Cancer Coalition Distinguished Cancer Clinicians and Scientists Program (YF), Ovarian Cancer Institute (JFM), NIH grant GM085261 (YF), and Georgia Tech. We thank L. DeEtte Walker for assistance in storage and handling of tumor samples.

.

CHAPTER 3: Histone H1.3 suppresses H19 oncogene expression and cell growth of OVCAR-3 ovarian cancer cells.

3.1. Abstract

Ovarian cancer is a deadly gynecological malignancy for which novel biomarkers and therapeutic targets are imperative for improving survival. Previous studies have suggested the expression pattern of linker histone variants as potential biomarkers for ovarian cancer. To investigate the role of histone H1 in ovarian cancer cells, we over-expressed one of the major somatic H1 variants, H1.3 in epithelial ovarian cancer cell line, OVCAR-3. We find that over-expression of H1.3 decreases the growth rate and colony formation of OVCAR-3 cells. We identify histone H1.3 as a specific repressor for non-coding oncogene H19. Over-expressing H1.3 suppresses H19 expression, whereas H1.3 knockdown increases its expression. Furthermore, we demonstrate that histone H1.3 over-expression leads to increased occupancy of H1.3 at the H19 regulator region encompassing the imprinting control region (ICR) concomitant with increased DNA methylation and reduced occupancy of insulator protein CTCF at the ICR. Moreover, we show that elevated expression of H19 increases proliferation, whereas its depletion suppresses growth rate of OVCAR-3 cells. Finally, we demonstrate that over-expression of H1.3 combined with H19 knockdown synergistically decreases growth rate of ovarian cancer cells.

3.2. Introduction

Ovarian cancer has the highest mortality rate among gynecological malignancies, and is currently the fourth most common cancer in women. Each year, more than 22,000 women are diagnosed with ovarian cancer and about 15,000 women die of the disease, primarily due to difficulty in detecting its presence in earlier, often-

asymptomatic stages [121,253]. The survival rate of women who suffer from ovarian cancer can be improved if diagnostic tests of high specificity and accuracy are clinically available. In order to reach this goal, new therapeutic targets and novel biomarkers need to be characterized on a molecular basis.

The etiology of ovarian cancers involves both genetic and epigenetic alterations. The genetic components of malignant transformations are not well understood, although mutations in BRCA1, TP53, RB1, PTEN and other genes are sporadically found in ovarian cancer cases (reviewed in [176]). Epigenetic aberrations, such as DNA methylation, histone modifications, nucleosome positioning and post-transcriptional gene regulation by microRNAs, are well established in the development and progression of ovarian cancer (reviewed in [177,254]).

Organization of chromatin, DNA stabilization, and facilitation of nucleosome folding are the major structural functions of H1 linker histones [255]. H1 linker histones interact with linker DNA at the dyad axis of the nucleosome at the entry and exit sites of the nucleosomal DNA and participate in multiple cellular processes occurring on the chromatin template, such as gene expression, DNA replication and repair [13,14,16,256].

In mammals, there are 11 H1 variants. Five major somatic H1 subtypes: H1.1 – H1.5 variously are expressed in both dividing and non-dividing cells. Also a somatic H1.0 mainly accumulates in differentiated cells. Tissue specific H1s include testis-specific H1t, H1T2, and HILS1, as well as the oocyte-specific H1oo. The recently identified H1x is present in very low amount and found to have higher expression in neuroendocrine cells [41,42,229,232,257]. Their heterogeneity is conserved among species and suggests that the individual subtypes may have unique properties and functions in the cell [66].

Besides mediating higher order chromatin folding, linker histone H1 has been shown to regulate gene expression *in vivo* in a specific manner. However, it is not clear whether those genes are directly regulated by a specific H1 variant. Here, we

report the identification of an important non-coding oncogene H19 as a direct target specifically regulated by H1.3 in epithelial ovarian cancer cells.

Aberrant expression of H19 occurs in ovarian cancer and other types of cancers [258-260]. H19 is often over-expressed in ovarian cancer, and has been suggested as a biomarker for ovarian cancer [261]. H19 is an oncofetal gene located on human chromosome 11 and is highly expressed in fetal tissues but suppressed in most tissues after birth [262,263]. H19 belongs to an imprinted gene family controlled by the imprinting control region (ICR) important for mammalian development [264,265]. Expressed from the maternal allele, H19 encodes for a spliced, capped and polyadenylated non-coding RNA highly conserved in evolution [266]. It is also a precursor for a microRNA, miR-675, which targets genes essential for growth, development and carcinogenesis, such as RB and Igf1r [267-269]. The H19 locus was recently found to produce an antisense transcript, called H19 opposite tumor suppressor (HOTS) and a long intergenic transcript, 91H, which indicates the great complexity of this region [270,271]. H19 gene regulation has been shown to be regulated by chromatin structure and epigenetic mechanisms, including DNA methylation, CTCF isolator and enhancer activity (reviewed in [272,273]).

In this study we investigate the role of linker histone H1 variants in regulating H19 transcript in ovarian cancer. We utilize over-expression and shRNA knockdown approaches to modulate the expression levels of H1s and H19 mRNA in OVCAR-3 cells. We find that linker histone H1, as a potent epigenetic regulator, directly represses the expression of H19 gene that leads to phenotypic changes in ovarian cancer cells. The results suggest a novel mechanism by which H1.3 regulates H19 expression and tumorigenesis in epithelial ovarian cancer.

3.3. Materials and Methods

3.3.1. Cell culture

OVCAR-3 and 293T cells were cultured in RPMI-1640 (OVCAR-3) or DMEM (293T) media containing 10% and 20% fetal bovine serum, respectively, in a humidified incubator with 5% CO_2 at 37^{o}C.

3.3.2. Expression vectors construction and stable cell lines generation

Genomic DNA (gDNA) of OVCAR-3 cells was extracted with Allprep DNA/RNA Mini kit (Qiagen) and used as template DNA for amplification of the human H1 variant gene coding sequences by PCR. PCR products containing H1 variant coding sequence were cloned into a modified pcDNA3 cloning vector at the EcoRI/XhoI restriction sites, and sequence verified. The backbone of the modified pcDNA3 vector contained flag sequence (5'-GACTACAAAGACGATGACGACAAG-3') at the N-terminal to the start codon. The primers designed for cloning PCR are listed in Table A.1. The expressional vector of H19 was purchased from Genescript. The BamHI site was mutated into SacI, and the ApaI site was changed into BamHI using a site-directed mutagenesis kit according to the manufacturer's manual (Clontech). The H19 gene flanked by SacI and BamHI was inserted into pcDNA3 vector and sequence verified.

OVCAR-3 cells were transfected with pcDNA-H1s or pcDNA-H19 vectors by a Lipofectamine 2000 reagent according to the manufacturer's recommendations. Two days post-transfection, the cells were treated with 400 μg/ml G418 (Geneticin, Invitrogen) for 4 to 5 weeks and resistant clones were picked up and cultured.

3.3.3. Lentivirus production and inducible/stable cell lines generation

pTRIPz (inducible) and pGIPz (stable) shRNA lentiviral systems (Thermo Scientific) were utilized to knockdown H19 and histone H1.3 expression. 293T cells were co-transfected with lentiviral target vectors containing shRNAmir or H1s mRNA

and the TransLenti Viral Packing System (Thermo Scientific) to obtain viral particles capable of infecting OVCAR-3 cells. Virus titration, transduction of target cell lines, and puromycin selection were performed according to the manufacturer's protocol. The cells were sorted by Green Fluorescence Protein (GFP) or Red Fluorescence Protein (RFP) expression to enrich the populations with cells highly expressing shRNAmir or H1s mRNA respectively (BD FACS Aria III Cell Sorter, Beckman Coulter). Seven cell lines with integrated shRNA were generated: OV-3/scrambled-shRNA, OV-3/shH19(tz), OV-3/shH1.3(tz), OV-3/fl.H1.3(H)/scrambled-shRNA, OV-3/flH1.3(H)/shH19(tz), OV-3/flH1.3(H)/shH1.3(tz), OV-3/flH1.3(H)/shH1.3(gz).

3.3.4. RNA isolation and RT-PCR

RNAs were extracted with Trizol (Invitrogen) according to the manufacturer's instructions. RNA samples were further cleaned and concentrated using RNeasy Mini kit (Qiagen). The concentration and quality of RNAs were measured with Nanodrop (Nanodrop, Wilmington, DE) and verified by gel electrophoresis. 2.5 µg of total RNA were reverse transcribed into cDNA using Superscript III kit (Invitrogen) according to the manufacturer's protocol. Random hexamers and oligo-dT were used as primers in the reverse transcription reactions in 1:1 ratio. cDNAs were subsequently analyzed by real-time PCR analysis to quantitatively measure the expression levels of H1 histone subtypes, H19, and house-keeping genes, such as glyceraldehyde-3-phosphate dehydrogenase (GAPDH), which served as normalization controls. The sequences of H19 primers were as follows: F: 5'-ACCACTGCACTACCTGACTC-3' and R: 5'-CCGCAGGGGGTGGCCATGAA-3'. H1 subtypes and control primers used for the real-time quantitative PCR analysis were previously published [274]. The relative expression of selected genes were quantified and analyzed by real-time PCR using iQ SYBR Green PCR Supermix kit (Bio-Rad Laboratories, Hercules, CA) in a MyIQ Single Color real-time PCR Detection System

(Bio-Rad) as previously described [275]. All samples were typically analyzed in triplicates in at least 3 independent runs.

3.3.5. microRNA extraction

microRNAs were extracted from $5x10^6$ cells with mirVana miRNA Isolation kit (Invitrogen) according to the manufacturer's protocol. The quality of obtained microRNAs was confirmed by gel electrophoresis. Reverse transcription of 500 ng microRNAs was performed with miScript Reverse Transcription kit (Qiagen). Primers for miR-675 were as follows: F: 5'-GTTATTGGTGCGGAGAGGGCC-3', universal R: 5'- TGAATCGAGCACCAGTTACG-3', and internal control primer U6: F: 5'-GCGCAAGGATGACACGC.

3.3.6. Western blotting

The cells were lysed in Lysis buffer (30 mM Tris pH 8.0, 150 mM NaCl, 0.1% SDS, 0.5% Na-deoxycholate, 0.1% NP-40, Proteinase Inhibitor tablet) and total histones were extracted as previously described [275]. A Bradford Protein Assay (Bio-Rad) was performed to determine total protein concentration of each sample. Samples were boiled at 95ºC for 5 minutes with Loading Buffer (4% SDS, 20% Glycerol, 100 mM Tris pH 7.0, 200 mM DTT, Coomassie Blue dye). Samples were run in 12% SDS-PAGE gels and transferred to nitrocellulose members (Trans-blot Transfer Medium, Bio-Rad) for two hours. The membranes were blocked for one hour in 4% non-fat milk in PBS at room temperature, incubated over night at 4ºC with primary antibody against: flag-tagged proteins M2 (Sigma, Cat. F1804), H1.2 (Abcam, Cat. ab4086), H1.3 (Abcam, Cat. ab24174), phospho-H1.4 (Sigma, Cat. H7664), H1.5 (Abcam, Cat. ab24175), H1.0 (Santa Cruz, Cat. sc-56695), H3 (Abcam. Cat. ab1791), beta-actin (Sigma, Cat. A5441) and then with secondary antibodies: IRDye680 Goat anti-Rabbit (Li-COR, Cat. 926-32221), IRDye800 Goat anti-Rabbit (Rockland, Cat. 611-0132-122) or Goat anti-Mouse (Molecular Probes,

Cat. A21058) for one hour at room temperature in a 1:10000 ratio. Bands were visualized using Odyssey Infrared Imaging System (LI-COR Biosciences).

3.3.7. Growth curves, MTT and clonogenic assays

The growth rate assay of selected cell lines was performed by seeding $3x10^4$ cells per well in triplicates and counting them every 2 days with Multisizer Coulter Counter (Beckman Coulter). After 16 days, a growth curve was generated and compared with control cell lines. MTT assay was performed to evaluate the metabolic activity of the tested cells. The clones and control cell lines were seeded at the density of 1500 cells per well in 96-well plate. Triplicates of each cell line were tested every other day for 16 days. Two hours after incubation with MTT compound (yellow), mitochondrial succinate dehydrogenase in metabolically active cells formed insoluble formazan crystals (purple), which were resolubilized with stop solution (10% SDS, 0.1% HCl). The amount of formazan crystals produced by the cells was proportional to metabolic activity (of living cells), which was measured by spectrometer at 570 nm wavelength. For colony forming (clonogenic) assay, 0.1 ml, 0.3 ml, and 1 ml of 10^3 cells per ml were seeded on 3.5-cm dishes in triplicates and were cultured in a humidified incubator with 5% CO_2 for 4 weeks as previously described with modifications [276]. RPMI-1640 medium with 20% FBS was changed every 3 days. After incubation, the cells were rinsed with cold PBS and fixed with PBS:Methanol (1:1 ratio) for 2 minutes, then incubated in Methanol for 10 minutes, and dried. 3 ml 1% Crystal violet was added to each dish for 10 minutes. The colonies were rinsed with H_2O and counted.

3.3.8. Cell cycle analysis

The cell cycle was determined after Propidium Iodide DNA staining followed by flow cytometry analysis. The cells were collected from an exponentially growing culture, washed with cold PBS and fixed in ice-cold ethanol. After 30 minutes of incubation at room temperature the cells were layered with bovine serum and

centrifuged for 5 minutes at 300xg to remove cellular debris. The cells were treated with RNase A (400 units/ml) for 30 minutes at 37° to eliminate the double-stranded RNA and stained with Propidium Iodide (50 µg/ml in 1.12% sodium citrate) for at least 30 minutes. The stained cells were detected by flow cytometer (BD FACSDiva, Beckman Coulter) and analyzed with FlowJo software.

3.3.9. Microarray and data analysis

Genome-wide expression profiles of OVCAR-3 and selected clones were compared to vector only transfected cell lines. Total RNAs were isolated with TRIzol reagent (Invitrogen), purified, labeled and used for microarray hybridization to human Affymetrix ST1.0 array at Einstein Genomic Facility. Data were analyzed using Expression Console (Affymetrix). Selected gene changes were confirmed using qRT-PCR. The results were normalized over the housekeeping gene GAPDH and compared with the controls. Cluster analysis was performed to group differentially expressed genes into subgroups according to their expression patterns (Cluster 1.0). A list of differentially expressed genes was further analyzed with Ingenuity IPA Software to determine the pathways or functional groups of genes involved.

3.3.10. High Performance Liquid Chromatography

Histone proteins were extracted using 0.2 N sulfuric acid as previously described [275]. 100 µg of total histone preparations were injected into a C18 reverse phase column (Vydac) on an AKTA UPC10 system (GE Healthcare). Fractions corresponding to the H1.2/H1.3/H1.4 peak from HPLC analysis were collected and subjected to mass spectrometry analysis on a Qstar XL MS/MS system (Applied Biosystems) with electrospray ionization (ESI) as the ionization method. Analyst QS software (Applied Biosystems) was used for data acquirement and analysis. Also, individual fractions were analyzed by Western blotting.

3.3.11. Chromatin Immunoprecipitation

ChIP assays were performed as previously described [73] with modifications. The following antibodies were used: anti-flag (Sigma, Cat. F1804), anti-CTCF (Santa Cruz, Cat. Sc15914), anti-H3 (Abcam, Cat. 1791) and anti-IgG (Millipore, Cat. 12-370). Briefly, cross-linked chromatin was sheared by sonication to DNA fragments ranged from 400 to 1,000 bp. Small portions of chromatin for each sample was aliquoted and stored for % Input. 20 µl of Dynabeads Protein G (Invitrogen) was incubated with 2 µg of antibody for 7 hours in 4°C. Dynabeads were washed three times with 1 ml PBS containing 0.5% BSA, then mixed with 50 µg of chromatin and left rotating overnight in 4°C. After incubation Dynabeads were washed five times with Washing Buffer (50 mM HEPES pH 7.6, 1 mM EDTA pH 8.0, 500 mM LiCl, 0.7% Sodium Deoxycholate, 1% NP-40) and once with PBS. Protein/DNA complexes were eluted in 100 µl Elution Buffer (50 mM Tris-Cl pH 8.0, 10 mM EDTA pH 8.0, 1% SDS) at 65°C for 20 minutes with agitation every 3 minutes, and incubated overnight at 65°C. DNA was purified with Qiagen DNA Isolation column (Qiagen). Lastly, the concentration of immunoprecipitated DNA was measured using Qubit Fluorometer (Invitrogen). The amount of each specific DNA fragment in immuno-precipitates was determined by real-time PCR. PCR reactions were prepared with the iQ SYBR Green Supermix (Bio-Rad) and were analyzed in a MyIQ Real-Time PCR Detection System (Bio-Rad). All samples were typically analyzed in triplicate in three independent experiments. The primers used to analyze H19 regulatory region and control primers are listed in Table A.2. All results were normalized over the % Input. The values from ChIP with control antibody (IgG) were typically less than 5% of the ChIP values.

3.3.12. Bisulfite treatment and DNA methylation analysis

Genomic DNA was isolated from cells with Qiamp DNA kit (Qiagen). 1 µg of DNA was treated with the pGenome DNA Modification kit (Millipore) according to the manufacturer's manual. Treated DNA was dissolved in 50 µl H_2O, and 1 µl of treated

DNA was used in each PCR reaction as previously described [73]. The primers used to generate PCR products from the bisulfite-converted DNA are listed in Table A.3. The PCR products were subsequently cloned using the TOPO TA cloning kit (Invitrogen), and clones containing the converted DNA inserts were selected for sequencing. DNA sequences were analyzed with BiQ analyzer.

3.4. Results

3.4.1. Determination and analysis of individual H1 variants in OVCAR-3 cells

OVCAR-3 cell line is a well-characterized epithelial ovarian cancer cell line frequently used to study molecular mechanisms of ovarian cancer malignancies. This cell line was derived from a patient with epithelial ovarian adenocarcinoma, which represents more than 90% of all ovarian cancer malignancies. We characterized the expression of individual histone H1 variants by combining HPLC, Mass Spectrometry and Western blotting methods (Figures 3.1 and 3.2).

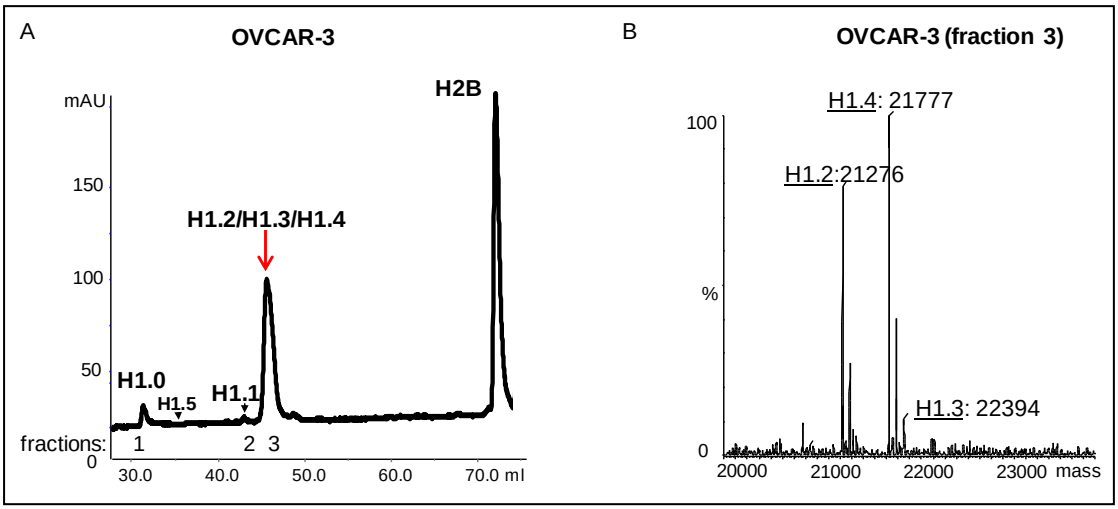

Figure 3.1: Expression of histone H1 subtypes in OVCAR-3 cell line. A: RP-HPLC of histone proteins. B: Mass spectrometry of fraction indicated with red arrow in (A).

Total histones were isolated from OVCAR-3 cells by sulfuric acid extraction and subjected to RP-HPLC. Increasing gradiant of Acetonitrile/0.1% TFA allows linker

histone H1 variants separation according to their hydrophobic/hydrophilic properties (Figure 3.1A). Three fractions of putative H1 subtypes were collected, lyophilized and analyzed by Mass spectrometry.

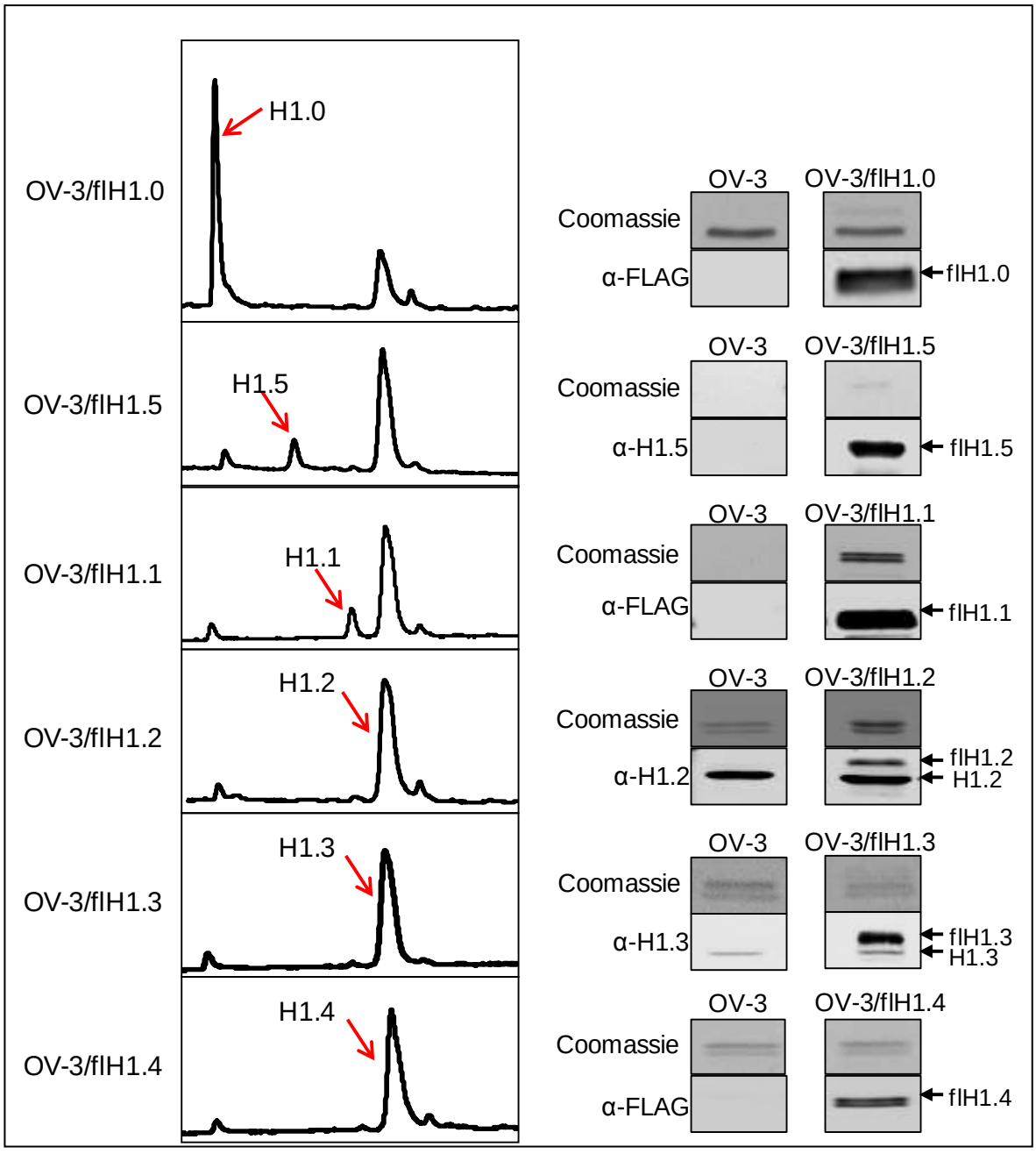

Figure 3.2: Characterization of peaks eluted from HPLC of histones extracted from OVCAR-3/H1 clones. Histone extracts from stable clones with over-expressed H1 subtypes were analyzed by HPLC (left). Individual peaks were collected and analyzed by Coomassie and Western blotting using indicated antibodies. Red arrows indicate the fractions collected for Western blotting analysis.

The fraction 3 was identified as a mixture of histones H1.2, H1.3 and H1.4 (Figure 3.1B). Since histone H1.3 is ubiquitously expressed among different cell types and we found mRNA transcripts present at high levels in OVCAR-3 (data not shown), we expected that its protein levels would be comparable to the other subtypes. Surprisingly, its amount occurred to be much lower that H1.2 and H1.4 (Figure 3.1B). To verify the identity of individual peaks of the HPLC fractions, we generated the cell clones with over-expressed N-terminally flagged histone H1 subtypes. The total histones were extracted and analyzed by HPLC and the eluted fractions were collected and verified by Western blotting (Figure 3.2). These results demonstrate the peak identity and the relative amount of each linker histone variant in HPLC profile from OVCAR-3/H1 cell lines.

3.4.2. Over-expression of histone H1.3 inhibits cell growth and colony formation

Histone H1.3 is a one of the major somatic H1 variants that is abundantly expressed in tissues as well as in both dividing and non-dividing cells, and play an important role in chromatin folding. However, its specific role in gene regulation and cellular functions remain elusive and it has often been omitted in cancer related studies despite its abundance. Surprisingly, compared with other somatic H1 variants, H1.3 protein level is particularly low in OVCAR-3 despite high levels of mRNA transcripts, suggesting that the endogeneous H1.3 is translationally inhibited in OVCAR-3 cells. The low expression of endogeneous H1.3 in OVCAR-3 cells provides a good experimental system for us to investigate the role of H1.3 in ovarian cancer cells using an over-expression approach.

Stable clones over-expressing FLAG-H1.3 were generated by transfecting pcDNA-H1.3 construct into OVCAR-3 cell line (Figure 3.3A). 48 clones resistant to G418 selection were selected and screened using an anti-FLAG antibody (Figure

3.3B). The clone with the highest FLAG-H1.3 levels (designated as OVCAR-3/H1.3(H)) was used for further characterization.

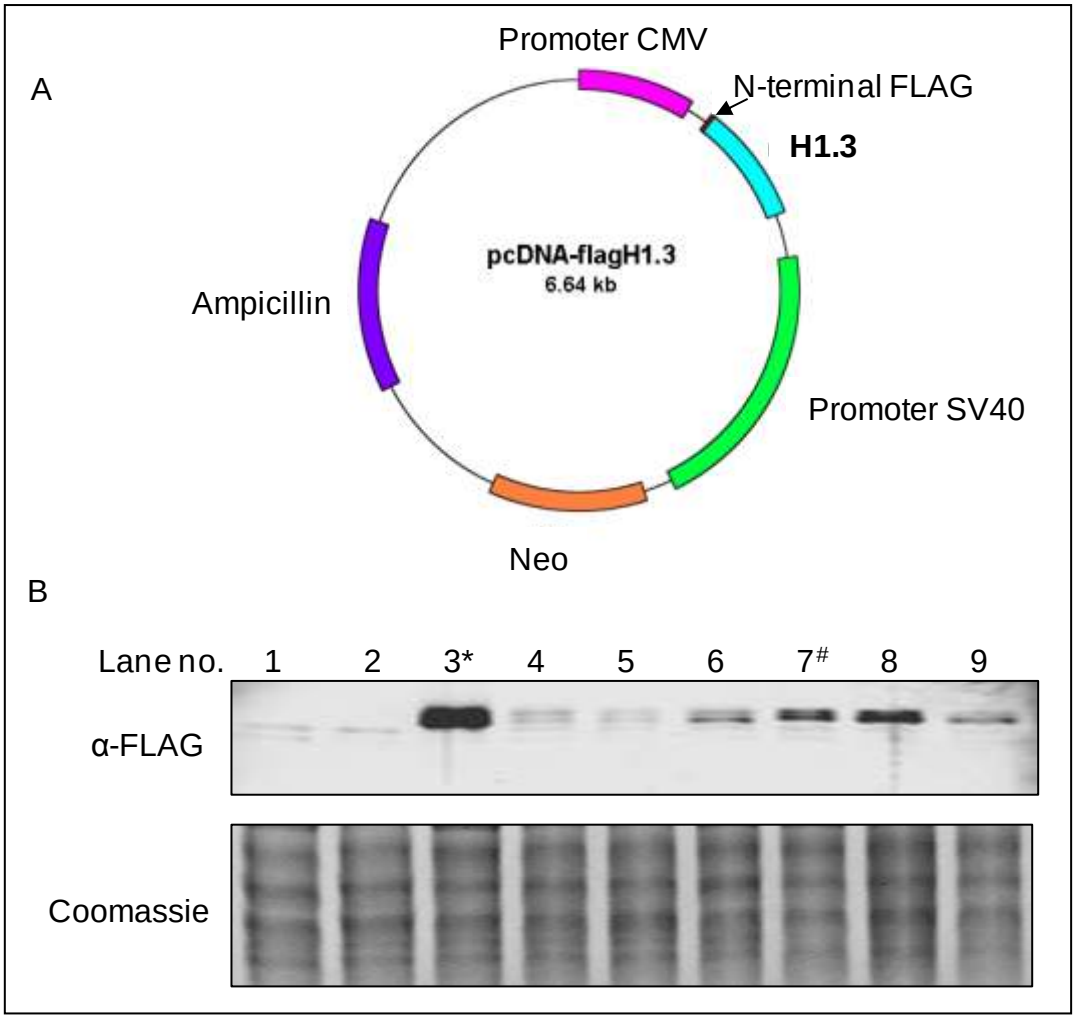

Figure 3.3: Generation of OVCAR-3/H1.3 clones. A: Vector containing N-terminally FLAG tagged H1.3 subtype. B: Western blotting of H1.3 over-expressed clones. OVCAR-3 cells were transfected with a pcDNA-FLAGH1.3 construct, G418 resistant clones were picked and analyzed by Western blotting using an anti-FLAG antibody. Coomassie staining shows equal loading of cell lysates. Lane 1: OVCAR-3; Lane 2: OVCAR-3 transfected with pcDNA3 vector (designated as OV-3/vector only); Lane 3-9: OVCAR-3/FLAGH1.3 clones. A clone (lane 3, marked with an asterisk) with the highest expression of FLAG-H1.3 was used for further investigation and A low expressing clone denoted with number sign was used in microarray analysis.

To determine the effects of over-expression of FLAGH1.3 on the expression of other H1 variants, HPLC and Western blotting were performed on OV-3/H1.3(H) clone as described above. The results indicated that FLAG-H1.3 co-eluded in the same fraction as the endogenous protein, proving that the biochemical properties of exogenous H1.3 does not differ from the endogeneous H1.3. The antibody against

H1.3 detected a strong band of FLAG-H1.3 in fraction 3 of the OV-3/H1.3(H) sample, indicating that the amount of FLAGH1.3 is several fold higher compared with the endogenous H1.3 (Figure 3.4A, D). However, quantitation of H1 to nucleosome ratio from the HPLC profile indicates that the total H1 levels are comparable in OV-3/H1.3(H) clones and OVCAR-3 cells (Figure 3.4B). The presence of FLAGH1.3 protein (23.2 kDa) in fraction 3 eluted from HPLC was further confirmed using Mass Spectrometry (Figure 3B). Interestingly, the protein levels of H1.0, H1.2 and H1.4 protein are all reduced to certain extent (Figure 3.4C,D, E) by calculation of individual H1 to nucleosome ratio from HPLC analysis (Figure 3.4C) and Western blotting using total histone extracts (Figure 3.4E). This phenomenon is reminiscent of H1 compensatory regulation that occurs during subtypes expression alterations by H1 subtype knockout [80,226,227].

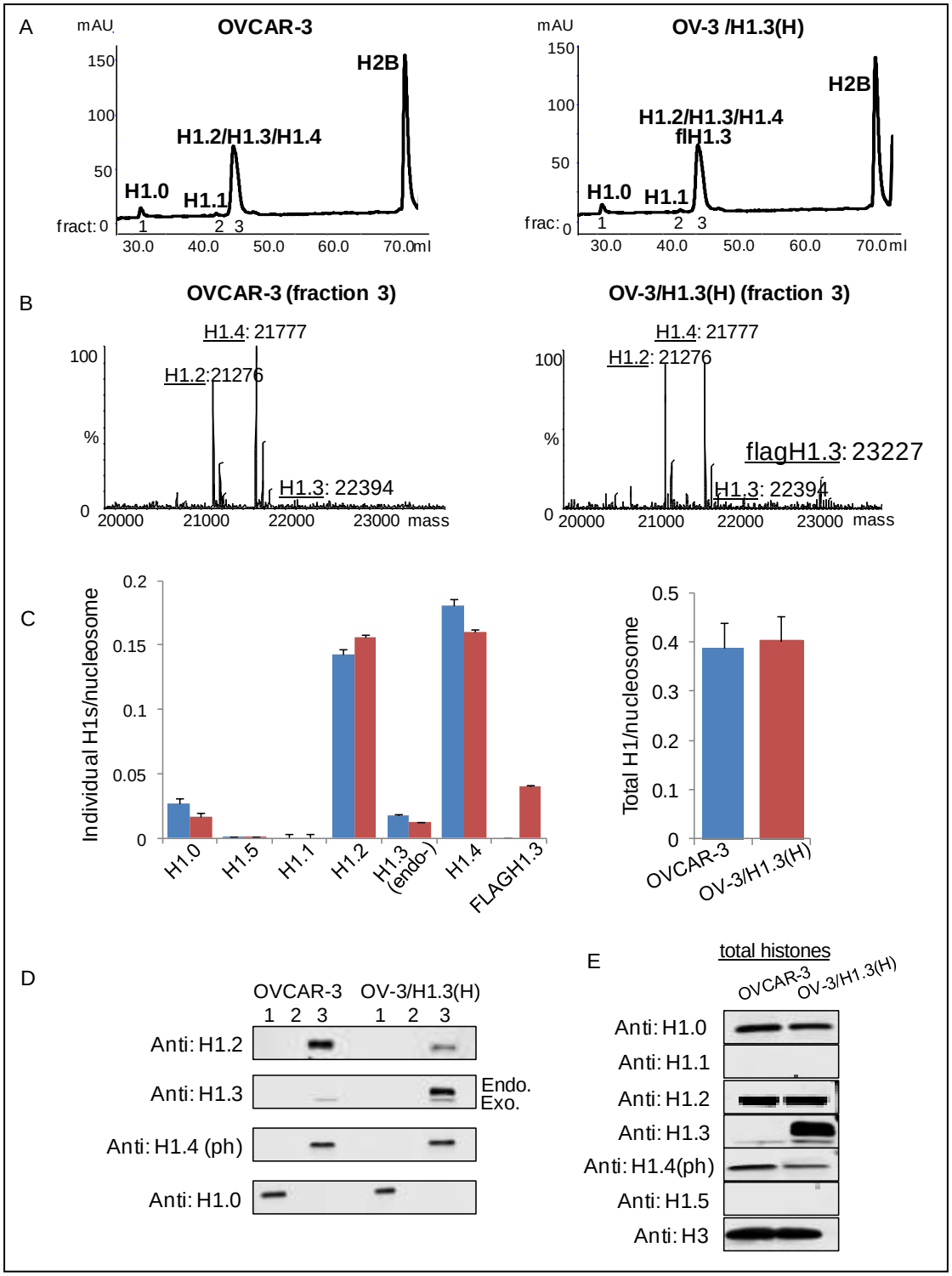

Figure 3.4. Over-expression of histone H1.3 modulates the amount of other linker histone subtypes in OV-3/H1.3(H). A: HPLC profile of linker histone H1 subtypes in OVCAR-3 and OV-3/H1.3(H) cells. B: Mass spectrometry profiles of fraction 3 obtained from HPLC of OVCAR-3 and OV-3/H1.3(H) cells. C: Calculation of individual H1 subtype per nucleosome as well as total H1s per nucleosome in OV-3/H1.3(H) and OVCAR-3 based on HPLC results. H1 to nucleosome is determined by the ratio of A214 values of individual H1 subtype to that of half of the H2B peak. Results were obtained from 3 independent experiments. D: The presence of histone H1 subtypes in fractions 1, 2, and 3 determined by Western blotting. 4. FLAGH1.3 co-elutes in the same fraction 3 as the endogenous H1.3 protein. E: The comparison of individual H1 subtypes in OV-3/H1.3(H) and OVCAR-3 by Western blotting.

To characterize the phenotypic changes by H1.3 over-expression, we compared the growth rate, metabolic activity, colony forming abilities and cell cycle profiles of OVCAR-3 and OV-3/H1.3(H). OV-3/H1.3(H) cells displayed reduced growth rate by growth curve and MTT assays (Figure 3.5). Cell cycle analysis indicated that OV-3/H1.3(H) cells have a higher population of G1 than OVCAR-3 cells as well as a lower percent of S phase cells compared with OVCAR-3 cells (Figure 3.6). These results indicate that over-expression of H1.3 subtype reduces cell proliferation and affects the metabolic activity in OVCAR-3 (Figure 3.5A and 3.5B).

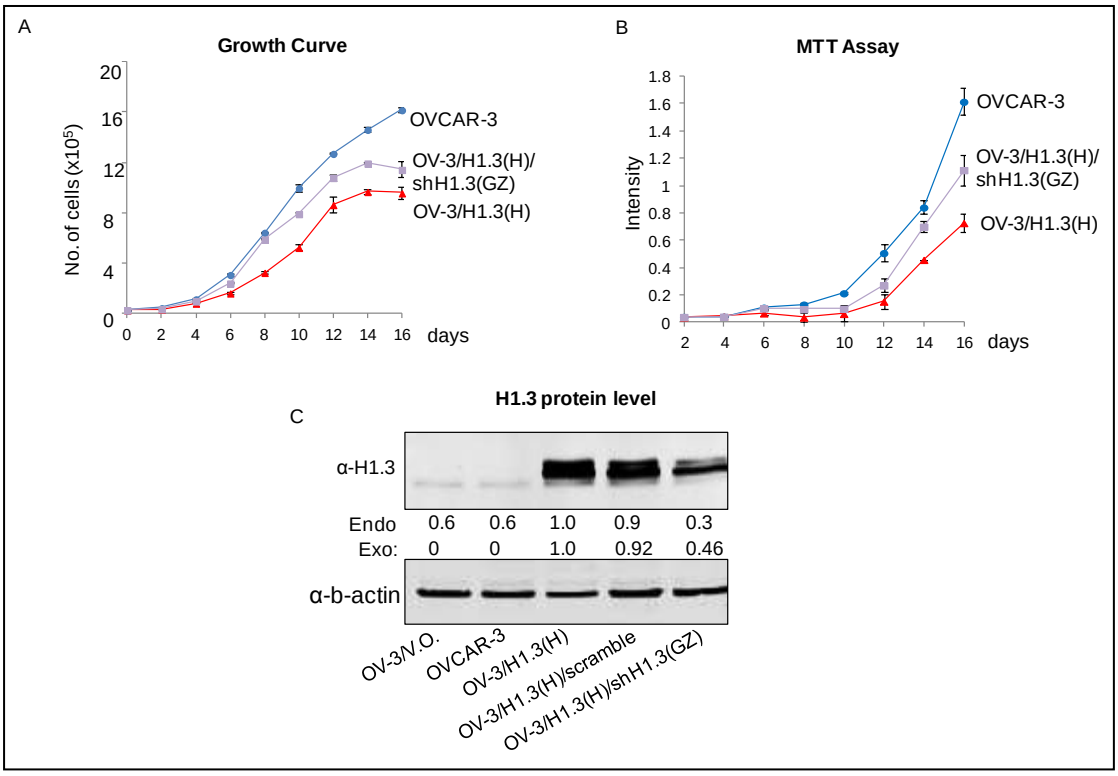

Figure 3.5: Histone H1.3 over-expression alters the growth rate in OVCAR-3 cell line. Analysis of A) growth rate, B) metabolic activity (MTT) and C) expression levels of H1.3 of OVCAR-3, OV-3/H1.3(H) and, OV-3/H1.3(H)/shH1.3(GZ) cell lines. p values: * < 0.05, **<0.01, ***<0.001.

To exclude the possibility that the inhibitory effects on cell proliferation in OV-3/H1.3(H) is due to clonal variation, OV-3/H1.3(H) cells were infected with a vector expressing shH1.3 to knockdown H1.3 levels in OV-3/H1.3(H) cells. H1.3 levels was knocked down more than 50% when OV-3/H1.3(H)/shH1.3(GZ) cells were compared

with OV-3/H1.3(H) cells (Figure 3.5C). The reduced growth rate in OV-3/H1.3(H) cells was alleviated in OV-3/H1.3(H)/shH1.3(GZ) cells (Figure 3.5A,B).

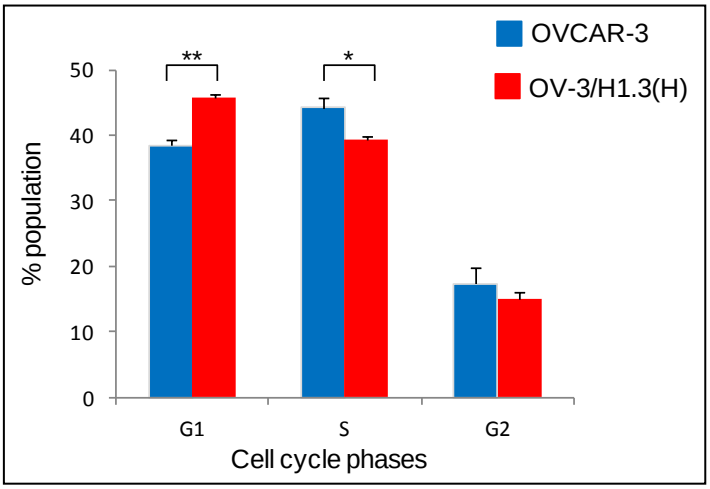

Figure 3.6: Cell cycle analysis of OVCAR-3 and OV-3/H1.3(H) cells. The cells were stained with Propidium Iodide and analyzed with flow cytometry. p values: * < 0.05, **<0.01.

We next examined the clonogenic capacity of these cells and found that OV-3/H1.3(H) clone formed between 10 to 15 times less colonies than OVCAR-3 cells, suggesting that increased levels of histone H1.3 impairs clonogenic abilities in OVCAR-3 cells (Figure 3.7). This inhibitory effect is partially abolished by H1.3 knockdown in OV-3/H1.3(H)/shH1.3(GZ) cells (Figure 3.7).

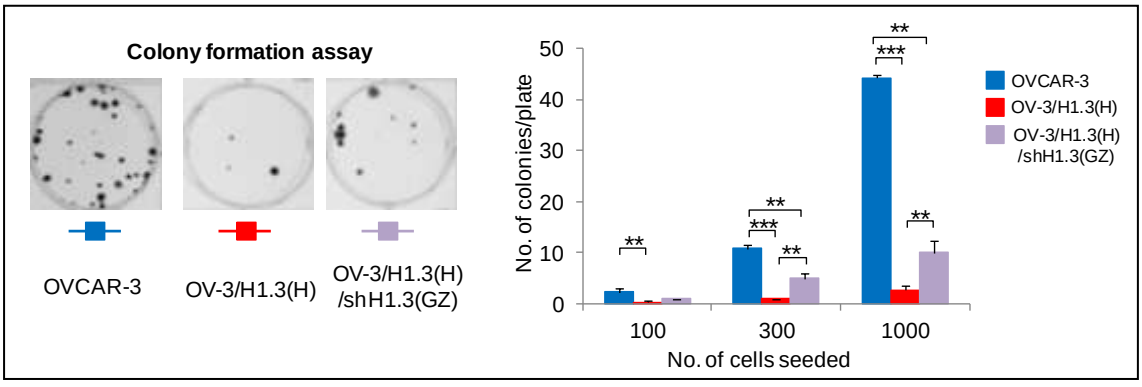

Figure 3.7: Histone H1.3 over-expression inhibits colony formation. A: Representative results of colony formation assay. B: The quantitation of colonies formed 4 weeks post seeding (in triplicates). p values: * <0.05, **<0.01, ***<0.001.

3.4.3. Over-expression of H1.3 leads to specific changes in gene expression

To identify genes and pathways affected by H1.3 subtype over-expression, we performed Affymetrix Human Gene 1.0 ST Array (Affymetrix, Santa Clara, CA) at Einstein Genomic Core Facility. We compared the genome-wide transcriptomes of OV-3/H1.3(H), OV-3/H1.3(L), OVCAR-3/V.O. and OVCAR-3 cell lines (Figure 3.8A & B). Two biological repeats were performed for each cell line and data were normalized over that from OVCAR-3/V.O. cells. Genes showing consistent changes of 2-fold or more were selected for cluster analysis (Cluster 3.0) (Figure 3.8). Among genes with significant expression changes, 76 were upregulated and 88 were downregulated genes in OV-3/H1.3(H) cells compared with OVCAR-3 cells. To confirm the results of microarray, several differently expressed genes were analyzed by RT-PCR (Figure 3.9), and all of them showed expression changes comparable to that from array analysis.

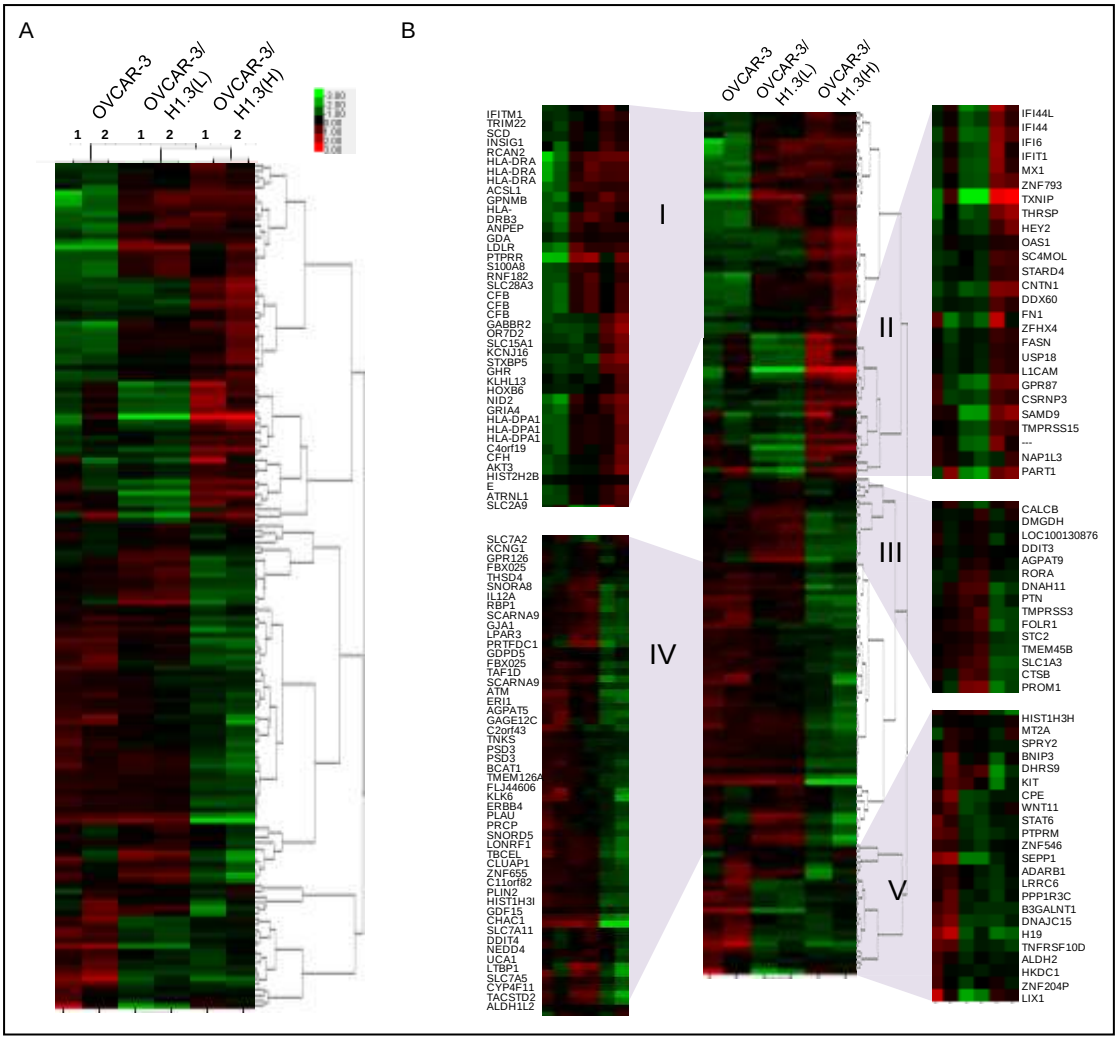

Figure 3.8: Comparison of global gene changes in OV/H1.3 and OVCAR-3 cells by microarray analysis. A: Genes with more than 2-fold expression difference were selected for analysis. The duplicates of OVCAR-3, OV-3/H1.3(H) and OV-3/H1.3(L) results were normalized over OV-3/V.O. and clustered by Cluster 1.0 software. B: Cluster of gene changes divided on subgroups with different expression patterns with adjacent gene list. Genes altered only in OV-3/H1.3(H) are shown in group II and IV, genes altered in both clones – group I and V, and genes altered only in OV-3/H1.3(L) – group III.

According to microarray, GJA1, RBP1 and Il12A genes were downregulated, whereas GDA, GHR and PTPRR genes had increased expression in OV-3/H1.3(H) in comparison to control cell lines. CTCF gene which expression did not alter in OV-3/H1.3(H), served as negative control (data not shown). Similar expression results were obtained by RT-PCR analysis (Figure 3.9).

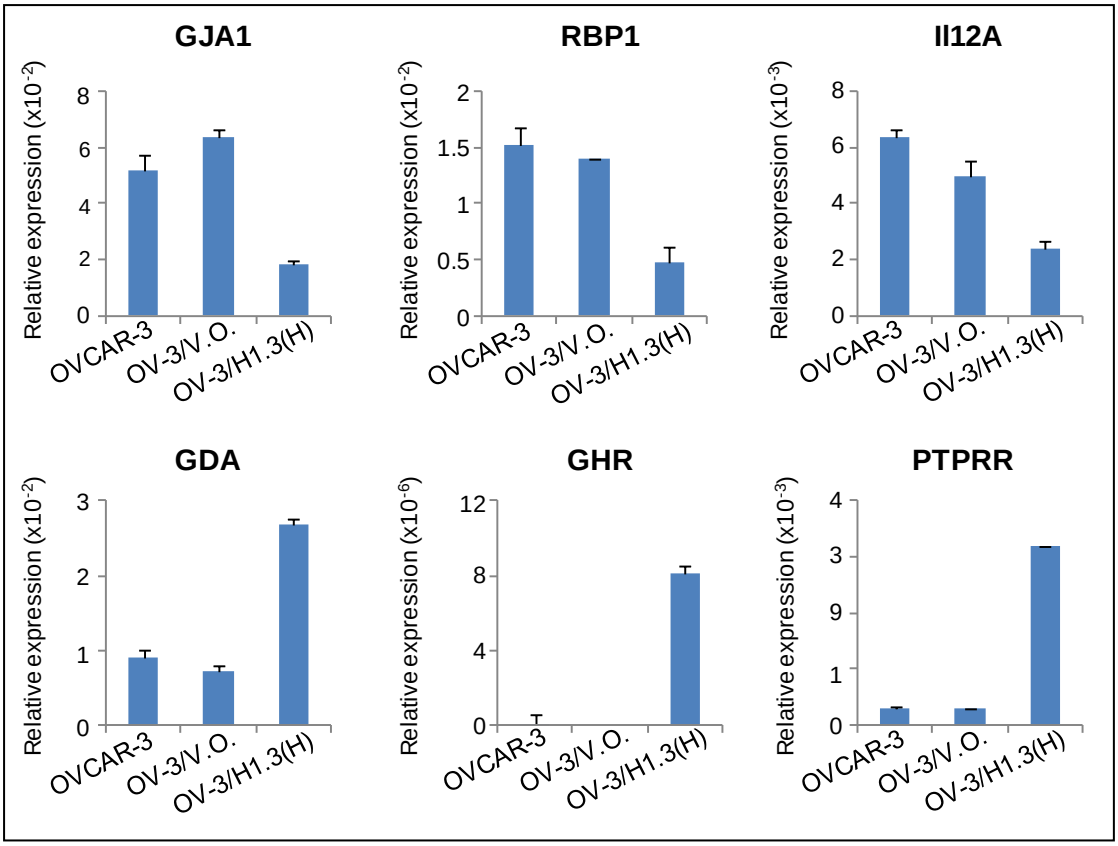

Figure 3.9: RT-PCR analysis of indicated genes in OVCAR-3 cells. Upper panels show representative genes downregulated in OV-3/H1.3(H), lower panels are three representative genes upregulated in OV-3/H1.3(H). Bar: SD.

H19 was found to be one of the genes most dramatically disregulated in OV-3/H1.3(H) cells. H19 expression was also significantly suppressed in OV-3/H1.3(L) clone which suggested that H19 gene is a target of linker histone H1.3. Analysis of the molecular pathways and cellular processes altered in OV-3/H1.3(H) cells using IPA software indicate that cell proliferation, cell adhesion, programmed cell death, cell migration and immune response were all affected. An representatitive IPA hit map including H19 gene is shown in Figure 3.10.

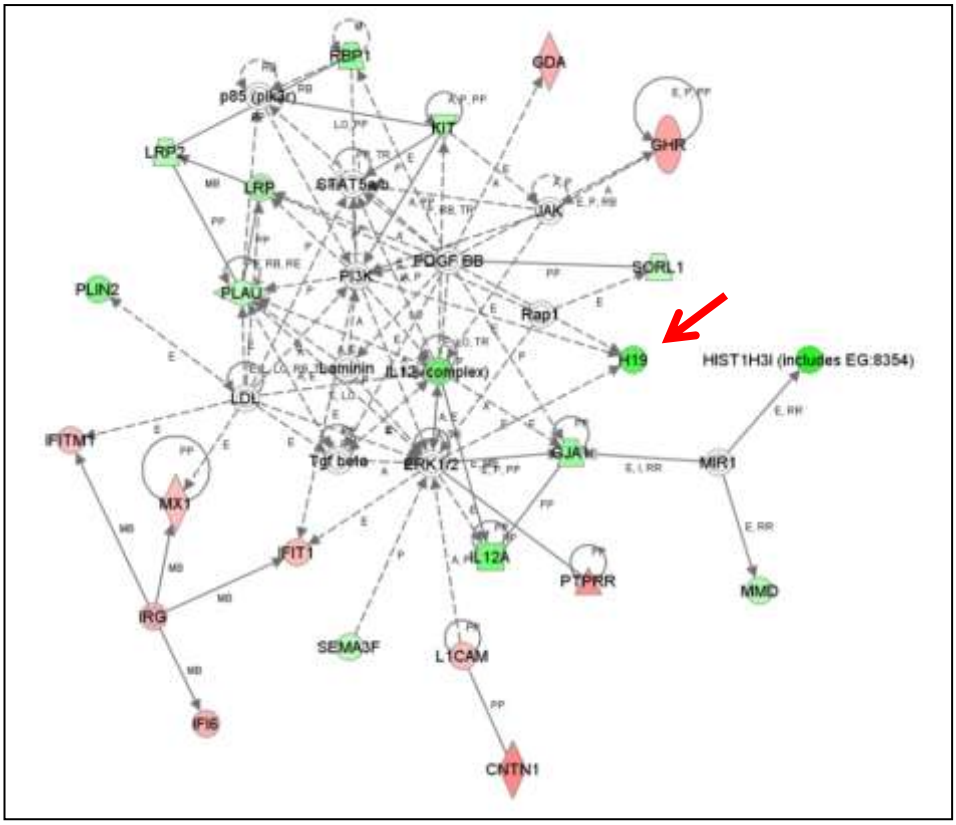

Figure 3.10: A selected hit map with genes altered in OV-3/H1.3(H) clone. H19 marked as a gene of interest.

3.4.4. Oncogene H19 is a direct target of H1.3 in OVCAR-3 cells.

The finding that H19 is down-regulated in OV-3/H1.3(H) cells combined with previous report that H19 is upregulated in H1.2/H1.3/H1.4 triple knockout mouse embryonic stem cells, prompted us to investigate if the regulation of H19 expression is specifically affected by H1.3 or other H1 subtypes. To investigate this, we utilized the stable OVCAR-3/H1 cell lines over-expressing one of the six somatic H1 subtypes (H1.0 - H1.5) as shown in Figure 3.2. The expression levels of exogenous FLAG-H1 were measured by Western blotting with an anti-FLAG antibody. While all of the OV-3/H1 cell lines exhibit comparable signals of exogenous FLAG-H1 for each individual H1 variant (Figure 3.11), H19 transcript level was only dramatically suppressed in OV-3/H1.3(H) line as measured by RT-PCR (Figure 3.12), suggesting that H19 is specifically repressed by H1.3 subtype in OVCAR-3 cells.

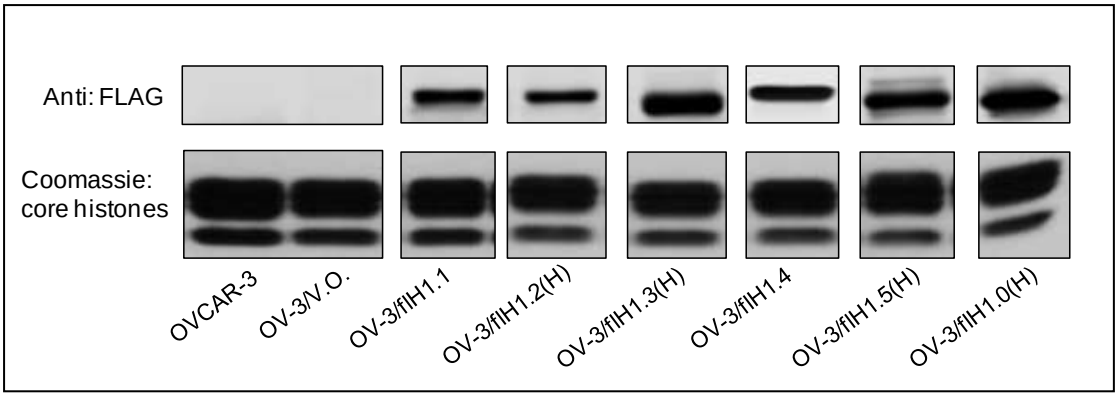

Figure 3.11: OV-3/H1 clones of each individual H1 variant express comparable levels of FLAG-H1 variants. 15 µg of total histone extracts were analyzed by Western blotting with an anti-FLAG antibody. Coomassie staining of core histones serves as loading control. OV-3/V.O.: OVCAR-3 cells transfected with pcDNA vector without inserted H1 genes.

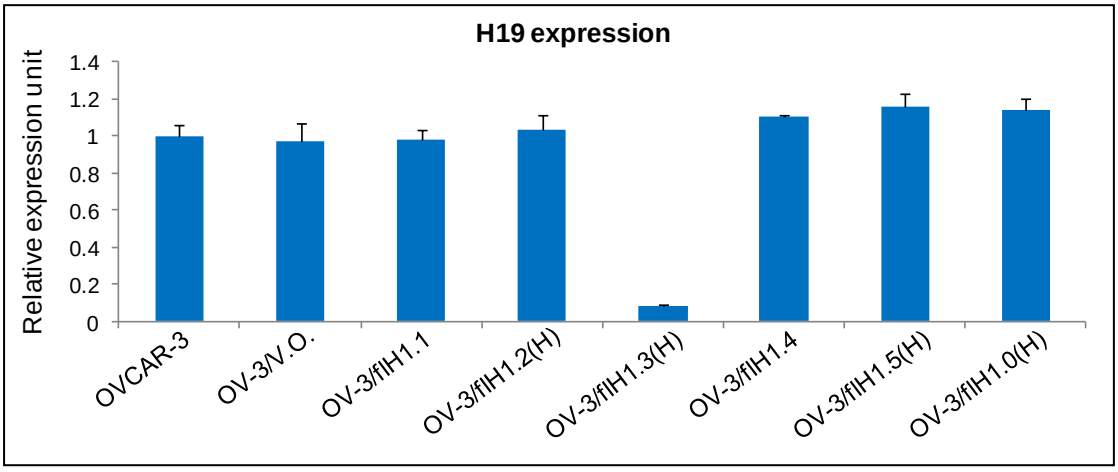

Figure 3.12: Relative expression of the H19 mRNA transcript level in each stable clone measured by RT-PCR. H19 expresion was normalized over GAPDH. Bar: SD

H19 is a precursor for miR-675 [267,268,277]. To determine if the repression of H1.3 on H19 expression also leads to reduction in miR-675 expression, we extracted low molecular weight enriched RNA from OVCAR-3, OV-3/V.O. and OV-3/H1.3(H) cells and analyzed miR-675 expression. RT-PCR results indicated that the relative amount of miR-675 is drastically suppressed in OV-3/H1.3(H) when compared with control cell lines (Figure 3.13), suggesting that over-expression of histone H1.3 also causes down-regulation of miR-675. Thus, in addition to H19, H1.3 may also control H19-dependent gene regulation, such as miR-675 targeted genes.

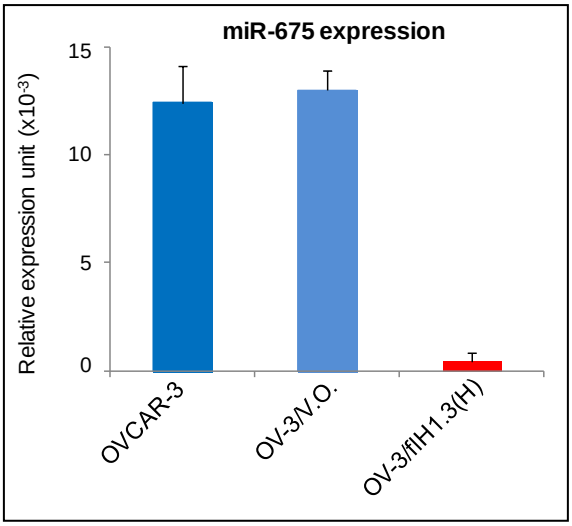

Figure 3.13: miR-675 is downregulated in OV-3/H1.3(H) cells. microRNAs were extracted from cells and relative expression of miR-675 was measured by RT-PCR. Bar:SD.

To further test if the expression of H19 is directly dependent on the amount of histone H1.3 in cells, we generated OV-3/shH1.3(TZ) cell line in which the expression of endogenous H1.3 level in OVCAR-3 cells can be knocked down under the induction by doxycycline to induce the expression of shRNA against H1.3 in a pTRIPZ vector.

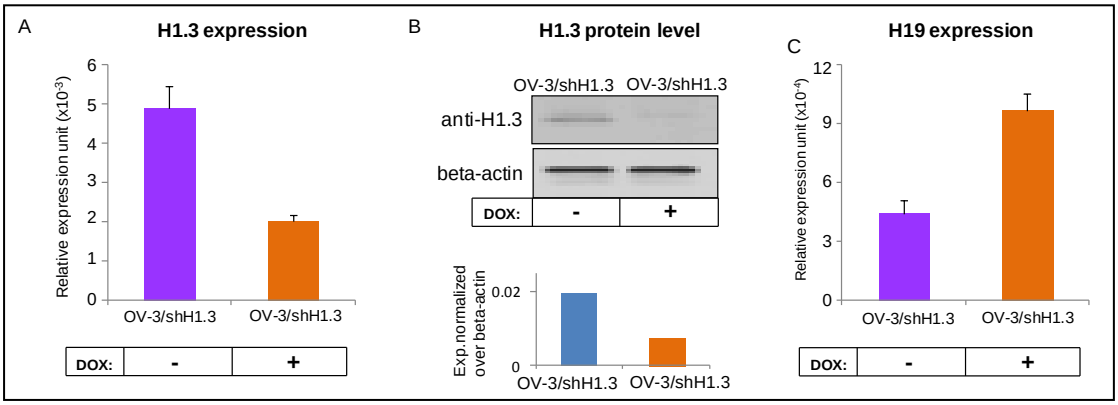

Figure 3.14: H19 expression is elevated by endogenous H1.3 knockdown in OVCAR-3 cells. A: The expression level of H1.3 in OV-3/shH1.3(TZ) cells 10 days post 1 μg/ml Doxycycline treatment. B: Protein level of histone H1.3 in OV-3/shH1.3(TZ) 10 days after Dox treament. C: The effect of H1.3 knockdown on H19 expression in OV-3/shH1.3(TZ)+Dox (10 days).

The efficiency of shH1.3 knockdown was determined using RT-PCR and Western blotting (Figure 3.14A & B). H1.3 knockdown by shRNA results in a 81% reduction of the endogenous H1.3 mRNA levels and a 60% reduction in protein levels. This

knockdown led to a 50% elevation in H19 mRNA transcript. Similarly, knockdown histone H1.3 level in OV-3/H1.3(H) cells using stable expression of shRNA against H1.3 (Figure 3.5C) led to an upregulation of H19 transcript (Figure 3.15).

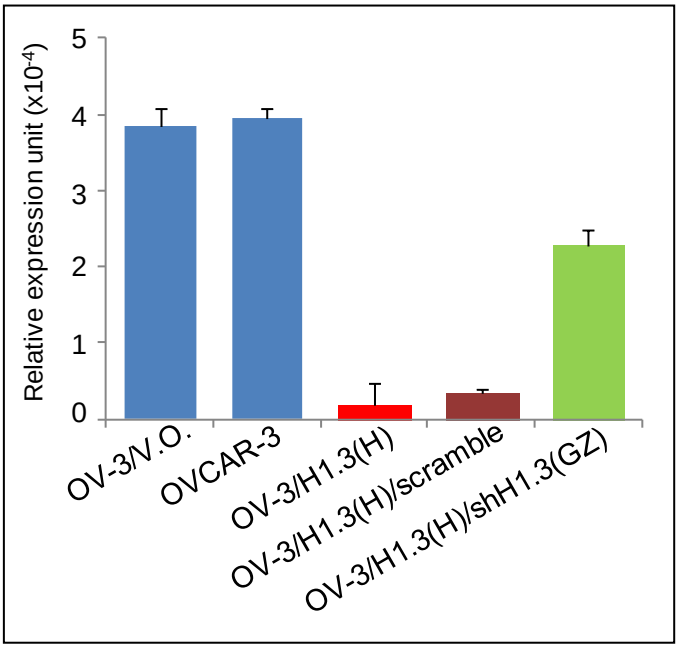

Figure 3.15: H1.3 knockdown in OV-3/H1.3(H) cells abolishes the repression effects of H1.3 on OVCAR-3 cells. H19 expression was measured by RT-PCR. Bar: SD.

3.4.5. Epigenetic mechanisms of H19 repression mediated by H1.3

Chromatin structure and epigenetic mechanisms play a key role in H19 expression regulation [278]. Aforementioned findings suggest that, among somatic H1 variants, H1.3 is the specific variant that represses H19 expression in OVCAR-3 cells. To investigate the potential mechanisms by which H1.3 regulates H19 expression in OVCAR-3 cells, we first set out to determine the binding profiles of H1.3 across entire H19 gene locus, including 5.2 kb upstream regulatory region, by Chromatin Immunoprecipitation.

Soluble chromatin from OV-3/H1.3(H), OV-3/H1.3(L) and OVCAR-3 cells were Immunoprecipitated using an anti-FLAG antibody (Sigma) and immunoprecipitated DNA was analyzed by quantitative real-time PCR to determine the enriched sequences occupied by H1.3 protein. The results showed that histone H1.3 occupies

the entire H19 upstream regulatory region with 3-5-fold higher signals than that in OV-3/H1.3(L) cells (Figure 3.16). These results indicate that H1.3 over-expression results in preferential accumulation of H1.3 at H19 regulatory regions.

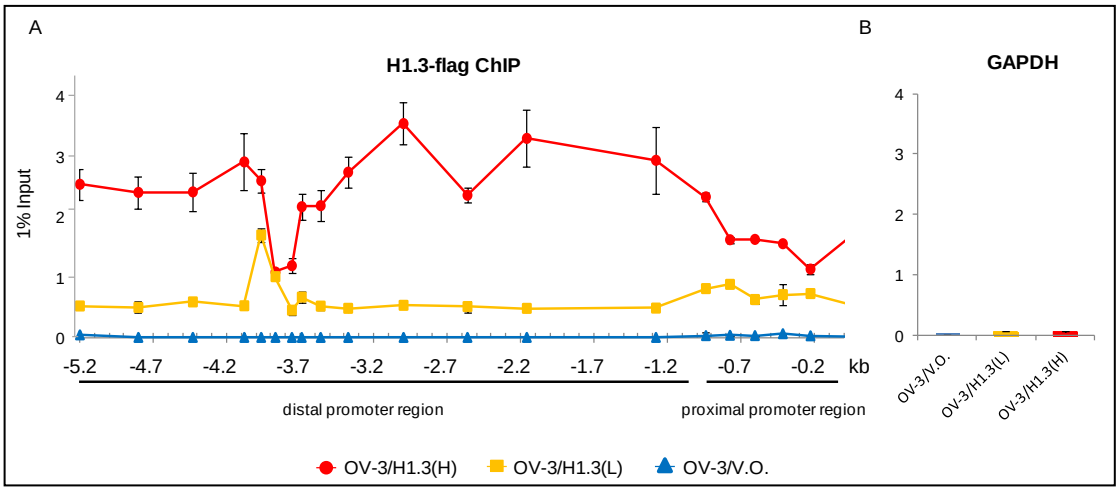

Figure 3.16: H1.3 over-expression preferentially increases H1.3 occupancy at H19 regulatory region. A: The occupancy of H1.3 was analyzed on distal and proximal promoter region. B: Control region - GAPDH promoter region, contains no H1.3. Bar: SD.

H19 expression is controlled by the imprinting control region (ICR) located within the H19 upstream regulatory region. In humans, this region also contains 7 CTCF binding sites, of which methylation status dictates accessibility for the CTCF isolator [279,280]. Previous studies have shown that DNA methylation at ICR region represses the expression of H19 with higher DNA methylation leads to reduced expression of H19. To determine if increased H1.3 binding at H19 ICR leads to changes in DNA methylation at H19 ICR, we picked two regions of highest increase in H1.3 binding (marked as region 1 (R1) and region 2 (R2)) as well as a region without dramatic H1.3 accumulation (R3) for analysis of DNA methylation by bisulfite sequencing.

As determined previously using quantitative bisulfite restriction analysis (QUBRA) [281] and confirmed by bisulfite sequencing in our experiment, H19-ICR region is hypomethylated in OVCAR-3 (Figure 3.17). Compared with OVCAR-3 cells, DNA

methylation of CpG sites surrounding CTCF binding sites R1 and R2 in OV-3/H1.3(H) cells are significantly increased by 2.3- and 5.8-times, respectively, whereas H19 proximal promoter (R3) remain hypermethylated in both OVCAR-3 and OV-3/H1.3(H) cells (Figure 3.17). Analysis of DNA methylation status of the rescue cell line OV-3/H1.3(H)/shH1.3 indicated a reduction of methylation in R1 and R2, but not in R3. These results indicate that increased occupancy of H1.3 at H19 distal promoter region leads to hypermethylation of the H19-ICR.

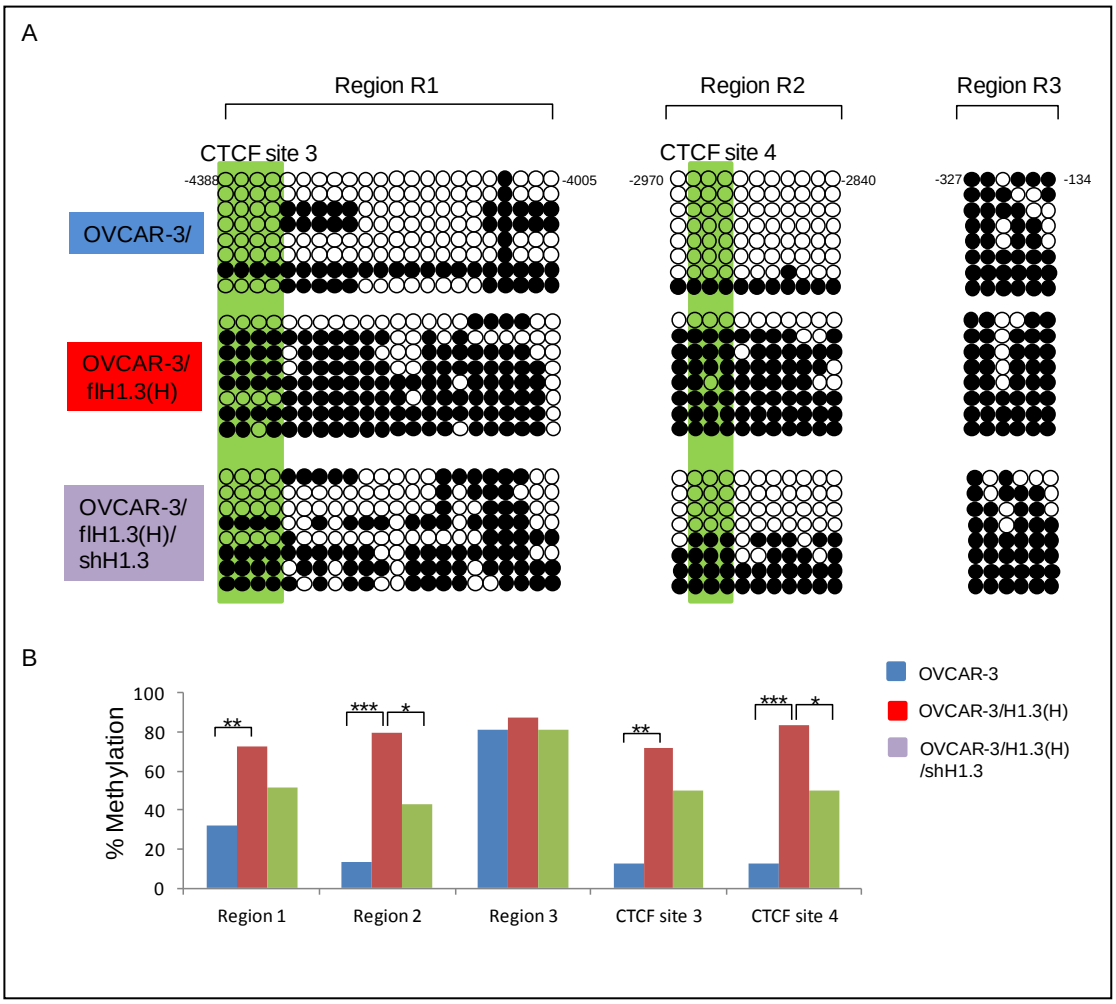

Figure 3.17: Increased H1.3 leads to higher DNA methylation at H19 regulatory regions. A: Methylation analysis was performed on CTCF (Region R1 and R2) and H19 proximal promoter region (Region R3). B: Calculations of percent methylation in analyzed regions and CTCF binding sites. ● CG methylated, ○ CG unmethylated. p values: **<0.01, ***<0.001.

It was previously documented that the methylation of CTCF binding sites in H19-ICR prevents CTCF binding [280]. CTCF ChIP results showed that CTCF occupancy

at H19-ICR is reduced in OV-3/H1.3(H) cells compared with that in OVCAR-3 (R1 and R2) cells. The c-myc site containing well-established CTCF binding sites is included as a positive control site, the c-myc gene body site was analyzed as a negative control site (Figure 3.18). The reduced occupancy of CTCF protein on H19-ICR in OV-3/H1.3(H) cells suggests that over-expression of histone H1.3 may prevent CTCF from binding to the H19 ICR region and regulating H19 expression in OVCAR-3 cells.

Taken together, these findings indicate that linker histone H1.3 directly regulates H19 expression in ovarian cancer cells by binding to H19-ICR, increasing DNA methylation and preventing CTCF from binding to CTCF sites in H19 ICR.

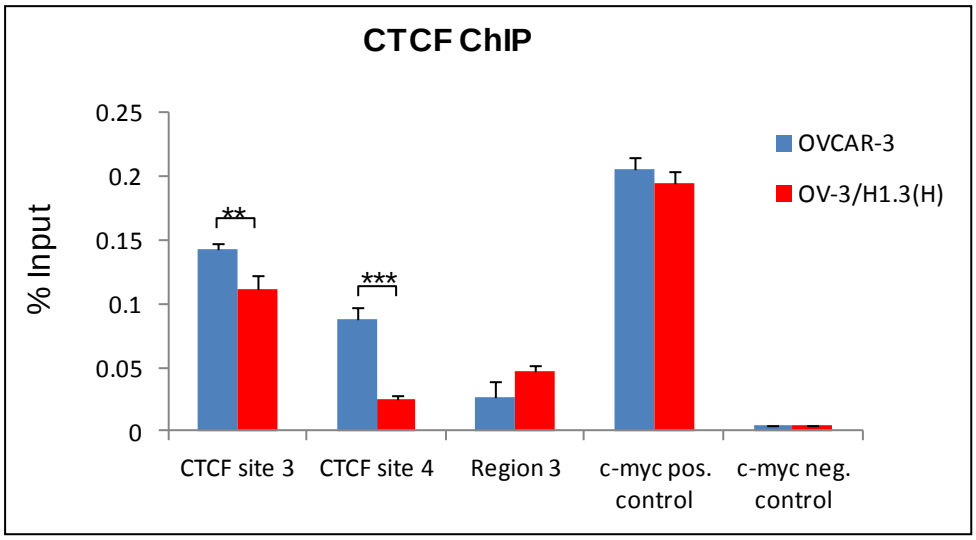

Figure 3.18: CTCF is partially depleted from H19-ICR in OV-3/H1.3(H).

3.4.6. Over-expression of histone H1.3 and reduction of H19 synergistically suppresses ovarian cancer cell growth

Previously, it was demonstrated that the expression of H19 mRNA promotes proliferation and enhances tumorigenesis in cancer cells [282-285]. To determine if the inhibitory effect of H1.3 on OVCAR-3 growth rate is mediated through its regulation on H19 expression, we first investigated the effects of modulation of H19 expression on OVCAR-3 growth.

Over-expressing H19 transcript in OVCAR-3 by transfecting the cells with a pcDNA-H19 vector (schematic diagram Figure 3.20A) increased H19 transcripts 20-fold in comparison with untransfected cells. This upregulation resulted in significant increase in cell growth rate when compared with non-transfected OVCAR-3 cells (Figure 3.20A & B). OV-3/H1.3(H)/H19 cell line in which H19 is over-expressed in OV-3/H1.3(H) cells will be generated to test if increase in H19 transcript can "rescue" the growth inhibitory effects by H1.3 over-expression. These experiments indicated that upregulation of H19 increases the growth rate of ovarian cancer cells.

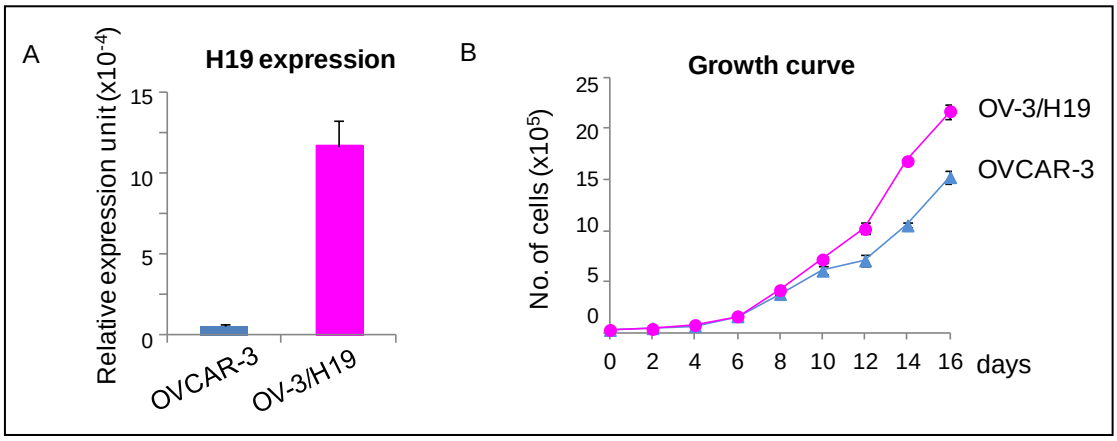

Figure 3.19: Over-expression of H19 transcript in OVCAR-3 cells leads to increased growth rate. A: RT-PCR analysis of H19 expression. H19 expression was normalized over GAPDH. B: Growth curves of OV-3/H19 and OVCAR-3 cells. Medium was supplemented with 1 µg/ml Doxycycline throughout the whole experiment Bar: SD.

In order to determine whether simultaneous over-expression of H1.3 and depletion of H19 would synergistically impair the growth of ovarian cancer cells, we established an OV-3/H1.3(H) cell line with knocked down H19 transcript by utilizing the commercially available pTRIPz lentiviral inducible system (schematic diagram Figure 3.20A). The induction effect by Dox can be visualized by RFP expression (Figure 3.20B). The generated stable cell line showed a 75% reduction in H19 expression at eight days post-induction in OVCAR-3 cells (Figure 3.20C) and 92% reduction in OV3/H1.3(H) cells (Figure 3.21A). Growth curve analysis of OVCAR-3/shH19 and OVCAR-3 cell lines indicated that depletion of H19 significantly reduced

growth rate in ovarian cancer cells after induction of shH19 by Doxycycline (Figure 3.20D & 3.21B).

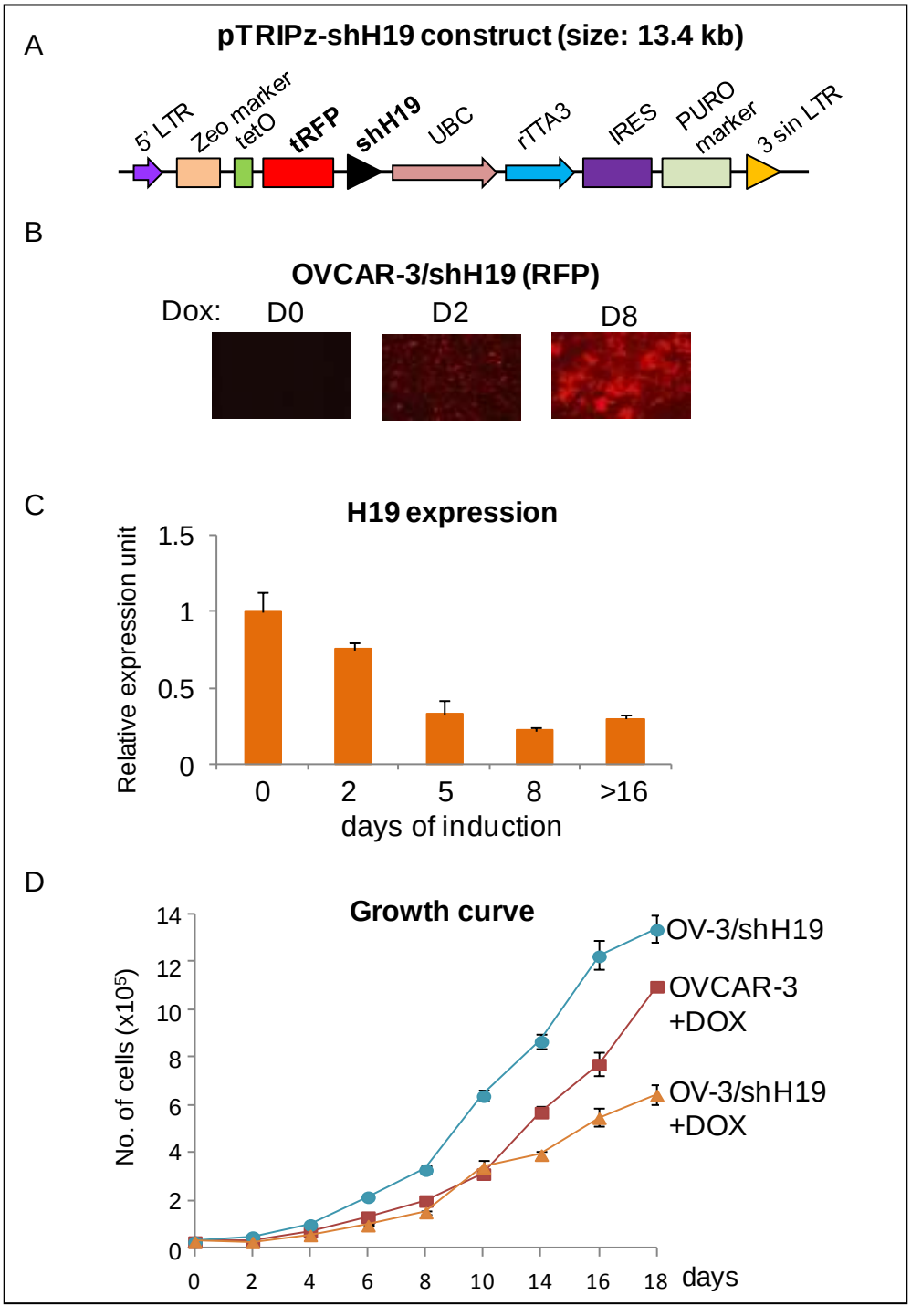

Figure 3.20: Modulation of H19 transcript affects the growth rate of OVCAR-3 cells. A: Schematic diagram of pTRIPz-shH19 vector. B: Doxycycline induced RFP expression at Day 2 and 8 in OV-3/shH19 cells. C: Efficiency of H19 knockdown induced by 16-day Doxycycline treatment measured using RT-PCR. D: Negative effect of H19 knockdown on OVCAR-3 growth rate. Medium was supplemented with 1 μg/ml Doxycycline throughout the whole experiment. Bar: SD.

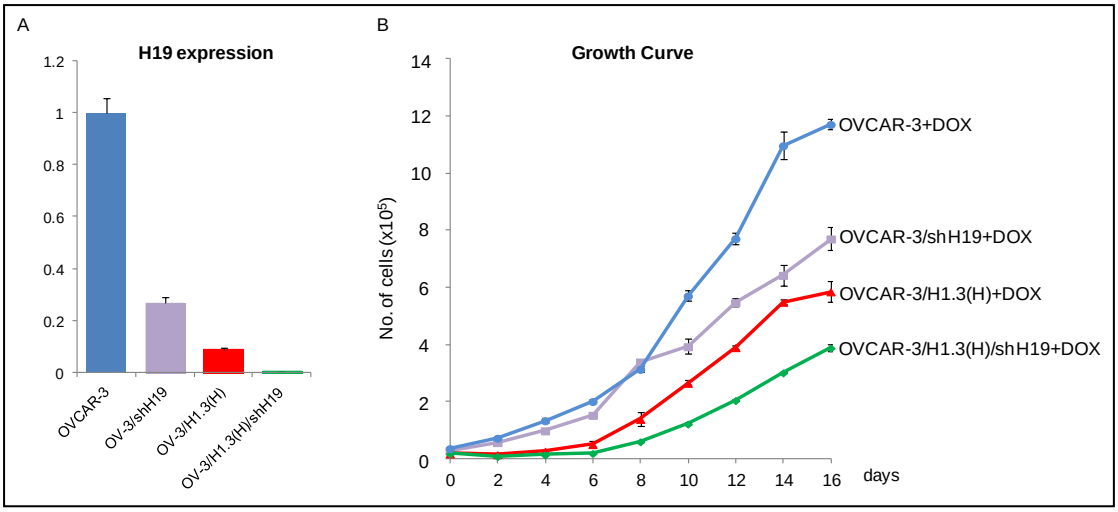

Figure 3.21: Synergistic effects of H1.3 over-expression and H19 depletion on OVCAR-3 growth rate. A: The expression of H19 in OVCAR-3, OV-3/shH19, OV-3/H1.3(H), OV-3/H1.3(H)/shH19. B: The growth curves of those cell lines. Medium was supplemented with 1 ug/ml Doxcycline for the entire experiment duration. Bar: SD.

These results suggest that over-expression of linker histone H1.3 and simultaneous depletion of H19 transcript synergistically suppress the growth rate in OVCAR-3 cells.

3.5. Discussion

H19 is an oncofetal gene whose expression is frequently elevated in many solid tumors [258,259,261,286]. Its upregulation has been associated with increased proliferation, tumorigenesis, cell cycle progression and cell migration [282,283,287,288]. However, tumor suppressor activity of H19 has also been reported in several studies [289,290], and thus the role of H19 in carcinogenesis is still controversial.

In this study, we uncovered a novel function of H1.3 in inhibiting ovarian cell growth, likely mediated through repression of H19 gene. By utilizing over-expression and knockdown approaches, we generated cell lines with modulated expression of

histone H1 subtypes and H19 transcript. Systematic analysis of generated clones demonstrated that linker histone H1.3 is the only somatic H1 variant capable of effective suppression of H19. Our results also suggest that this regulation is likely to be a direct effect. In addition, over-expression of histone H1.3 represses the growth rate and colony formation ability in OVCAR-3 cells suggesting its tumor suppressor properties. The synergistic effect of H1.3 over-expression and H19 depletion in ovarian cancer cells suggest a new strategy of combining H1.3 modulation with H19 for therapeutic intervention.

We have investigated the mechanism by which H19 is suppressed by H1.3 and found that H1.3 preferentially accumulates at H19 ICR, leading to increased DNA methylation and reduced binding of CTCF insulator binding protein at H19-ICR. These results suggest that H1.3 epigenetically represses H19 expression through DNA methylation as well as an antagonism between H1 and CTCF. Although a link between H1 and DNA methylation at regulating specific genes have been revealed in several previous studies [73,291,292], our study is the first one suggesting a highly specific regulation of H19 expression by H1.3 *in vivo*. However, this inhibitory effect appears to be regulated by H1.3 in a highly specific manner because other H1 variants did not repress the expression of H19 with the comparable levels of FLAG-H1 as to that of FLAG-H1.3. The mechanism by which H19 specifically repressed by H1.3 through DNA methylation can not be fully accounted by the interaction between H1 variants and DNA methyltransferases (DNMTs) ([207], Cao, Ho, and Fan, unpublished observation), because multiple H1 variants are found to interact with DNMTs. Other mechanisms may also contribute to the regulation of H19 by H1.3. For example, histone H1 was found to inhibit the remodeling activities of ySWI/SNF, hSWI/SNF, and xMi-2, whose functions are to move, destabilize, or restructure nucleosomes [293]. Thus, it is conceivable that histone H1.3 may act as a specific repressor of H19 gene by blocking the chromatin-remodeling complex to access H19 regulatory region.

Additionally, linker histone H1 has been shown to interact with SirT1 and histone lysine methyltransferase Ezh2 ([30], [29] reviewed in [294]). Histone H1 has been shown to be deacetylated at H1K26 by SirT1 and methylated by Ezh2. Methylated H1 binds heterochromatin protein 1 (HP1), which could lead to transcription repression of the target region [32]. Therefore, the direct effect of H1.3 on H19 gene silencing in human ovarian cancer cells may be due to direct interaction between linker histone H1 and other chromatin proteins or factors.

Histone H1 is increasingly being suggested to contribute to epigenetic regulation in cancer cells. Understanding the underlying molecular mechanisms may lead to new approaches to manipulate gene expression. In this study we generated stable cell lines with tagged H1 subtypes and we established inducible system in which protein levels of histone H1 variants can be readily modulated. Those cell lines will serve as valuable tools to study the role of H1 in epigenetic regulation in cancer cells.

CHAPTER 4: Expression analysis of mammalian linker histone subtypes

This chapter was published under the same name in the following article: Journal of visualized experiments, 2012 Mar 19;(61). pii: 3577. doi: 10.3791/3577.

Magdalena Medrzycki, Yunzhe Zhang, Kaixiang Cao, Yuhong Fan

School of Biology and the Parker H. Petit Institute of Bioengineering and Biosciences, Georgia Institute of Technology

4.1. Introduction

Linker histone H1 binds to the nucleosome core particle and linker DNA, facilitating folding of chromatin into higher order structure. H1 is essential for mammalian development [227] and regulates specific gene expression *in vivo* [10,23,206]. Among the highly conserved histone proteins, the family of H1 linker histones is the most heterogeneous group. There are 11 H1 subtypes in mammals that are differentially regulated during development and in different cell types. These H1 subtypes include 5 somatic H1s (H1a-e), the replacement H1.0, 4 germ cell specific H1 subtypes, and H1x [25]. The presence of multiple H1 subtypes that differ in DNA binding affinity and chromatin compaction ability [46,56,62,65] provides an additional level of modulation of chromatin function.

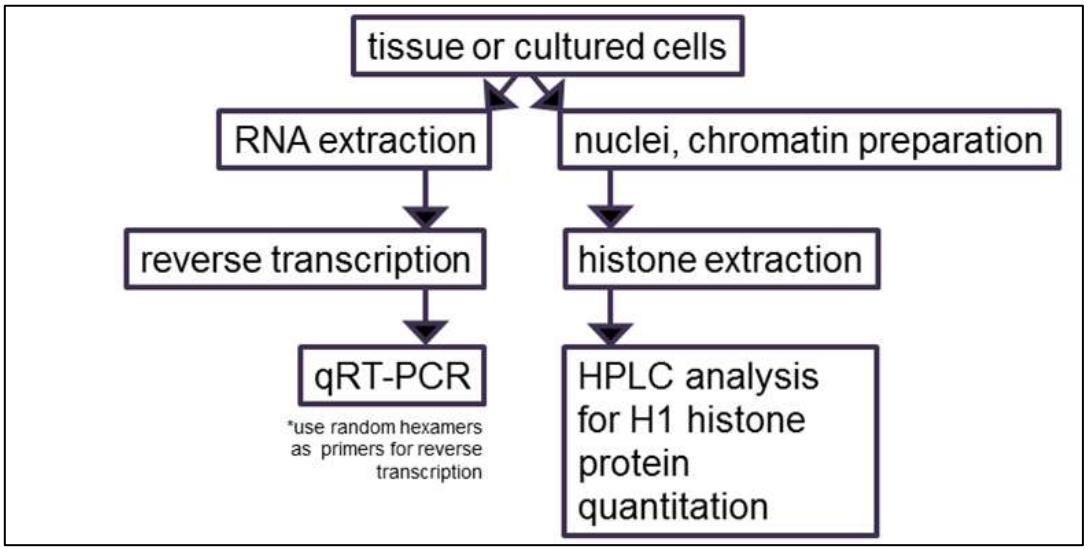

Figure 4.1: Overall scheme of expression analysis of mammalian linker-histone subtypes.

Thus, quantitative expression analysis of individual H1 subtypes, both of mRNA and proteins, is necessary for better understanding of the regulation of higher order chromatin structure and function.

Here we describe a set of assays designed for analyzing the expression levels of individual H1 subtypes (Figure 4.1). mRNA expression of various H1 variant genes is measured by a set of highly sensitive and quantitative reverse transcription-PCR (qRT-PCR) assays, which are faster, more accurate and require much less samples compared with the alternative approach of Northern blot analysis. Unlike most other cellular mRNA messages, mRNAs for most histone genes, including the majority of H1 genes, lack a long poly-A tail, but contain a stem-loop structure at the 3' untranslated region (UTR) [223]. Therefore, cDNAs are prepared from total RNA by reverse transcription using random primers instead of oligo-dT primers. Real-time PCR assays with primers specific to each H1 subtypes (Table 4.1) are performed to obtain highly quantitative measurement of mRNA levels of individual H1 subtypes. Expression of housekeeping genes are analyzed as controls for normalization.

The relative abundance of proteins of each H1 subtype and core histones is obtained through reverse phase high-performance liquid chromatography (RP-HPLC) analysis of total histones extracted from mammalian cells [225,226,295]. The HPLC method and elution conditions described here give optimum separations of mouse H1 subtypes. By quantifying the HPLC profile, we calculate the relative proportion of individual H1 subtypes within H1 family, as well as determine the H1 to nucleosome ratio in the cells.

4.2. Protocol

4.2.1. Sample preparation and RNA extraction

4.2.1.1) Before RNA extraction, all working surfaces and pipettes should be wiped with 70% ethanol and treated with RNase decontamination solution, such as RNase Zap®. This practice reduces the chances of RNase contamination and RNA degradation. Wear gloves for all procedures.

4.2.1.2) To extract RNA from mouse tissue, dissect the organ of interest from euthanized mouse, and wash the tissue in ice cold Phosphate Buffered Saline (PBS: 0.13 M NaCl, 5 mM Sodium phosphate dibasic heptahydrate, 5 mM Sodium dihydrogen phosphate heptahydrate, pH 7.4). Proceed immediately to RNA extraction in step 4.2.1.4. If fresh tissue is not to be processed for RNA extraction, the tissue samples should be snap frozen in liquid nitrogen immediately and be stored at -80^{o}C for later use.

4.2.1.3) If RNA is to be extracted from adherent cell culture, aspirate culture media, rinse with sufficient amount of PBS, and add Trizol Reagent (Invitrogen) onto the plate and proceed to step 4.2.1.4. For cells grown in suspension, harvest the cells and pellet cells by centrifugation. Discard media, rinse the pellets briefly with PBS, and pellet the cells with centrifugation. Add Trizol Reagent and proceed to step 4.2.1.4.

4.2.1.4) Sufficient Trizol Reagent is necessary for obtaining high quality RNA. Use 1 ml Trizol Reagent to extract RNA from 50 - 100 mg tissue, 5 - 10 x 10^{6} cells (for suspension cultures) or per 3.5 cm plate (for adherent cultures). Homogenize the tissue in Trizol Reagent with Polytron PT2100 homogenizer (or equivalent). Proceed to extract RNA from tissue samples or cells according to the manufacturer's manual for Trizol Reagent (Invitrogen).

4.2.1.5) RNA concentration is measured using Nanodrop 1000 (Thermo Scientific) and RNA quality is analyzed by gel electrophoresis. The typical yield ranges from 1-10 µg of RNA per mg of tissue or 5-15 µg of RNA per 1 x 10^6 cultured cells. To eliminate the potential contamination of RNA from trace amount of genomic DNA, RNA samples are treated with RNase-free DNase (Sigma AMP-D1) according to the manufacturer's instruction. Repeat RNA concentration determination and gel electrophoresis to ensure no degradation of RNA from this treatment. Store extracted RNA at -80^{o}C.

*Note: RNA may also be extracted using RNAeasy kit (Qiagen) according to the kit manual, or by DNA/RNA kit (Qiagen) if both DNA and RNA are desired.

4.2.2. Quantitative reverse transcription PCR (qRT-PCR)

4.2.2.1) Total RNA is reverse transcribed into cDNA using Superscript III First-strand Synthesis System (Invitrogen). Since mRNA of most H1 genes lack poly-A tails, it is critical to use random hexamers instead of oligo-dT as primers for cDNA synthesis. However, if expression analysis of genes with polyadenylated messages at low levels is also desired, a mixture of random hexamers and oligo-dT should be used in the reverse transcription (RT) reaction to improve the reverse transcription efficiency of polyadenylated mRNAs.

4.2.2.2) Perform the RT reaction according to the manufacturer's manual. Briefly,

- In a 0.5 ml PCR tube, combine 5 µg of total RNA, 1 µl of 50 ng/µl random hexamers, 2 µl of 10 mM dNTP mix, and add DEPC-treated H_2O to make the total reaction volume as 10 µl. Mix well and incubate for 5 minutes at 65ºC, followed by 1 minute incubation on ice.

• Prepare 10 µl of cDNA Synthesis Mix: 2 µl of 10xRT buffer, 4 µl of 25 mM $MgCl_2$, 2 µl of 0.1M DTT, 1 µl of RNaseOut (40U/µl), 1 µl of SuperScript III RT (200 U/µl) and add it to RNA/primer mixture.

Table 4.1: Histone H1 subtype nomenclature in mouse and human.

Histone subtypes	Mouse histone nomenclature		Human histone nomenclature	
	Gene name	Accession no.	Gene name	Accession no.
Histone H1a	Hist1h1a	NM_030609	HIST1H1A (H1.1)	NM_005325
Histone H1b	Hist1h1b	NM_020034	HIST1H1B (H1.5)	NM_005322
Histone H1c	Hist1h1c	NM_015786	HIST1H1C (H1.2)	NM_005319
Histone H1d	Hist1h1d	NM_145713	HIST1H1D (H1.3)	NM_005320
Histone H1e	Hist1h1e	NM_015787	HIST1H1E (H1.4)	NM_005321
Histone H1.0	H1f0	NM_008197	H1F0	NM_005318
Histone H1oo	H1foo	NM_183811	H1FOO	NM_153833
Histone H1t	Hist1h1t	NM_010377	HIST1H1T	NM_005323
Histone H1t2	H1fnt	NM_027304	H1FNT	NM_181788
Histone H1x	H1fx	NM_198622	H1FX	NM_006026
Histone Hils1	Hils1	NM_081792	HILS1	AY286318

- Incubate for 10 minutes at 25ºC, followed by 50 minutes at 50ºC and terminate the reaction at 85ºC for 5 minutes.

- Each reaction typically yields 100-250 ng/µl of cDNA product. Store cDNA products at -20ºC or proceed immediately for real-time quantitative PCR (qPCR).

4.2.2.3) qPCR can accurately quantify the target sequence copies with high efficiency and reproducibility [296]. We choose qPCR measured by SYBR Green dye, which gives a fluorescent signal only when it intercalates with double-stranded DNA (dsDNA). Although not as specific as Taqman assay [296], this method is more cost effective, easier to be adopted in the laboratory, and gives more versatility to qPCR. Therefore, it is important to examine the amplification plot (Figure 4.2A) and the derivative melting curves of the qPCR product (Figure 4.2B) to ensure reaction efficiency and specificity.

4.2.2.4) Design forward and reverse PCR primers specific for each H1 gene (Table 4.1). Due to the high sequence similarity among somatic H1s, particularly in the region corresponding to the central globular domain, it is critical to ensure that the primers designed for a specific H1 subtype do not align with other H1 genes, or cross amplify other H1 subtypes. It is also important to note that most H1 genes do not contain introns. Thus intron-spanning primers that typically adopted for RT-PCR to avoid genomic contamination are not available. Instead, RNA samples should be pre-treated with DNase (see 4.2.1.5) to eliminate any trace amount of genomic contamination. In addition, RT(-)-qPCR should be performed in parallel to validate the lack of genomic contamination in the cDNA samples.

4.2.2.5) Also design primers for internal reference genes, whose expression are not changed among samples. Often housekeeping genes, such as glyceraldehyde-3-phosphate dehydrogenase (GAPDH) and beta-actin genes, are chosen as reference genes. qPCR signals of housekeeping genes serve as normalization controls.

4.2.2.6) Prepare each PCR reaction (total volume 25 µl) as following: 12.5 µl of 2x IQ SYBR Green Supermix (Bio-Rad) (containing dNTPs, 50 U/ml iTaq DNA polymerase, 6 mM $MgCl_2$, SYBR Green I and 20 nM fluorescein), 2 µl of 4 ng/µl cDNA, 1.25 ul of 10 nM forward/reverse primer mix, and 9.25 µl of ddH_2O, and mix well in Microseal 96-well PCR plate. Use Microseal 'B' Adhesive Seals (Bio-Rad) to ensure that the plate cover is sealed to the plate. Tap or briefly vortex the PCR plate, and spin down the reaction mixtures by a short centrifugation. Place the plate in MyIQ Single Color real-time PCR Detection System (Bio-Rad) for qPCR.

4.2.2.7) We use the following qPCR conditions: 95ºC for 3 minutes, followed by 40 cycles of 95ºC for 10 seconds, 60ºC for 20 seconds, 72ºC for 30 seconds. Examine the amplification curves (Figure 4.2A) for PCR efficiency and Ct (Threshold of cycle) values. The threshold line can be automatically set by the IQ5 Optical System Software Version 2.0.

4.2.2.8) The primer efficiency and optimal cDNA concentration needed can be tested by a standard curve assay, in which a serial dilution of genomic DNA is used for qPCR and Ct values are plotted against log of template DNA amount. An optimized qPCR assay with primers of high specificity and efficiency will give a linear standard curve, with the coefficient of determination (R2)>0.98. Avoid primers with amplicon length longer than 200 bp, which tend to have poor amplification efficiency.

4.2.2.9) Because SYBR Green detects any dsDNA, it is critical to perform a melting curve run following the qPCR to ensure that the desired amplicon, but not primer dimers or contaminants, are amplified and detected. For melt-curve analysis, program the qPCR instrument to heat the samples from 55ºC to 95ºC in 0.5ºC increments with data collection. The default setting of melt-curve analysis for MyIQ (Bio-Rad) instrument is the following: 95ºC for 1 minute, 55ºC for 1 minute, followed

by 81 cycles of 10 seconds at set-point 55ºC, melt curve, + temp 0.5ºC (camera collects data at each cycle).

4.2.2.10) Since melting temperature (Tm) of dsDNA is dependent on amplicon length and GC content, different amplicons will have different Tm(s). Examine the derivative melting curves of the qPCR products to confirm the specific melting temperature of desired amplicons as well as the lack of noise amplicon peaks (Figure 4.3B).

4.2.2.11) Prepare duplicate or triplicate reactions for each assay for statistical analysis. Include negative controls for qRT-PCR, such as RT(-)-qPCR (qPCR with RNA as template without reverse transcription) and qPCR with no cDNA, RNA or DNA source added in the PCR mix. RT(-)-qPCR can serve as control for potential genomic DNA contamination (RT(-) in Figure 4.2 & 4.3).

4.2.2.12) Analyze qPCR data with IQ5 Optical System Software Version 2.0 (Bio-rad). Normalize the expression values of H1 isoform genes with the expression of housekeeping gene (e.g. GAPDH, ß-actin, HPRT) to obtain relative expression levels of H1 genes.

4.2.3. Preparation of total histones

4.2.3.1) Dissect mouse tissue and rinse it with ice cold PBS. (If not proceed to extraction immediately, snap freeze and store the samples as described in step 4.2.1.2.) Mince the tissue into pieces with razor blade. Transfer mince to a dounce homogenizer (B pestle). Add 10 ml Sucrose Buffer (0.3 M Sucrose, 15 mM NaCl, 10 mM HEPES [pH 7.9], 2 mM EDTA, 0.5 mM PMSF, Complete mini proteinase inhibitor cocktail tablet, add fresh) per gram of tissue. Homogenize the tissue with 10-15 strokes.

4.2.3.2) Transfer the homogenates to a 15 ml tube, spin at 500 rpm for 30 seconds (centrifuge model: Eppendorf 5810R); carefully transfer the supernatant to a new tube (discard the pellet-tissue debris), and centrifuge at 2000 rpm for 5 minutes, to pellet cells. Proceed to step 4.2.3.4.

4.2.3.3) If histones and chromatin are to be extracted from cells grown in monolayer, rinse with PBS, add PBS to the culture dish, and harvest the cells using cell scraper, and pellet cells by centrifugation. For cells grown in suspension, pellet cells by centrifugation.

4.2.3.4) Resuspend the cell pellet in 10 ml Sucrose Buffer supplemented with 0.5% NP-40 (per gram starting tissue amount or 10^8 cells). Transfer the sample to a Dounce homogenizer (B pestle) and dounce 10 strokes within 20 minutes incubation. At this point, nuclei are obtained. Examine the nuclei quality under a microscope. Pellet the nuclei by centrifugation at 2000 rpm for 5 minutes. Discard the supernatant.

4.2.3.5) Resuspend the nuclei pellet in 3 ml High Salt Buffer (0.35 M KCl, 10 mM Tris [pH 7.2], 5 mM $MgCl_2$, 0.5 mM PMSF - add fresh before each use) per 1 g of tissue or 10^8 cells. Transfer the sample to a small Dounce homogenizer (B pestle) and homogenize with 5-10 strokes.

4.2.3.6) Aliquot the suspension into 3 Eppendorf tubes (1 ml each), incubate on ice for 20 minutes, followed by centrifugation at 14,000 rpm for 10 minutes to pellet chromatin. Discard the supernatant.

4.2.3.7) Add 0.8 ml 0.2 N H_2SO_4 to each chromatin pellet. Use an eppendorf tube pestle dounce to grind the pellet well until the pellet is completely dissociated. Incubate the samples on a rotating platform at 4ºC overnight. Total histones are extracted with this step of acid treatment.

4.2.3.8) Centrifuge at 14,000 rpm for 10 minutes. Transfer the supernatant (histone extracts) into two Eppendorf tubes (400 ul/tube). Discard the pellet. Add 2.5 volumes (1 ml) of ice cold ethanol to each tube. Keep the samples at -20ºC overnight.

4.2.3.9) Centrifuge at 14,000 rpm for 10 minutes to pellet total histones, discard the supernatant. Wash the pellet three times with 70% EtOH, leave on bench for 20-30 minutes to air dry. Store the dried proteins at -80ºC or dissolve them in ddH_2O and proceed to HPLC analysis immediately. Dried proteins can be stored at -80ºC for up to 1 year.

4.2.4. HPLC analysis of linker histones

4.2.4.1) Resuspend the histone pellet in the recommended volume of ddH_20 depending on the capacity of reverse-phase column and the HPLC instrument. We use C18 reverse phase column 250 x 4.6 mm (Vydac) and Äktapurifier UPC 10 instrument (GE healthcare) for HPLC analysis. We typically dissolve 50-100 µg of total histones in 100 µl of ddH_20 for analysis.

4.2.4.2) Centrifuge at 14,000 rpm for 5 minutes to remove insoluble residues. Bradford protein assay is used to determine the amount of protein to be injected onto the column. Inject 50-100 µg of total protein into the reverse phase column on HPLC system. Loading an excess amount of protein should be avoided to prevent clogging of the column.

4.2.4.3) Fractionate the linker histones and core histones with an increasing acetonitrile gradient as listed in Table 4.2.

Table 4.2: Increasing acetonitrile gradient over time.

Time (Min.)	Acetonitrile/ 0.1% TFA (%)	0.1% TFA/ddH_2O (%)
0	0	100
1	5	95
11	25	75
26	30	70
45	35	65
66	40	60
75	43	57
126	55	45
131	90	10
136	5	95

4.2.4.4) The effluent is monitored at 214 nm, and the HPLC profiles (Figure 4.4) are recorded and analyzed using Äktapurifier UPC 10 (GE Healthcare) with UNICORN 5.11 software (GE Healthcare). The protein fractions can be also collected with fraction auto-collector (Frac-920 - GE) for further analysis, e.g. SDS-PAGE and mass spectroscopy.

4.2.4.5) The A214 values of the peaks of each H1 subtype and H2B are normalized by the number of peptide bonds of each corresponding histone protein. The relative proportion of individual H1 histone subtypes within the H1 family, as well as the ratio of H1 subtypes to nucleosome core particles can be calculated from these normalized A214 values (Figure 4.5).

4.3. Representative Results

The list of mammalian H1 subtypes, overall flowchart and representative results of the expression analysis of individual histone H1 genes are shown in Table 4.1, Figure 4.1 and Figures 4.2-4.5, respectively. Figure 4.2A shows typical amplification curves of H1a qPCR reactions using cDNA prepared from mouse liver and mESCs, whereas Figure 4.2B shows the derivative melting curves of the corresponding amplicons. The melting curve displays a single characteristic peak at melting temperature (Tm) at 86^0C for the H1a PCR amplicon, and lacks non-specific background peaks, suggesting high specificity of H1a qPCR assay. Evaluation of the amplification plot (Figure 4.A) shows that the triplicate qPCR reactions of each sample gave consistent signals with almost identical Ct values, suggesting high reproducibility. The lack of amplicons build-up from RT(-)-qPCR reactions indicates that genomic DNA contamination was not present, or minimal.

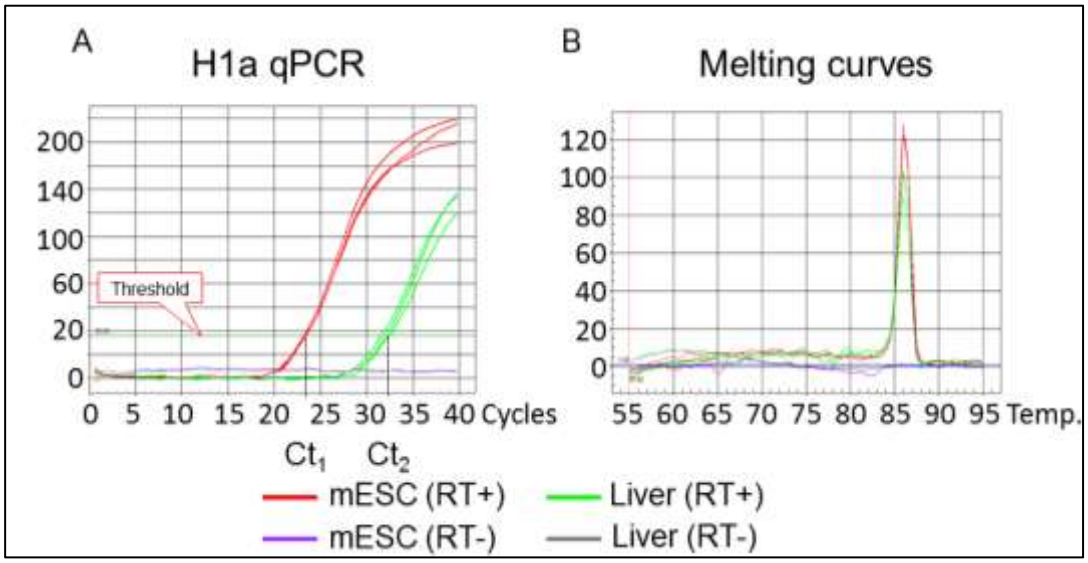

Figure 4.2: Representative results of H1a qPCR assay. A: Amplification plot of H1a qPCR assay. The threshold line and Ct values set by the IQ5 Optical System Software are indicated. B: Derivative melt-curves of qPCR products shown in (A).

Utilizing the Ct values of H1 genes and housekeeping genes, such as GAPDH, the relative RNA expression levels of each H1 gene is calculated. Examples of

calculated results for H1.0 and H1a genes are shown in Figure 4.3. The relative expression levels of H1a mRNA are higher in mESCs compared with mouse liver, whereas H1.0 expression is much higher in liver than in mESCs.

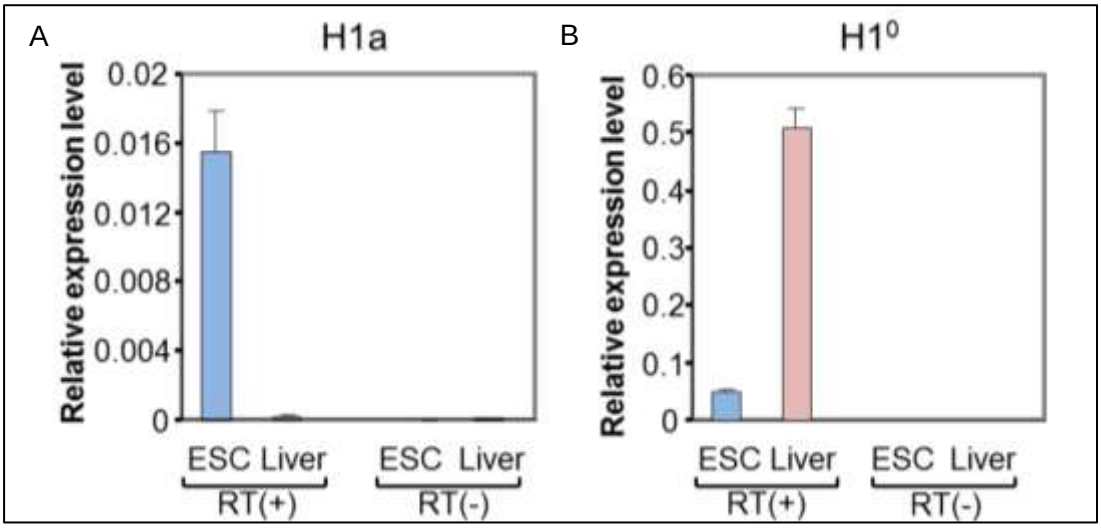

Figure 4.3: qRT-PCR analysis of mRNA levels of H1a and H1.0 in mESCs and adult mouse liver. Y axis represents relative expression levels of H1 genes to that of the reference gene GAPDH. qPCR with RT(-) samples (RNA without reverse transcription) shows minimal or no signals.

The difference in expression of H1a or H1.0 in mESC versus adult mouse liver is also evident from HPLC profiles of histone proteins (Figure 4.4). H1.0, the differentiation specific H1, is accumulated to a large amount in mature tissues, accounting for 27.2% of total H1 in adult liver (Figure 4.5A). In contrast, H1.0 protein is nearly absent in undifferentiated mESCs (Figure 4.4B). On the other hand, H1a is highly expressed, both in mRNA transcripts and proteins, in mESCs (Figure 4.3 & 4.4B). Through quantification of H1 peaks in HPLC profile, the relative proportion of each individual H1 subtype within the H1 family is determined (Figure 4.5A). Furthermore, the values of individual H1 subtype (or total H1) per nucleosome can be calculated by the ratio of the normalized A214 peak value of corresponding H1 subtypes (or sum of total H1) to one-half of the normalized A214 values for H2B (Figure 4.5B).

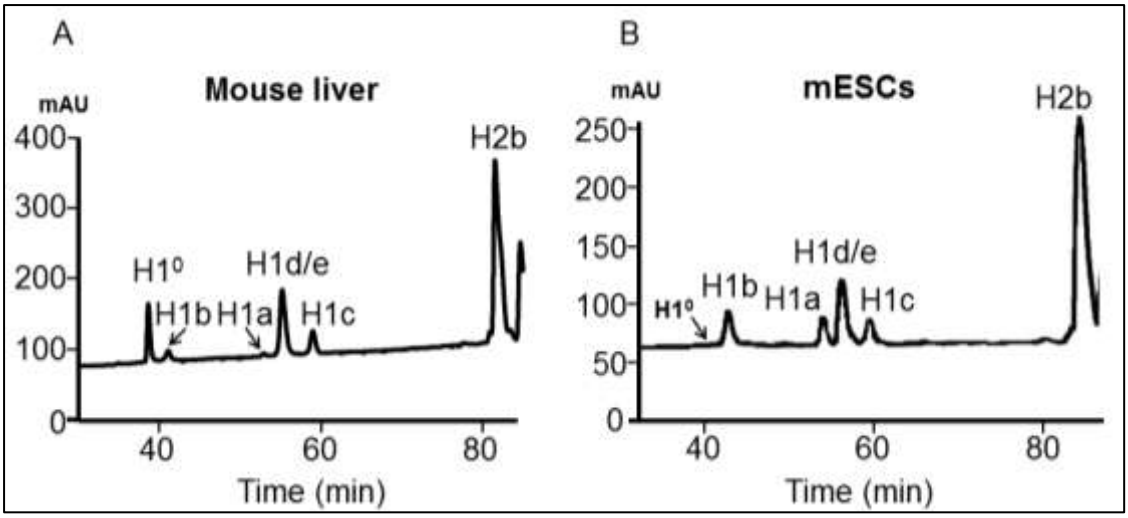

Figure 4.4: HPLC analysis of histones extracted from mammalian cells. Reverse-phase HPLC analysis of 100 µg total histones extracted from adult mouse liver (A) and mouse ESCs (B). X axis: elution time. Y axis: mAU, milli-abosorbency units.

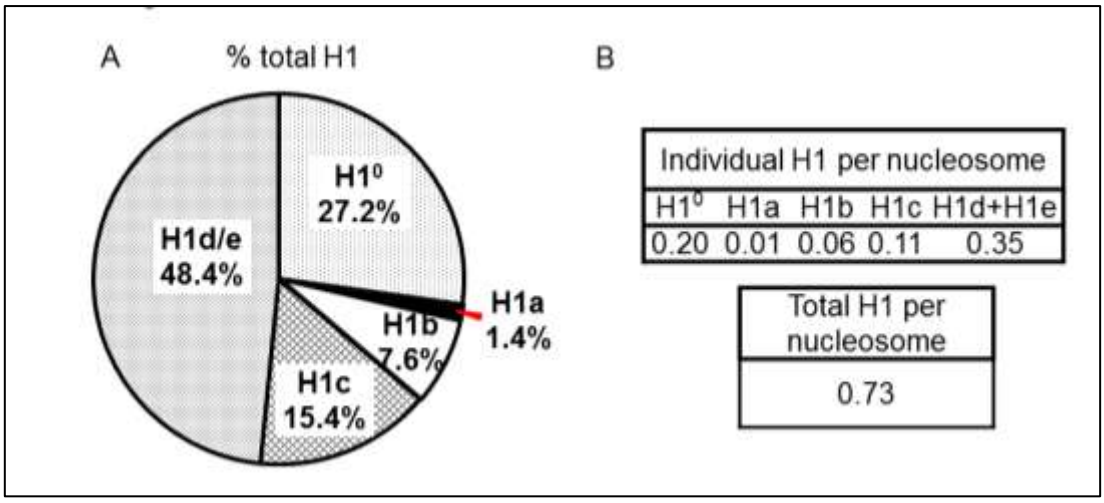

Figure 4.5: H1 subtype composition and H1 per nucleosome ratios in adult mouse liver. The A_{214} values of the peak area for each H1 isoform and H2B are calculated using UNICORN 5.11 software (GE Healthcare), and normalized by the number of peptide bonds present in the corresponding histone protein. The sum of normalized A_{214} values of all H1 subtypes is obtained as the value for total H1. The percentage of total H1 for each H1 subtype (A) as well as the ratio of H1 to nucleosome (represented by one-half of the normalized A_{214} values of H2B) (B) in adult mouse liver are calculated from the HPLC profile shown in Fig. 4.4A.

4.4. Discussion

The set of assays presented here enable comprehensive analysis of the expression levels of mammalian linker histone subtypes. Properly designed qRT-PCR assays provide highly sensitive and accurate measurements of RNA messages from any mammalian histone H1 genes. The critical part of qRT-PCR assays for linker histone subtype genes is the preparation of cDNA using random primer based reverse transcription. mRNA of most histone genes, including most H1 genes, do not contain a long poly-A tail presented in other cellular mRNAs. Thus the traditional reverse transcription method with oligo-dT primers will not efficiently produce H1 cDNAs. Expression analysis of the few H1 genes with mRNA transcripts containing poly-A tails, such as H1.0, is equally effective with random hexamers based qRT-PCR (Figure 4.3), probably due to the high abundance of H1 RNAs. Nevertheless, a mixture of oligo-dT primers and the random hexamers for RT reaction can be adopted to improve RT efficiency of polyadenylated mRNAs that are of low copy numbers, allowing broader coverage of genes analyzed by qRT-PCR. qRT-PCR of internal reference genes, such as housekeeping gene GAPDH, is included so that the relative expression level of specific H1 genes across different tissues or cell types can be compared (Figure 4.3). By combining qRT-PCR with standard curve analysis, it is also possible to obtain absolute copy numbers of H1 cDNAs from various samples (data not shown).

Here we also describe the protocols for histone extraction and HPLC analysis of histone proteins. The advantage of this method is that one can determine the relative proportions of each H1 subtype within the pool of total H1 proteins as well as quantify the ratio of individual H1 subtype (and total H1) per nucleosome. In addition, compared with other protein analysis methods, such as Western blotting, the HPLC analysis provides more quantitative and reproducible measurements of all H1 subtypes. The different levels and composition of H1 subtypes in the cell modulate

chromatin higher order chromatin structure. The ratio of H1 to nucleosome has been shown to correlate with chromatin compaction and is a determinant for nucleosome repeat length in chromatin [10]. Thus, the methods we described here should have wide applications in chromatin research.

4.5. Table of specific reagents and equipment

Name of the reagent	Company	Catalogue number
RNase Zap®	Applied Biosystems	AM9780
Trizol Reagent	Invitrogen	15596-018
SuperScript III	Invitrogen	18080-051
Absolute Ethanol	Fisher Scientific	BP2818-4
IQ SYBR Green	Bio-Rad	170-8880
RNeasy Mini Kit	Qiagen	74104
Deoxyribonuclease I	Sigma	AMP-D1
Microseal 96-well PCR plate	Bio-Rad	MSP-9605
Microseal 'B' Adhesive Seals	Bio-Rad	MSB-1001
Sucrose	Agros Organics	AC40594
Sodium phosphate dibasic heptahydrate ($Na_2HPO_4 \cdot 7H_2O$)	Fisher Scientific	BP332
Sodium chloride (NaCl)	American Bioanalytical	AB01915
Sodium dihydrogen phosphate heptahydrate ($NaH_2PO_4 \cdot 7H_2O$)	Fisher Scientific	BP-330

HEPES	Fisher Scientific	BP310
Complete Mini proteinase inhibitor cocktail tablet	Roche Applied Science	11836153001
EDTA	Sigma	E-5134
Phenylmethanesulfonyl fluoride (PMSF)	American Bioanalytical	AB01620
Nonidet-40 (NP-40)	American Bioanalytical	AB01425
Potassium chloride (KCl)	Fisher Scientific	BP366
Tris [hydroxymethyl aminomethane]	American Bioanalytical	AB02000
Magnesium chloride ($MgCl_2$)	Fisher Scientific	BP214
Sulfuric acid (H_2SO_4)	VWR	VW3648-3
Ammonium hydroxide (NH_4OH)	Agros Organics	AC42330
Bradford Protein Assay	Bio-Rad	500-0001
Acetonitrile	EMD	AX0145-1
Trifluoroacetic acid (TFA)	J.T.Baker	9470-01

4.6. Acknowledgements

This work is supported by NIH grant GM085261 and a Georgia Cancer Coalition Distinguished Scholar Award (to Y.F.).

CHAPTER 5: Conclusions

Ovarian cancer is one of the most common women malignancies, leading to death in 63% of cases diagnosed. Despite intensive research searching for new therapies and preventive screenings of higher efficiency and specificity, the 5-year survival rate of ovarian cancer patients remains low and largely unchanged for the past 50 years.

Epigenetic mechanisms play an important role in regulating expression of genes that are necessary for ovarian cancer progression. Unlike genetic modifications, epigenetics does not involve any changes in nucleotide sequence, and thus opens great opportunities for therapeutic intervention. DNA methylation, posttranslational histone modifications and microRNA expression have all been shown to be disregulated in ovarian cancers [177-180,297]. Additionally, the advanced stages of ovarian malignancy correlate well with accumulation of epigenetic alterations in tumors (reviewed in [298]). Therefore, components or inhibitors of epigenetic machineries or factors, such as chromatin modififying enzymes, micro-RNAs, are actively tested as potential therapeutic targets for ovarian cancer.

Linker histone H1, one of the major chromatin structural proteins, is emerging as an important epigenetic factor. Previously thought to act as a general repressor, H1 is now recognized as specific regulator of gene expression from many *in vivo* studies. Although much is known about the biochemical and structural properties of H1 variants, little is understood regarding the mechanisms of the epigenetic mechanisms regulated by H1 variants or the role of H1 in occurrence and progression of diseases, such as cancer. In addition, studying H1 subtypes in ovarian cancer seemed to be especially relavant, because recent evidence indicated that several genes

abnormally expressed in adenocarcinomas might be targeted by linker histone H1 variants [40,73,206,207].

Here, we begin to systematically study the role of H1 variants in ovarian cancer. Establishing a comprehensive set of quantitative assays for analysis of RNA and protein expression levels of individual H1 subtypes in mammalian cells (Chapter 4) allowed us to accurately determine the H1 transcript levels in ovarian adenomas and adenocarcinoma samples (Chapter 2). Profiling of H1 variants in ovarian tumors indicates dramatically different expression pattern of H1 variants in malignant adenocarcinomas compared with benign adenomas. H1.1, H1.4, H1.x, and H1.0 are downregulated and the total H1 expression level is lower in malignant adenocarcinomas compared with benign adenomas, whereas the expression of other H1 variants was not significantly altered or even elevated in malignant tumors. Importantly, we find that H1 subtype profiling combined with computational cluster analysis can accurately segregate adenomas and adenocarcinomas with overall 97% accuracy (Chapter 2). This study establishes expression patterns of H1 variants as ovarian cancer biomarkers.

To determine the functional role of H1 variants in ovarian cancer cells, we initiated a program to modulate the levels of individual H1 variants in the OVCAR-3 epithelial ovarian cancer cell line and to characterize the effects of over-expressing specific H1 variants in these cells. Toward this end, we report the identification of a novel function of histone H1.3 in inhibiting ovarian cancer cell growth and colony formation as well as in directly suppressing oncogene H19 expression through epigenetic regulation. Expressional analysis of OVCAR-3 cells reveals a surprisingly low level of H1.3 protein which are often present in abundant amount in adult tissues. Over-expression of H1.3 leads to increased doubling time and reduced colony formation of OVCAR-3 cells, as well as changes in cell cycle distribution. mRNA microarray analysis revealed many genes are affected, with both genes upregulated or downregulated by histone H1.3 over-expression. Network and pathway analysis indicate multiple pathways are affected. Interestingly, H19 is one of the most dramatically affected genes by H1.3 over-

expression. H19 expression was severely repressed in OV-3/H1.3(H) clone, but unchanged in cell lines expressing other FLAG-H1 to a comparable level to that of FLAG-H1.3. H19 gene is an oncofetal gene highly over-expressed in ovarian cancer cells. While over-expression of H1.3 effectively represses H19 expression, knockdown of H1.3 alleviates the repression on H19. Furthermore, by analyzing DNA methylation, H1.3 occupancy and CTCF binding at H19-ICR, we establish an interplay relationship among these epigenetic regulations. Our data suggest that over-expression of H1.3 leads to its preferential binding at H19 upstream regulatory regions which in turn leads to increase DNA methylation and reduced CTCF binding.

Through this study, we have found, for the first time, a functional role of H1.3 in regulating H19 expression and ovarian cancer cell growth. Additionally, we demonstrate a synergistic effect of H1.3 over-expression and H19 knockdown in inhibiting ovarian cancer cell proliferation. These findings may lead to new strategies to ovarian cancer therapeutic intervention. It would also be interesting to test if the effect of over-expressed H1.3 on H19 regulation also exist in other cancer cells, such as breast cancer cells. In addition, other novel H1 target genes may be identified from these studies.

CHAPTER 6: Future Studies

There are many unresolved questions regarding the role of histone H1 subtypes in gene regulation in ovarian cancer. Here, we demonstrated that histone H1.3 directly targets H19 gene and represses its expression in OVCAR-3 cells. To date, this repression by a specific H1 variant was only thoroughly examined in the ovarian cancer cell line. It would be interesting to analyze the effect of H1.3 over-expression on H19 regulation in other cancers, in which H19 transcript is significantly elevated, such as breast, bladder, liver, and testicular cancers. The H1 variant expression vectors as well as the inducible H1.3 shRNA knockdown system established in this study should be useful tools for such future studies. These investigations would determine whether H19 regulation by histone H1.3 is specific for ovarian cancer cells or occurs in other cancer models as well.

In this study, we also find increased levels of DNA methylation as well as depleted CTCF binding within the H19 regulatory region as a result of increased H1.3 occupancy in H1.3 over-expressing OVCAR-3 cells. DNA methylation occurring on the H19 regulatory region could be due to interaction between linker histone H1 variants and DNA methyltransferases (DNMTs) which have been shown both *in vitro* and in mouse ESCs ([207], Cao, Ho, and Fan, unpublished observation). Whether an interaction between histone H1.3 and DNMTs exists in OVCAR-3 cells is not clear. To test this possibility, nuclear extracts from OVCAR-3, OVCAR-3/V.O. and OV-3/H1.3(H) cells can be used for Co-Immunoprecipitation (co-IP). Co-immunoprecipitation with anti-FLAG antibody using OVCAR-3 cell lines over-expressing other H1 variants can be performed in parallel to determine if the specificity among H1 variants in repression H19 is due to their differential binding capacities to DNMTs in OVCAR-3. Given that multiple H1 variants can interact with

DNMTs *in vitro* and in mESCs, these co-IP experiments would provide crucial insights as to the specificity of H1 variants under different cellular milieu.

On the other hand, the sequences of reduced CTCF binding and increased DNA methylation in repressing H19 expression under H1.3 over-expression in OVCAR-3 cells are not determined in this study. Future studies utilizing shRNA knockdown of the level of CTCF expression in OVCAR-3 and OV-3/H1.3(H) cells followed by examination of H19 expression and DNA methylation at H19-ICR could help determine if depleted CTCF occupancy acts upstream or downstream of increased DNA methylation in regulating H19 expression in these cells. To facilitate the analysis of the sequence of the events as well as to avoid the lethal effects associated with dramatic knockdown of CTCF [299,300], an inducible shRNA lentiviral system that is well-established in our lab will be employed in such studies.

Synergistic effects of over-expression of histone H1.3 with downregulation of H19 transcript in ovarian cancer cells in severe impairment in OVCAR-3 cells' growth rate point to an attractive avenue for potential future therapeutic intervention in ovarian cancers. However, it is not tested whether the effects of H1.3 on impairment of OVCAR-3 growth is mainly due to repression of H19. To investigate this possibility, H19 expression vector will be transfected into OV-3/H1.3(H) cell line to obtain OV-3/H1.3(H)/H19 cells in which H19 transcript level is increased to that comparable to OVCAR-3 cells. The growth curves of OV-3/H1.3(H)/H19 cells will be measured to determine if the growth inhibitory effect by H1.3 over-expression is alleviated in these cells, which will indicate a "rescue" effect by H19 over-expression in these cells.

In this study we generated ovarian cancer cell lines with over-expressed individual somatic linker histone variants. We mainly concentrated on linker histone H1.3 and its role in H19 gene regulation. However, according to microarray results, H1.3 over-expressed clones contained many genes with expression changed in dose-dependent manners when compared with control cell lines. Those genes could be further characterized, and new, potentially important networks can be investigated in order to

obtain a more comprehensive view of the effect of linker histone H1.3 in ovarian cancer cells. Global gene expression changes may be examined in other H1 variants over-expressed OVCAR-3 cell lines as well. These analyses would identify new target genes important in tumorigenesis, and would significantly enrich our knowledge in understanding the role of H1 variants in ovarian cancer.

APPENDIX A: Supplemental tables and graphs

A.1 Linker histone subtype primers designed for subcloning into pcDNA3.0 expressional vector.

Gene name	Accession number	Sequence	Product size (bp)	Annealing temp.
H1.1	HIST1H1A: NM_005325	F' -GCTGGAATTCTGTCTGAAACAGTGCC-5'	669	56^{o}C
		R' - ATGCATGCTCGAGTTACTTTTTCTTG-5'		
H1.2	HIST1H1C: NM_005319	F' - GCTGGAATTCTGTCCGAGACTGCTCCTG-5'	662	60^{o}C
		R' - TGCATGCTCGAGCTATTTCTTCTTGGGC-5'		
H1.3	HIST1H1D: NM_005320	F' - GCTGGAATTCTGTCGGAGACTGC-5'	683	56^{o}C
		R' - CATGCTCGAGTCACTTTTTCTTC-5'		
H1.4	HIST1H1E: NM_005321	F' - CTGGAATTCTGTCCGAGACTGCGCCT-5'	679	59^{o}C
		R' - TGCATGCTCGAGCTACTTTTTCTTGGC-5'		
H1.5	HIST1H1B: NM_005322	F' - GCTGGAATTCTGTCGGAAACCGCTCC-5'	696	60^{o}C
		R' - GCTCGAGCTACTTCTTTTTGGCAGCC-5'		
H1.0	H1F0: NM_005318	F' – GACGATGACGACAAGGGATCCACTAG TAACGGCCGCCAGTGTGCTGGAATTCT GACCGAGAATTCCACGTC-5'	612	61^{o}C
		R' – CTAGATGCATGCTCGAGTCACTTCTTCT TGCCGGCCC-5'		

A.2. Primers designed to detect enrichment of H1 signal on H19 ICR region

Primer name	Position	Sequence	Product size (bp)
Ch1.1	Chr11: 2,024,177-2,024,292	F' - AATCGGCTGTACGTGTGGAAT-5'	115
		R' - CTGGGAGACCTGGGACGTTTC-5'	
Ch1.2	Chr11: 2,023,751-2,023,894	F' - GGTGCAGAATCGGTTGTAGTT-5'	143
		R' - TGAACCTTGCGGCACCTAGCT-5'	
Ch1.3	Chr11: 2,023,414-2,023,523	F' - ACGCTTCCCCTTCTGTCTCAC-5'	109
		R' - GGGCTTGGGCTGTGATGTGTG-5'	
Ch1.4	Chr11: 2,023,231-2,023,318	F' - GAGCCACACCACGTCTTCGTA-5'	107
		R' - GCGGGTAGGCGTGACTTGAGT-5'	
Ch1.5	Chr11: 2,022,957-2,023,058	F' - TTCCACATCCATCCCAGAGCA-5'	84
		R' - TGGGGAGGCAATTGTCAGTTC-5'	
Ch1.5.1	Chr11: 2,022,755-2,022,849	F' – GGCCAGACATTAACATTCCCA-5'	101
		R' - ACCCCAGAATAAAGCAGCAGTG-5'	
Ch1	Chr11: 2,022,831-2,022,956	F' - GGGGTCTAGGATCCTTGTGTT-5'	130
		R' - GCAATTGGGCACAGACCGCA-5'	
Ch1.5.2	Chr11: 2,022,755-2,022,828	F' - GCGGTCTGTGCCCAATTGCCTG-5'	94
		R' - AGGCTCTGGAAAATGCACTGTC-5'	
Ch1.6	Chr11: 2,022,672-2,022,782	F' - GAGCCTGACAGTGCATTTTCC-5'	110
		R' - AGGTGATACGGGGCCATGGTC-5'	
Ch1.6.1	Chr11: 2,022,570-2,022,653	F' - GGGACAGGAGAGCAGAGACTTC-5'	83
		R' - ATGCGCTTGAGTCCTTGGGTCC-5'	
Ch1.7	Chr11: 2,022,346-2,022,466	F' - GCCACGGAATCAGTTGAAGGT-5'	120
		R' - TGTTGACCCGGGATGTTTCTG-5'	
Ch1.8	Chr.11: 2,022,231- 2,022,333	F' - CATTGGTTCGCGAGGGTCATC-5'	102
		R' - TCATCTCCCCAACCTTCAACA-5'	
Ch2	Chr11: 2,021,916-2,022,089	F' - GGCTTCCCCTTCAGTCTCAC-5'	173
		R' - GTGAACCCTGCGGCGCCTGG-5'	

Ch3	Chr11: 2,021,530-2,021,654	F' - GGCACGGAATTGGTTGTAGTT-5' R' - CTTGGATGACCTGGGATGTTT-5'	124
Ch4	Chr11: 2,021,113-2,021,250	F' - ATGGCACGGAATTGGTTGTAG-5' R' - GCGACGCGTGGCTTGGGTGAC-5'	137
Ch4.1	Chr11: 2,020,175-2,020,322	F' - CCTTGGGTCTTGGGTGCTGTC-5' R' - CAGCCTTGGGTCACCTTCAGA-5'	135
Ch5	Chr11: 2,019,925-2,020,031	F' - CGCGGCCAGCCCTTCCACATC-5' R' - AGTCTCGAGTGTCAAAGCCG-5'	147
Ch6	Chr11: 2,019,746-2,019,867	F' - TGACCGACGGACCCACAGCG-5' R' - TGACAAGCGGTGGGCGGCCT-5'	121
Ch7	Chr11: 2,019,590-2,019,697	F' - TCAGACAGGAAAGTGGCCGC-5' R' - TTCCCATCCAGTTGACCGAG-5'	107
Ch8	Chr11: 2,019,406-2,019,507	F' - AGGAACGTGAGGTCTGAGCC-5' R' - CATACTTTGCACATGGCTGG-5'	101
Ch9	Chr11: 2,019,201-2,019,319	F' - AGGGAGGTGATGGGGCAATG-5' R' - CAGTTCCAGCACACGTCTCT-5'	118
Ch10	Chr11: 2,018,665-2,018,778	F' - GCCAGGCATTCATCCCGGTCA-5' R' - TGCCAGCTACACCTCCGTTGC-5'	114
Ch11	Chr11: 2,017,396-2,017,526	F' - GGCCTTCCTGGTGAGCGTGTC-5' R' - CCGCAGCCCCACCAGCCTAAG-5'	130
Ch12	Chr11: 2,016,500-2,016,602	F' - CTCCATCTGGGCCGGGTGACT-5' R' - TTGAAGGCTGCTCCGTGATGT-5'	102
Ch13	Chr11: 2,015,970- 2,016,083	F' - CAAACCATCCCCGAGCGAGTG-5' R' - GTGACTGGGGTAGAGCTGGCC-5'	113
Ch14	Chr11: 2,014,860-2,014,979	F' - CCCTACAGGCCAATTTGACTT-5' R' - TGCAGAGTTGGATGTTTATAA-5'	119
Ch15	Chr11: 2,014,185-2,014,365	F' - GAGCAGGACGTGTACTCAGG-5' R' – TGAACGCTGCCCCCACCACC-5'	180
Ch16	Chr11: 2,012,587-2,012,722	F' - AGGGGGATTGGAAGGTTCGA-5'	135

		R’ - GGAGAAAGAGAAAGGAGAGG-5'	
Enh.3	Chr11: 2,008,762-2,008,852	F’ - CCCAGCCTAGACCCCCAGCAT-5'	91
		R - CGGGTGGAGTGGGCGATGGT-5'	
c-myc5	Chr8: 128,748,541-128,748,630	F- GGCGGCCGGCTAGGGTGGAAGA-5'	131
		R- CGGACCGCTGGCTGGGGGATCA-5'	
c-myc7	Chr8: 128,750,078-128,750,182	F - CGCCTCTCGCCTTCTCCTTCAG-5'	125
		R - GCGGCAGAGGAATCGAAATCGG-5'	

A.3. Primers used in bisulfite sequencing analysis

Primer name	Position	Sequence 5'	Product size (bp)	Annealing temp.(^{o}C)
bisulf.**H19**BC3	chr11: 2,023,188-2,023,480	F - TTGTAAGTGTGGATTTAAAAGT	294	55.8^{o}C
		R - ATTAAAATTTACTATACTCATC		
bisulf.**H19**BC4	chr11: 2,021,918 - 2,022,096	F - TTTTGGAGGTTTTTTTTTA	179	57.6^{o}C
		R - AAACCCTACAACACCTAACT		
bisul.**H19** promoter	chr11: 2,019,225 - 2,019,482	F - GGTGGTAGGAAGGGGTTTTT R - CCCAACACCCATCCTAAAAT	255	55.4^{o}C

REFERENCES

1. Oudet P, Gross-Bellard M, Chambon P (1975) Electron microscopic and biochemical evidence that chromatin structure is a repeating unit. Cell 4: 281-300.

2. Ramakrishnan V (1997) Histone structure and the organization of the nucleosome. Annu Rev Biophys Biomol Struct 26: 83-112.

3. McGhee JD, Felsenfeld G (1980) Nucleosome structure. Annu Rev Biochem 49: 1115-1156.

4. Khorasanizadeh S (2004) The nucleosome: from genomic organization to genomic regulation. Cell 116: 259-272.

5. Henikoff S, Ahmad K (2005) Assembly of variant histones into chromatin. Annu Rev Cell Dev Biol 21: 133-153.

6. Carruthers LM, Hansen JC (2000) The core histone N termini function independently of linker histones during chromatin condensation. J Biol Chem 275: 37285-37290.

7. Jenuwein T, Allis CD (2001) Translating the histone code. Science 293: 1074-1080.

8. Gardner KE, Allis CD, Strahl BD (2011) Operating on chromatin, a colorful language where context matters. J Mol Biol 409: 36-46.

9. Stewart MD, Li J, Wong J (2005) Relationship between histone H3 lysine 9 methylation, transcription repression, and heterochromatin protein 1 recruitment. Mol Cell Biol 25: 2525-2538.

10. Woodcock CL, Skoultchi AI, Fan Y (2006) Role of linker histone in chromatin structure and function: H1 stoichiometry and nucleosome repeat length. Chromosome Res 14: 17-25.

11. Happel N, Doenecke D, Sekeri-Pataryas KE, Sourlingas TG (2008) H1 histone subtype constitution and phosphorylation state of the ageing cell system of human peripheral blood lymphocytes. Exp Gerontol 43: 184-199.

12. Szerlong HJ, Hansen JC (2011) Nucleosome distribution and linker DNA: connecting nuclear function to dynamic chromatin structure. Biochem Cell Biol 89: 24-34.

13. Konishi A, Shimizu S, Hirota J, Takao T, Fan Y, et al. (2003) Involvement of histone H1.2 in apoptosis induced by DNA double-strand breaks. Cell 114: 673-688.

14. Brown DT (2003) Histone H1 and the dynamic regulation of chromatin function. Biochem Cell Biol 81: 221-227.

15. Alexandrow MG, Hamlin JL (2005) Chromatin decondensation in S-phase involves recruitment of Cdk2 by Cdc45 and histone H1 phosphorylation. J Cell Biol 168: 875-886.

16. Downs JA, Kosmidou E, Morgan A, Jackson SP (2003) Suppression of homologous recombination by the Saccharomyces cerevisiae linker histone. Mol Cell 11: 1685-1692.

17. Okamura H, Yoshida K, Amorim BR, Haneji T (2008) Histone H1.2 is translocated to mitochondria and associates with Bak in bleomycin-induced apoptotic cells. J Cell Biochem 103: 1488-1496.

18. Barra JL, Rhounim L, Rossignol JL, Faugeron G (2000) Histone H1 is dispensable for methylation-associated gene silencing in Ascobolus immersus and essential for long life span. Mol Cell Biol 20: 61-69.

19. Lu X, Wontakal SN, Kavi H, Kim BJ, Guzzardo PM, et al. (2013) Drosophila H1 regulates the genetic activity of heterochromatin by recruitment of Su(var)3-9. Science 340: 78-81.

20. Patterton HG, Landel CC, Landsman D, Peterson CL, Simpson RT (1998) The biochemical and phenotypic characterization of Hho1p, the putative linker histone H1 of Saccharomyces cerevisiae. J Biol Chem 273: 7268-7276.

21. Hayashi T, Hayashi H, Iwai K (1987) Tetrahymena histone H1. Isolation and amino acid sequence lacking the central hydrophobic domain conserved in other H1 histones. J Biochem 102: 369-376.

22. Ushinsky SC, Bussey H, Ahmed AA, Wang Y, Friesen J, et al. (1997) Histone H1 in Saccharomyces cerevisiae. Yeast 13: 151-161.

23. Shen X, Gorovsky MA (1996) Linker histone H1 regulates specific gene expression but not global transcription in vivo. Cell 86: 475-483.

24. Hellauer K, Sirard E, Turcotte B (2001) Decreased expression of specific genes in yeast cells lacking histone H1. J Biol Chem 276: 13587-13592.

25. Happel N, Doenecke D (2009) Histone H1 and its isoforms: contribution to chromatin structure and function. Gene 431: 1-12.

26. Garcia BA, Busby SA, Barber CM, Shabanowitz J, Allis CD, et al. (2004) Characterization of phosphorylation sites on histone H1 isoforms by tandem mass spectrometry. J Proteome Res 3: 1219-1227.

27. Wisniewski JR, Zougman A, Kruger S, Mann M (2007) Mass spectrometric mapping of linker histone H1 variants reveals multiple acetylations, methylations, and phosphorylation as well as differences between cell culture and tissue. Mol Cell Proteomics 6: 72-87.

28. Ramakrishnan V, Finch JT, Graziano V, Lee PL, Sweet RM (1993) Crystal structure of globular domain of histone H5 and its implications for nucleosome binding. Nature 362: 219-223.

29. Vaquero A, Scher M, Lee D, Erdjument-Bromage H, Tempst P, et al. (2004) Human SirT1 interacts with histone H1 and promotes formation of facultative heterochromatin. Mol Cell 16: 93-105.

30. Kuzmichev A, Jenuwein T, Tempst P, Reinberg D (2004) Different EZH2-containing complexes target methylation of histone H1 or nucleosomal histone H3. Mol Cell 14: 183-193.

31. Hale TK, Contreras A, Morrison AJ, Herrera RE (2006) Phosphorylation of the linker histone H1 by CDK regulates its binding to HP1alpha. Mol Cell 22: 693-699.

32. Daujat S, Zeissler U, Waldmann T, Happel N, Schneider R (2005) HP1 binds specifically to Lys26-methylated histone H1.4, whereas simultaneous Ser27 phosphorylation blocks HP1 binding. J Biol Chem 280: 38090-38095.

33. Albig W, Meergans T, Doenecke D (1997) Characterization of the H1.5 gene completes the set of human H1 subtype genes. Gene 184: 141-148.

34. Doenecke D, Albig W, Bode C, Drabent B, Franke K, et al. (1997) Histones: genetic diversity and tissue-specific gene expression. Histochem Cell Biol 107: 1-10.

35. Gjerset R, Gorka C, Hasthorpe S, Lawrence JJ, Eisen H (1982) Developmental and hormonal regulation of protein H1 degrees in rodents. Proc Natl Acad Sci U S A 79: 2333-2337.

36. Lennox RW, Cohen LH (1983) The histone H1 complements of dividing and nondividing cells of the mouse. J Biol Chem 258: 262-268.

37. Franke K, Drabent B, Doenecke D (1998) Expression of murine H1 histone genes during postnatal development. Biochim Biophys Acta 1398: 232-242.

38. Rasheed BK, Whisenant EC, Ghai RD, Papaioannou VE, Bhatnagar YM (1989) Biochemical and immunocytochemical analysis of a histone H1 variant from the mouse testis. J Cell Sci 94 (Pt 1): 61-71.

39. Karhu I, Mahonen A, Palvimo J (1988) Separation and quantification of histone H1 subtypes and high-mobility-group proteins by reversed-phase liquid chromatography: protein levels in rat tissues during postnatal development. J Chromatogr 426: 65-73.

40. Zhang Y, Cooke M, Panjwani S, Cao K, Krauth B, et al. (2012) Histone h1 depletion impairs embryonic stem cell differentiation. PLoS Genet 8: e1002691.

41. Martianov I, Brancorsini S, Catena R, Gansmuller A, Kotaja N, et al. (2005) Polar nuclear localization of H1T2, a histone H1 variant, required for spermatid elongation and DNA condensation during spermiogenesis. Proc Natl Acad Sci U S A 102: 2808-2813.

42. Tanaka M, Hennebold JD, Macfarlane J, Adashi EY (2001) A mammalian oocyte-specific linker histone gene H1oo: homology with the genes for the oocyte-specific cleavage stage histone (cs-H1) of sea urchin and the B4/H1M histone of the frog. Development 128: 655-664.

43. Yamamoto T, Horikoshi M (1996) Cloning of the cDNA encoding a novel subtype of histone H1. Gene 173: 281-285.

44. Talbert PB, Ahmad K, Almouzni G, Ausio J, Berger F, et al. (2012) A unified phylogeny-based nomenclature for histone variants. Epigenetics Chromatin 5: 7.

45. Tanaka M, Kihara M, Hennebold JD, Eppig JJ, Viveiros MM, et al. (2005) H1FOO is coupled to the initiation of oocytic growth. Biol Reprod 72: 135-142.

46. Clausell J, Happel N, Hale TK, Doenecke D, Beato M (2009) Histone H1 subtypes differentially modulate chromatin condensation without preventing ATP-dependent remodeling by SWI/SNF or NURF. PLoS One 4: e0007243.

47. Marzluff WF (2005) Metazoan replication-dependent histone mRNAs: a distinct set of RNA polymerase II transcripts. Curr Opin Cell Biol 17: 274-280.

48. Marzluff WF, Gongidi P, Woods KR, Jin J, Maltais LJ (2002) The human and mouse replication-dependent histone genes. Genomics 80: 487-498.

49. Cheng GH, Nandi A, Clerk S, Skoultchi AI (1989) Different 3'-end processing produces two independently regulated mRNAs from a single H1 histone gene. Proc Natl Acad Sci U S A 86: 7002-7006.

50. Marzluff WF, Wagner EJ, Duronio RJ (2008) Metabolism and regulation of canonical histone mRNAs: life without a poly(A) tail. Nat Rev Genet 9: 843-854.

51. Doenecke D, Tonjes R, Kress H (1988) The H1 and core histone subtypes: differential gene expression and varied primary structures. Adv Enzyme Regul 27: 107-120.

52. Khochbin S (2001) Histone H1 diversity: bridging regulatory signals to linker histone function. Gene 271: 1-12.

53. Lennox RW, Oshima RG, Cohen LH (1982) The H1 histones and their interphase phosphorylated states in differentiated and undifferentiated cell lines derived from murine teratocarcinomas. J Biol Chem 257: 5183-5189.

54. Hall JM, Cole RD (1985) Modulation in proportions of H1 histone subfractions by differential changes in synthesis and turnover during butyrate treatment of neuroblastoma cells. Biochemistry 24: 7765-7771.

55. Dominguez V, Pina B, Suau P (1992) Histone H1 subtype synthesis in neurons and neuroblasts. Development 115: 181-185.

56. Th'ng JP, Sung R, Ye M, Hendzel MJ (2005) H1 family histones in the nucleus. Control of binding and localization by the C-terminal domain. J Biol Chem 280: 27809-27814.

57. Sun JM, Wiaderkiewicz R, Ruiz-Carrillo A (1989) Histone H5 in the control of DNA synthesis and cell proliferation. Science 245: 68-71.

58. Lever MA, Th'ng JP, Sun X, Hendzel MJ (2000) Rapid exchange of histone H1.1 on chromatin in living human cells. Nature 408: 873-876.

59. Misteli T, Gunjan A, Hock R, Bustin M, Brown DT (2000) Dynamic binding of histone H1 to chromatin in living cells. Nature 408: 877-881.

60. Phair RD, Scaffidi P, Elbi C, Vecerova J, Dey A, et al. (2004) Global nature of dynamic protein-chromatin interactions in vivo: three-dimensional genome scanning and dynamic interaction networks of chromatin proteins. Mol Cell Biol 24: 6393-6402.

61. Catez F, Yang H, Tracey KJ, Reeves R, Misteli T, et al. (2004) Network of dynamic interactions between histone H1 and high-mobility-group proteins in chromatin. Mol Cell Biol 24: 4321-4328.

62. Khadake JR, Rao MR (1995) DNA- and chromatin-condensing properties of rat testes H1a and H1t compared to those of rat liver H1bdec; H1t is a poor condenser of chromatin. Biochemistry 34: 15792-15801.

63. Liao LW, Cole RD (1981) Condensation of dinucleosomes by individual subfractions of H1 histone. J Biol Chem 256: 10124-10128.

64. Talasz H, Sapojnikova N, Helliger W, Lindner H, Puschendorf B (1998) In vitro binding of H1 histone subtypes to nucleosomal organized mouse mammary tumor virus long terminal repeat promotor. J Biol Chem 273: 32236-32243.

65. Orrego M, Ponte I, Roque A, Buschati N, Mora X, et al. (2007) Differential affinity of mammalian histone H1 somatic subtypes for DNA and chromatin. BMC Biol 5: 22.

66. Brown DT (2001) Histone variants: are they functionally heterogeneous? Genome Biol 2: REVIEWS0006.

67. Montes de Oca R, Lee KK, Wilson KL (2005) Binding of barrier to autointegration factor (BAF) to histone H3 and selected linker histones including H1.1. J Biol Chem 280: 42252-42262.

68. Kaludov NK, Pabon-Pena L, Seavy M, Robinson G, Hurt MM (1997) A mouse histone H1 variant, H1b, binds preferentially to a regulatory sequence within a mouse H3.2 replication-dependent histone gene. J Biol Chem 272: 15120-15127.

69. Lakhani SR, Manek S, Penault-Llorca F, Flanagan A, Arnout L, et al. (2004) Pathology of ovarian cancers in BRCA1 and BRCA2 carriers. Clin Cancer Res 10: 2473-2481.

70. Jin KL, Pak JH, Park JY, Choi WH, Lee JY, et al. (2008) Expression profile of histone deacetylases 1, 2 and 3 in ovarian cancer tissues. J Gynecol Oncol 19: 185-190.

71. Wierzbicki AT, Jerzmanowski A (2005) Suppression of histone H1 genes in Arabidopsis results in heritable developmental defects and stochastic changes in DNA methylation. Genetics 169: 997-1008.

72. Fan Y, Braut SA, Lin Q, Singer RH, Skoultchi AI (2001) Determination of transgenic loci by expression FISH. Genomics 71: 66-69.

73. Fan Y, Nikitina T, Zhao J, Fleury TJ, Bhattacharyya R, et al. (2005) Histone H1 depletion in mammals alters global chromatin structure but causes specific changes in gene regulation. Cell 123: 1199-1212.

74. Alizadeh AA, Eisen MB, Davis RE, Ma C, Lossos IS, et al. (2000) Distinct types of diffuse large B-cell lymphoma identified by gene expression profiling. Nature 403: 503-511.

75. Drabent B, Benavente R, Hoyer-Fender S (2003) Histone H1t is not replaced by H1.1 or H1.2 in pachytene spermatocytes or spermatids of H1t-deficient mice. Cytogenet Genome Res 103: 307-313.

76. Furuya M, Tanaka M, Teranishi T, Matsumoto K, Hosoi Y, et al. (2007) H1foo is indispensable for meiotic maturation of the mouse oocyte. J Reprod Dev 53: 895-902.

77. Sancho M, Diani E, Beato M, Jordan A (2008) Depletion of human histone H1 variants uncovers specific roles in gene expression and cell growth. PLoS Genet 4: e1000227.

78. Bhan S, May W, Warren SL, Sittman DB (2008) Global gene expression analysis reveals specific and redundant roles for H1 variants, H1c and H1(0), in gene expression regulation. Gene 414: 10-18.

79. Brown DT, Alexander BT, Sittman DB (1996) Differential effect of H1 variant overexpression on cell cycle progression and gene expression. Nucleic Acids Res 24: 486-493.

80. Sirotkin AM, Edelmann W, Cheng G, Klein-Szanto A, Kucherlapati R, et al. (1995) Mice develop normally without the H1(0) linker histone. Proc Natl Acad Sci U S A 92: 6434-6438.

81. Gabrilovich DI, Cheng P, Fan Y, Yu B, Nikitina E, et al. (2002) H1(0) histone and differentiation of dendritic cells. A molecular target for tumor-derived factors. J Leukoc Biol 72: 285-296.

82. Vani G, Vanisree AJ, Shyamaladevi CS (2006) Histone H1 inhibits the proliferation of MCF 7 and MDA MB 231 human breast cancer cells. Cell Biol Int 30: 326-331.

83. Class R, Lindman S, Fassbender C, Leinenbach HP, Rawer S, et al. (1996) Histone H1 suppresses tumor growth of leukemia cells in vitro, ex vivo and in an animal model suggesting extracellular functions of histones. Am J Clin Oncol 19: 522-531.

84. Gine E, Crespo M, Muntanola A, Calpe E, Baptista MJ, et al. (2008) Induction of histone H1.2 cytosolic release in chronic lymphocytic leukemia cells after genotoxic and non-genotoxic treatment. Haematologica 93: 75-82.

85. Hiemstra PS, Eisenhauer PB, Harwig SS, van den Barselaar MT, van Furth R, et al. (1993) Antimicrobial proteins of murine macrophages. Infect Immun 61: 3038-3046.

86. Konopinska D, Nawrocka E, Siemion IZ, Slopek S, Szymaniec S, et al. (1977) Partial sequences of histones with tuftsin activity. Int J Pept Protein Res 9: 71-77.

87. Tsoneva I, Nikolova B, Georgieva M, Guenova M, Tomov T, et al. (2005) Induction of apoptosis by electrotransfer of positively charged proteins as Cytochrome C and Histone H1 into cells. Biochim Biophys Acta 1721: 55-64.

88. (2013) American Cancer Society: Cancer Facts and Figures 2013. American Cancer Society.

89. Siegel R, Naishadham D, Jemal A (2013) Cancer statistics, 2013. CA Cancer J Clin 63: 11-30.

90. Oktem O, Oktay K (2008) The ovary: anatomy and function throughout human life. Ann N Y Acad Sci 1127: 1-9.

91. Chen VW, Ruiz B, Killeen JL, Cote TR, Wu XC, et al. (2003) Pathology and classification of ovarian tumors. Cancer 97: 2631-2642.

92. Creasman WT (2012) Clinical gynecologic oncology. Elsevier Health Sciences.

93. Nicosia SV, Johnson JH (1984) Surface morphology of ovarian mesothelium (surface epithelium) and of other pelvic and extrapelvic mesothelial sites in the rabbit. Int J Gynecol Pathol 3: 249-260.

94. Ozols RF, Bookman MA, Connolly DC, Daly MB, Godwin AK, et al. (2004) Focus on epithelial ovarian cancer. Cancer Cell 5: 19-24.

95. Scully RE (1995) Pathology of ovarian cancer precursors. J Cell Biochem Suppl 23: 208-218.

96. Bell DA (2005) Origins and molecular pathology of ovarian cancer. Mod Pathol 18 Suppl 2: S19-32.

97. Auersperg N, Wong AS, Choi KC, Kang SK, Leung PC (2001) Ovarian surface epithelium: biology, endocrinology, and pathology. Endocr Rev 22: 255-288.

98. Okamura H, Katabuchi H, Nitta M, Ohtake H (2006) Structural changes and cell properties of human ovarian surface epithelium in ovarian pathophysiology. Microsc Res Tech 69: 469-481.

99. Salazar H, Godwin AK, Daly MB, Laub PB, Hogan WM, et al. (1996) Microscopic benign and invasive malignant neoplasms and a cancer-prone phenotype in prophylactic oophorectomies. J Natl Cancer Inst 88: 1810-1820.

100. Fathalla MF (1971) Incessant ovulation--a factor in ovarian neoplasia? Lancet 2: 163.

101. Schildkraut JM, Bastos E, Berchuck A (1997) Relationship between lifetime ovulatory cycles and overexpression of mutant p53 in epithelial ovarian cancer. J Natl Cancer Inst 89: 932-938.

102. Fleming JS, Beaugie CR, Haviv I, Chenevix-Trench G, Tan OL (2006) Incessant ovulation, inflammation and epithelial ovarian carcinogenesis: revisiting old hypotheses. Mol Cell Endocrinol 247: 4-21.

103. Biglia N, Gadducci A, Ponzone R, Roagna R, Sismondi P (2004) Hormone replacement therapy in cancer survivors. Maturitas 48: 333-346.

104. Capen CC (2004) Mechanisms of hormone-mediated carcinogenesis of the ovary. Toxicol Pathol 32 Suppl 2: 1-5.

105. Landen CN, Jr., Birrer MJ, Sood AK (2008) Early events in the pathogenesis of epithelial ovarian cancer. J Clin Oncol 26: 995-1005.

106. Mani SA, Guo W, Liao MJ, Eaton EN, Ayyanan A, et al. (2008) The epithelial-mesenchymal transition generates cells with properties of stem cells. Cell 133: 704-715.

107. Pearce CL, Templeman C, Rossing MA, Lee A, Near AM, et al. (2012) Association between endometriosis and risk of histological subtypes of ovarian cancer: a pooled analysis of case-control studies. Lancet Oncol 13: 385-394.

108. Vo C, Carney ME (2007) Ovarian cancer hormonal and environmental risk effect. Obstet Gynecol Clin North Am 34: 687-700, viii.

109. Rebbeck TR, Lynch HT, Neuhausen SL, Narod SA, Van't Veer L, et al. (2002) Prophylactic oophorectomy in carriers of BRCA1 or BRCA2 mutations. N Engl J Med 346: 1616-1622.

110. Hunn J, Rodriguez GC (2012) Ovarian cancer: etiology, risk factors, and epidemiology. Clin Obstet Gynecol 55: 3-23.

111. Boyd J (1998) Molecular genetics of hereditary ovarian cancer. Oncology (Williston Park) 12: 399-406; discussion 409-310, 413.

112. Meindl A, Ditsch N, Kast K, Rhiem K, Schmutzler RK (2011) Hereditary breast and ovarian cancer: new genes, new treatments, new concepts. Dtsch Arztebl Int 108: 323-330.

113. Aarnio M, Mecklin JP, Aaltonen LA, Nystrom-Lahti M, Jarvinen HJ (1995) Life-time risk of different cancers in hereditary non-polyposis colorectal cancer (HNPCC) syndrome. Int J Cancer 64: 430-433.

114. Nicolaides NC, Papadopoulos N, Liu B, Wei YF, Carter KC, et al. (1994) Mutations of two PMS homologues in hereditary nonpolyposis colon cancer. Nature 371: 75-80.

115. Lacey JV, Jr., Mink PJ, Lubin JH, Sherman ME, Troisi R, et al. (2002) Menopausal hormone replacement therapy and risk of ovarian cancer. JAMA 288: 334-341.

116. Riman T, Dickman PW, Nilsson S, Correia N, Nordlinder H, et al. (2002) Hormone replacement therapy and the risk of invasive epithelial ovarian cancer in Swedish women. J Natl Cancer Inst 94: 497-504.

117. Rodriguez C, Patel AV, Calle EE, Jacob EJ, Thun MJ (2001) Estrogen replacement therapy and ovarian cancer mortality in a large prospective study of US women. JAMA 285: 1460-1465.

118. Duckitt K, Templeton AA (1998) Cancer in women with infertility. Curr Opin Obstet Gynecol 10: 199-203.

119. Potashnik G, Lerner-Geva L, Genkin L, Chetrit A, Lunenfeld E, et al. (1999) Fertility drugs and the risk of breast and ovarian cancers: results of a long-term follow-up study. Fertil Steril 71: 853-859.

120. Ness RB, Cramer DW, Goodman MT, Kjaer SK, Mallin K, et al. (2002) Infertility, fertility drugs, and ovarian cancer: a pooled analysis of case-control studies. Am J Epidemiol 155: 217-224.

121. Goff BA, Mandel L, Muntz HG, Melancon CH (2000) Ovarian carcinoma diagnosis. Cancer 89: 2068-2075.

122. Goff BA (2012) Ovarian cancer: screening and early detection. Obstet Gynecol Clin North Am 39: 183-194.

123. Yurkovetsky ZR, Linkov FY, D EM, Lokshin AE (2006) Multiple biomarker panels for early detection of ovarian cancer. Future Oncol 2: 733-741.

124. Weissman SM, Weiss SM, Newlin AC (2012) Genetic testing by cancer site: ovary. Cancer J 18: 320-327.

125. Gagnon A, Ye B (2008) Discovery and application of protein biomarkers for ovarian cancer. Curr Opin Obstet Gynecol 20: 9-13.

126. Kaku T, Ogawa S, Kawano Y, Ohishi Y, Kobayashi H, et al. (2003) Histological classification of ovarian cancer. Med Electron Microsc 36: 9-17.

127. Serov SF, Scully, R.E., Robin I.H. (1973) Histological typing of ovarian tumors: international histological classification of tumors. World Health Organization.

128. http://www.ovariancancer.org/ Ovarian Cancer National Alliance.

129. Bristow RE, del Carmen MG, Kaufman HS, Montz FJ (2003) Radical oophorectomy with primary stapled colorectal anastomosis for resection of locally advanced epithelial ovarian cancer. J Am Coll Surg 197: 565-574.

130. Armstrong DK, Bundy B, Wenzel L, Huang HQ, Baergen R, et al. (2006) Intraperitoneal cisplatin and paclitaxel in ovarian cancer. N Engl J Med 354: 34-43.

131. Bristow RE, Santillan A, Salani R, Diaz-Montes TP, Giuntoli RL, 2nd, et al. (2007) Intraperitoneal cisplatin and paclitaxel versus intravenous carboplatin and paclitaxel chemotherapy for Stage III ovarian cancer: a cost-effectiveness analysis. Gynecol Oncol 106: 476-481.

132. Markman M, Bundy BN, Alberts DS, Fowler JM, Clark-Pearson DL, et al. (2001) Phase III trial of standard-dose intravenous cisplatin plus paclitaxel versus moderately high-dose carboplatin followed by intravenous paclitaxel and intraperitoneal cisplatin in small-volume stage III ovarian carcinoma: an intergroup study of the Gynecologic Oncology Group, Southwestern Oncology Group, and Eastern Cooperative Oncology Group. J Clin Oncol 19: 1001-1007.

133. Omura GA, Brady MF, Homesley HD, Yordan E, Major FJ, et al. (1991) Long-term follow-up and prognostic factor analysis in advanced ovarian carcinoma: the Gynecologic Oncology Group experience. J Clin Oncol 9: 1138-1150.

134. Tewari K, Cappuccini F, Disaia PJ, Berman ML, Manetta A, et al. (2000) Malignant germ cell tumors of the ovary. Obstet Gynecol 95: 128-133.

135. Smith HO, Berwick M, Verschraegen CF, Wiggins C, Lansing L, et al. (2006) Incidence and survival rates for female malignant germ cell tumors. Obstet Gynecol 107: 1075-1085.

136. Collaborative Group on Epidemiological Studies of Ovarian C, Beral V, Doll R, Hermon C, Peto R, et al. (2008) Ovarian cancer and oral contraceptives: collaborative reanalysis of data from 45 epidemiological studies including 23,257 women with ovarian cancer and 87,303 controls. Lancet 371: 303-314.

137. Hartge P, Whittemore AS, Itnyre J, McGowan L, Cramer D (1994) Rates and risks of ovarian cancer in subgroups of white women in the United States. The Collaborative Ovarian Cancer Group. Obstet Gynecol 84: 760-764.

138. La Vecchia C (2006) Oral contraceptives and ovarian cancer: an update, 1998-2004. Eur J Cancer Prev 15: 117-124.

139. Bristow RE, Karlan BY (1996) Ovulation induction, infertility, and ovarian cancer risk. Fertil Steril 66: 499-507.

140. Hankinson SE, Colditz GA, Hunter DJ, Willett WC, Stampfer MJ, et al. (1995) A prospective study of reproductive factors and risk of epithelial ovarian cancer. Cancer 76: 284-290.

141. Rosenblatt KA, Thomas DB (1993) Lactation and the risk of epithelial ovarian cancer. The WHO Collaborative Study of Neoplasia and Steroid Contraceptives. Int J Epidemiol 22: 192-197.

142. Pruthi S, Gostout BS, Lindor NM (2010) Identification and Management of Women With BRCA Mutations or Hereditary Predisposition for Breast and Ovarian Cancer. Mayo Clin Proc 85: 1111-1120.

143. Chadha S, Rao BR, Slotman BJ, van Vroonhoven CC, van der Kwast TH (1993) An immunohistochemical evaluation of androgen and progesterone receptors in ovarian tumors. Hum Pathol 24: 90-95.

144. Cardillo MR, Petrangeli E, Aliotta N, Salvatori L, Ravenna L, et al. (1998) Androgen receptors in ovarian tumors: correlation with oestrogen and progesterone receptors in an immunohistochemical and semiquantitative image analysis study. J Exp Clin Cancer Res 17: 231-237.

145. Edmondson RJ, Monaghan JM, Davies BR (2002) The human ovarian surface epithelium is an androgen responsive tissue. Br J Cancer 86: 879-885.

146. Karlan BY, Jones J, Greenwald M, Lagasse LD (1995) Steroid hormone effects on the proliferation of human ovarian surface epithelium in vitro. Am J Obstet Gynecol 173: 97-104.

147. Evangelou A, Jindal SK, Brown TJ, Letarte M (2000) Down-regulation of transforming growth factor beta receptors by androgen in ovarian cancer cells. Cancer Res 60: 929-935.

148. Okamoto S, Okamoto A, Nikaido T, Saito M, Takao M, et al. (2009) Mesenchymal to epithelial transition in the human ovarian surface epithelium focusing on inclusion cysts. Oncol Rep 21: 1209-1214.

149. Sundfeldt K, Piontkewitz Y, Ivarsson K, Nilsson O, Hellberg P, et al. (1997) E-cadherin expression in human epithelial ovarian cancer and normal ovary. Int J Cancer 74: 275-280.

150. Maines-Bandiera SL, Auersperg N (1997) Increased E-cadherin expression in ovarian surface epithelium: an early step in metaplasia and dysplasia? Int J Gynecol Pathol 16: 250-255.

151. Van Niekerk CC, Ramaekers FC, Hanselaar AG, Aldeweireldt J, Poels LG (1993) Changes in expression of differentiation markers between normal ovarian cells and derived tumors. Am J Pathol 142: 157-177.

152. Huber MA, Kraut N, Beug H (2005) Molecular requirements for epithelial-mesenchymal transition during tumor progression. Curr Opin Cell Biol 17: 548-558.

153. Cavallaro U, Christofori G (2004) Cell adhesion and signalling by cadherins and Ig-CAMs in cancer. Nat Rev Cancer 4: 118-132.

154. Elloul S, Elstrand MB, Nesland JM, Trope CG, Kvalheim G, et al. (2005) Snail, Slug, and Smad-interacting protein 1 as novel parameters of disease

aggressiveness in metastatic ovarian and breast carcinoma. Cancer 103: 1631-1643.

155. Symowicz J, Adley BP, Gleason KJ, Johnson JJ, Ghosh S, et al. (2007) Engagement of collagen-binding integrins promotes matrix metalloproteinase-9-dependent E-cadherin ectodomain shedding in ovarian carcinoma cells. Cancer Res 67: 2030-2039.

156. Clezardin P (1998) Recent insights into the role of integrins in cancer metastasis. Cell Mol Life Sci 54: 541-548.

157. Naora H, Montell DJ (2005) Ovarian cancer metastasis: integrating insights from disparate model organisms. Nat Rev Cancer 5: 355-366.

158. Nagy JA, Masse EM, Herzberg KT, Meyers MS, Yeo KT, et al. (1995) Pathogenesis of ascites tumor growth: vascular permeability factor, vascular hyperpermeability, and ascites fluid accumulation. Cancer Res 55: 360-368.

159. Senger DR, Van de Water L, Brown LF, Nagy JA, Yeo KT, et al. (1993) Vascular permeability factor (VPF, VEGF) in tumor biology. Cancer Metastasis Rev 12: 303-324.

160. Geva E, Jaffe RB (2000) Role of vascular endothelial growth factor in ovarian physiology and pathology. Fertil Steril 74: 429-438.

161. Viglietto G, Romano A, Maglione D, Rambaldi M, Paoletti I, et al. (1996) Neovascularization in human germ cell tumors correlates with a marked increase in the expression of the vascular endothelial growth factor but not the placenta-derived growth factor. Oncogene 13: 577-587.

162. Shweiki D, Itin A, Soffer D, Keshet E (1992) Vascular endothelial growth factor induced by hypoxia may mediate hypoxia-initiated angiogenesis. Nature 359: 843-845.

163. Warren RS, Yuan H, Matli MR, Ferrara N, Donner DB (1996) Induction of vascular endothelial growth factor by insulin-like growth factor 1 in colorectal carcinoma. J Biol Chem 271: 29483-29488.

164. Ferrara N, Davis-Smyth T (1997) The biology of vascular endothelial growth factor. Endocr Rev 18: 4-25.

165. Hicklin DJ, Ellis LM (2005) Role of the vascular endothelial growth factor pathway in tumor growth and angiogenesis. J Clin Oncol 23: 1011-1027.

166. Nishida N, Yano H, Komai K, Nishida T, Kamura T, et al. (2004) Vascular endothelial growth factor C and vascular endothelial growth factor receptor 2 are related closely to the prognosis of patients with ovarian carcinoma. Cancer 101: 1364-1374.

167. Paley PJ, Staskus KA, Gebhard K, Mohanraj D, Twiggs LB, et al. (1997) Vascular endothelial growth factor expression in early stage ovarian carcinoma. Cancer 80: 98-106.

168. Mesiano S, Ferrara N, Jaffe RB (1998) Role of vascular endothelial growth factor in ovarian cancer: inhibition of ascites formation by immunoneutralization. Am J Pathol 153: 1249-1256.

169. Rubin SC, Finstad CL, Federici MG, Scheiner L, Lloyd KO, et al. (1994) Prevalence and significance of HER-2/neu expression in early epithelial ovarian cancer. Cancer 73: 1456-1459.

170. Molina R, Escudero JM, Munoz M, Auge JM, Filella X (2012) Circulating levels of HER-2/neu oncoprotein in breast cancer. Clin Chem Lab Med 50: 5-21.

171. Shayesteh L, Lu Y, Kuo WL, Baldocchi R, Godfrey T, et al. (1999) PIK3CA is implicated as an oncogene in ovarian cancer. Nat Genet 21: 99-102.

172. Bellacosa A, de Feo D, Godwin AK, Bell DW, Cheng JQ, et al. (1995) Molecular alterations of the AKT2 oncogene in ovarian and breast carcinomas. Int J Cancer 64: 280-285.

173. Mills GB, Lu Y, Fang X, Wang H, Eder A, et al. (2001) The role of genetic abnormalities of PTEN and the phosphatidylinositol 3-kinase pathway in breast and ovarian tumorigenesis, prognosis, and therapy. Semin Oncol 28: 125-141.

174. Singer G, Stohr R, Cope L, Dehari R, Hartmann A, et al. (2005) Patterns of p53 mutations separate ovarian serous borderline tumors and low- and high-grade carcinomas and provide support for a new model of ovarian carcinogenesis: a mutational analysis with immunohistochemical correlation. Am J Surg Pathol 29: 218-224.

175. Berchuck A, Kohler MF, Hopkins MP, Humphrey PA, Robboy SJ, et al. (1994) Overexpression of p53 is not a feature of benign and early-stage borderline epithelial ovarian tumors. Gynecol Oncol 52: 232-236.

176. Schuijer M, Berns EM (2003) TP53 and ovarian cancer. Hum Mutat 21: 285-291.

177. Balch C, Fang F, Matei DE, Huang TH, Nephew KP (2009) Minireview: epigenetic changes in ovarian cancer. Endocrinology 150: 4003-4011.

178. Houshdaran S, Hawley S, Palmer C, Campan M, Olsen MN, et al. (2010) DNA methylation profiles of ovarian epithelial carcinoma tumors and cell lines. PLoS One 5: e9359.

179. Wei SH, Brown R, Huang TH (2003) Aberrant DNA methylation in ovarian cancer: is there an epigenetic predisposition to drug response? Ann N Y Acad Sci 983: 243-250.

180. Chen J, Wang L, Matyunina LV, Hill CG, McDonald JF (2011) Overexpression of miR-429 induces mesenchymal-to-epithelial transition (MET) in metastatic ovarian cancer cells. Gynecol Oncol 121: 200-205.

181. Murphy SK, Jirtle RL (2000) Imprinted genes as potential genetic and epigenetic toxicologic targets. Environ Health Perspect 108 Suppl 1: 5-11.

182. Costello JF, Fruhwald MC, Smiraglia DJ, Rush LJ, Robertson GP, et al. (2000) Aberrant CpG-island methylation has non-random and tumour-type-specific patterns. Nat Genet 24: 132-138.

183. Shi H, Yan PS, Chen CM, Rahmatpanah F, Lofton-Day C, et al. (2002) Expressed CpG island sequence tag microarray for dual screening of DNA hypermethylation and gene silencing in cancer cells. Cancer Res 62: 3214-3220.

184. Press JZ, De Luca A, Boyd N, Young S, Troussard A, et al. (2008) Ovarian carcinomas with genetic and epigenetic BRCA1 loss have distinct molecular abnormalities. BMC Cancer 8: 17.

185. Zhang H, Zhang S, Cui J, Zhang A, Shen L, et al. (2008) Expression and promoter methylation status of mismatch repair gene hMLH1 and hMSH2 in epithelial ovarian cancer. Aust N Z J Obstet Gynaecol 48: 505-509.

186. Arnold JM, Cummings M, Purdie D, Chenevix-Trench G (2001) Reduced expression of intercellular adhesion molecule-1 in ovarian adenocarcinomas. Br J Cancer 85: 1351-1358.

187. Caslini C, Capo-chichi CD, Roland IH, Nicolas E, Yeung AT, et al. (2006) Histone modifications silence the GATA transcription factor genes in ovarian cancer. Oncogene 25: 5446-5461.

188. Suzuki F, Akahira J, Miura I, Suzuki T, Ito K, et al. (2008) Loss of estrogen receptor beta isoform expression and its correlation with aberrant DNA

methylation of the 5'-untranslated region in human epithelial ovarian carcinoma. Cancer Sci 99: 2365-2372.

189. Katsaros D, Cho W, Singal R, Fracchioli S, Rigault De La Longrais IA, et al. (2004) Methylation of tumor suppressor gene p16 and prognosis of epithelial ovarian cancer. Gynecol Oncol 94: 685-692.

190. Mirza A, McGuirk M, Hockenberry TN, Wu Q, Ashar H, et al. (2002) Human survivin is negatively regulated by wild-type p53 and participates in p53-dependent apoptotic pathway. Oncogene 21: 2613-2622.

191. Rose SL, Fitzgerald MP, White NO, Hitchler MJ, Futscher BW, et al. (2006) Epigenetic regulation of maspin expression in human ovarian carcinoma cells. Gynecol Oncol 102: 319-324.

192. Litkouhi B, Kwong J, Lo CM, Smedley JG, 3rd, McClane BA, et al. (2007) Claudin-4 overexpression in epithelial ovarian cancer is associated with hypomethylation and is a potential target for modulation of tight junction barrier function using a C-terminal fragment of Clostridium perfringens enterotoxin. Neoplasia 9: 304-314.

193. Cheng W, Jiang Y, Liu C, Shen O, Tang W, et al. (2010) Identification of aberrant promoter hypomethylation of HOXA10 in ovarian cancer. J Cancer Res Clin Oncol 136: 1221-1227.

194. Turner BM (2005) Reading signals on the nucleosome with a new nomenclature for modified histones. Nat Struct Mol Biol 12: 110-112.

195. Nowak SJ, Corces VG (2004) Phosphorylation of histone H3: a balancing act between chromosome condensation and transcriptional activation. Trends Genet 20: 214-220.

196. Shilatifard A (2006) Chromatin modifications by methylation and ubiquitination: implications in the regulation of gene expression. Annu Rev Biochem 75: 243-269.

197. Nathan D, Ingvarsdottir K, Sterner DE, Bylebyl GR, Dokmanovic M, et al. (2006) Histone sumoylation is a negative regulator in Saccharomyces cerevisiae and shows dynamic interplay with positive-acting histone modifications. Genes Dev 20: 966-976.

198. Sterner DE, Berger SL (2000) Acetylation of histones and transcription-related factors. Microbiol Mol Biol Rev 64: 435-459.

199. Mutskov V, Felsenfeld G (2004) Silencing of transgene transcription precedes methylation of promoter DNA and histone H3 lysine 9. EMBO J 23: 138-149.

200. Sengupta N, Seto E (2004) Regulation of histone deacetylase activities. J Cell Biochem 93: 57-67.

201. Santos-Rosa H, Schneider R, Bannister AJ, Sherriff J, Bernstein BE, et al. (2002) Active genes are tri-methylated at K4 of histone H3. Nature 419: 407-411.

202. Schneider R, Bannister AJ, Myers FA, Thorne AW, Crane-Robinson C, et al. (2004) Histone H3 lysine 4 methylation patterns in higher eukaryotic genes. Nat Cell Biol 6: 73-77.

203. Schickel R, Boyerinas B, Park SM, Peter ME (2008) MicroRNAs: key players in the immune system, differentiation, tumorigenesis and cell death. Oncogene 27: 5959-5974.

204. Peters L, Meister G (2007) Argonaute proteins: mediators of RNA silencing. Mol Cell 26: 611-623.

205. Iorio MV, Visone R, Di Leva G, Donati V, Petrocca F, et al. (2007) MicroRNA signatures in human ovarian cancer. Cancer Res 67: 8699-8707.

206. Alami R, Fan Y, Pack S, Sonbuchner TM, Besse A, et al. (2003) Mammalian linker-histone subtypes differentially affect gene expression in vivo. Proc Natl Acad Sci U S A 100: 5920-5925.

207. Yang SM, Kim BJ, Norwood Toro L, Skoultchi AI (2013) H1 linker histone promotes epigenetic silencing by regulating both DNA methylation and histone H3 methylation. Proc Natl Acad Sci U S A 110: 1708-1713.

208. Jemal A, Siegel R, Ward E, Hao Y, Xu J, et al. (2008) Cancer statistics, 2008. CA Cancer J Clin 58: 71-96.

209. http://documents.cancer.org/acs/groups/cid/documents/webcontent/003130-pdf.pdf.

210. Widschwendter M, Jiang G, Woods C, Muller HM, Fiegl H, et al. (2004) DNA hypomethylation and ovarian cancer biology. Cancer Res 64: 4472-4480.

211. Kwon MJ, Kim SS, Choi YL, Jung HS, Balch C, et al. (2010) Derepression of CLDN3 and CLDN4 during ovarian tumorigenesis is associated with loss of repressive histone modifications. Carcinogenesis 31: 974-983.

212. Cai KQ, Caslini C, Capo-chichi CD, Slater C, Smith ER, et al. (2009) Loss of GATA4 and GATA6 expression specifies ovarian cancer histological subtypes and precedes neoplastic transformation of ovarian surface epithelia. PLoS One 4: e6454.

213. Ozdag H, Teschendorff AE, Ahmed AA, Hyland SJ, Blenkiron C, et al. (2006) Differential expression of selected histone modifier genes in human solid cancers. BMC Genomics 7: 90.

214. Wolffe AP (1998) Chromatin: Structure and Function. . Academic Press, San Diego, CA.

215. Vignali M, Workman JL (1998) Location and function of linker histones. Nat Struct Biol 5: 1025-1028.

216. Bouvet P, Dimitrov S, Wolffe AP (1994) Specific regulation of Xenopus chromosomal 5S rRNA gene transcription in vivo by histone H1. Genes Dev 8: 1147-1159.

217. Gunjan A, Brown DT (1999) Overproduction of histone H1 variants in vivo increases basal and induced activity of the mouse mammary tumor virus promoter. Nucleic Acids Res 27: 3355-3363.

218. Lee H, Habas R, Abate-Shen C (2004) MSX1 cooperates with histone H1b for inhibition of transcription and myogenesis. Science 304: 1675-1678.

219. Lee HL, Archer TK (1998) Prolonged glucocorticoid exposure dephosphorylates histone H1 and inactivates the MMTV promoter. EMBO J 17: 1454-1466.

220. Steinbach OC, Wolffe AP, Rupp RA (1997) Somatic linker histones cause loss of mesodermal competence in Xenopus. Nature 389: 395-399.

221. Veron M, Zou Y, Yu Q, Bi X, Selmi A, et al. (2006) Histone H1 of Saccharomyces cerevisiae inhibits transcriptional silencing. Genetics 173: 579-587.

222. Kim K, Choi J, Heo K, Kim H, Levens D, et al. (2008) Isolation and characterization of a novel H1.2 complex that acts as a repressor of p53-mediated transcription. J Biol Chem 283: 9113-9126.

223. Wang ZF, Sirotkin AM, Buchold GM, Skoultchi AI, Marzluff WF (1997) The mouse histone H1 genes: gene organization and differential regulation. J Mol Biol 271: 124-138.

224. Rabini S, Franke K, Saftig P, Bode C, Doenecke D, et al. (2000) Spermatogenesis in mice is not affected by histone H1.1 deficiency. Exp Cell Res 255: 114-124.

225. Fan Y, Skoultchi AI (2004) Genetic analysis of H1 linker histone subtypes and their functions in mice. Methods Enzymol 377: 85-107.

226. Fan Y, Sirotkin A, Russell RG, Ayala J, Skoultchi AI (2001) Individual somatic H1 subtypes are dispensable for mouse development even in mice lacking the H1(0) replacement subtype. Mol Cell Biol 21: 7933-7943.

227. Fan Y, Nikitina T, Morin-Kensicki EM, Zhao J, Magnuson TR, et al. (2003) H1 linker histones are essential for mouse development and affect nucleosome spacing in vivo. Mol Cell Biol 23: 4559-4572.

228. Lin Q, Inselman A, Han X, Xu H, Zhang W, et al. (2004) Reductions in linker histone levels are tolerated in developing spermatocytes but cause changes in specific gene expression. J Biol Chem 279: 23525-23535.

229. Happel N, Schulze E, Doenecke D (2005) Characterisation of human histone H1x. Biol Chem 386: 541-551.

230. Stoldt S, Wenzel D, Schulze E, Doenecke D, Happel N (2007) G1 phase-dependent nucleolar accumulation of human histone H1x. Biol Cell 99: 541-552.

231. Takata H, Matsunaga S, Morimoto A, Ono-Maniwa R, Uchiyama S, et al. (2007) H1.X with different properties from other linker histones is required for mitotic progression. FEBS Lett 581: 3783-3788.

232. Warneboldt J, Haller F, Horstmann O, Danner BC, Fuzesi L, et al. (2008) Histone H1x is highly expressed in human neuroendocrine cells and tumours. BMC Cancer 8: 388.

233. Zlatanova J, Doenecke D (1994) Histone H1 zero: a major player in cell differentiation? FASEB J 8: 1260-1268.

234. Lennox RW, Cohen LH (1984) The alterations in H1 histone complement during mouse spermatogenesis and their significance for H1 subtype function. Dev Biol 103: 80-84.

235. Yan W, Ma L, Burns KH, Matzuk MM (2003) HILS1 is a spermatid-specific linker histone H1-like protein implicated in chromatin remodeling during mammalian spermiogenesis. Proc Natl Acad Sci U S A 100: 10546-10551.

236. Becker M, Becker A, Miyara F, Han Z, Kihara M, et al. (2005) Differential in vivo binding dynamics of somatic and oocyte-specific linker histones in oocytes and during ES cell nuclear transfer. Mol Biol Cell 16: 3887-3895.

237. Gorka C, Brocard MP, Curtet S, Khochbin S (1998) Differential recognition of histone H10 by monoclonal antibodies during cell differentiation and the arrest of cell proliferation. J Biol Chem 273: 1208-1215.

238. Eisen MB, Spellman PT, Brown PO, Botstein D (1998) Cluster analysis and display of genome-wide expression patterns. Proc Natl Acad Sci U S A 95: 14863-14868.

239. Alonso A, Breuer B, Bouterfa H, Doenecke D (1988) Early increase in histone H1(0) mRNA during differentiation of F9 cells to parietal endoderm. EMBO J 7: 3003-3008.

240. Cheng GH, Skoultchi AI (1989) Rapid induction of polyadenylated H1 histone mRNAs in mouse erythroleukemia cells is regulated by c-myc. Mol Cell Biol 9: 2332-2340.

241. Zhu CQ, Pintilie M, John T, Strumpf D, Shepherd FA, et al. (2009) Understanding prognostic gene expression signatures in lung cancer. Clin Lung Cancer 10: 331-340.

242. Quackenbush J (2006) Microarray analysis and tumor classification. N Engl J Med 354: 2463-2472.

243. Weinberg RA (2007) The biology of cancer. Garland Science, Taylor & Francis Group LLC, New York.

244. Bond UM, Yario TA, Steitz JA (1991) Multiple processing-defective mutations in a mammalian histone pre-mRNA are suppressed by compensatory changes in U7 RNA both in vivo and in vitro. Genes Dev 5: 1709-1722.

245. Pehrson JR, Cole RD (1982) Histone H1 subfractions and H10 turnover at different rates in nondividing cells. Biochemistry 21: 456-460.

246. Sekeri-Pataryas KE, Sourlingas TG (2007) The differentiation-associated linker histone, H1.0, during the in vitro aging and senescence of human diploid fibroblasts. Ann N Y Acad Sci 1100: 361-367.

247. De S, Brown DT, Lu ZH, Leno GH, Wellman SE, et al. (2002) Histone H1 variants differentially inhibit DNA replication through an affinity for chromatin mediated by their carboxyl-terminal domains. Gene 292: 173-181.

248. Grigoryev SA, Bulynko YA, Popova EY (2006) The end adjusts the means: heterochromatin remodelling during terminal cell differentiation. Chromosome Res 14: 53-69.

249. Hashimoto H, Takami Y, Sonoda E, Iwasaki T, Iwano H, et al. (2010) Histone H1 null vertebrate cells exhibit altered nucleosome architecture. Nucleic Acids Res 38: 3533-3545.

250. Murga M, Jaco I, Fan Y, Soria R, Martinez-Pastor B, et al. (2007) Global chromatin compaction limits the strength of the DNA damage response. J Cell Biol 178: 1101-1108.

251. Gerlitz G, Bustin M (2011) The role of chromatin structure in cell migration. Trends Cell Biol 21: 6-11.

252. Gerlitz G, Bustin M (2010) Efficient cell migration requires global chromatin condensation. J Cell Sci 123: 2207-2217.

253. Jemal A, Siegel R, Ward E, Hao Y, Xu J, et al. (2009) Cancer statistics, 2009. CA Cancer J Clin 59: 225-249.

254. Nephew KP, Balch C, Zhang S, Huang TH (2009) Epigenetics and ovarian cancer. Cancer Treat Res 149: 131-146.

255. Rundquist I, Lindner HH (2006) Analyses of linker histone--chromatin interactions in situ. Biochem Cell Biol 84: 427-436.

256. Yang G, Leuba SH, Bustamante C, Zlatanova J, van Holde K (1994) Role of linker histones in extended chromatin fibre structure. Nat Struct Biol 1: 761-763.

257. Meergans T, Albig W, Doenecke D (1997) Varied expression patterns of human H1 histone genes in different cell lines. DNA Cell Biol 16: 1041-1049.

258. Adriaenssens E, Dumont L, Lottin S, Bolle D, Lepretre A, et al. (1998) H19 overexpression in breast adenocarcinoma stromal cells is associated with tumor values and steroid receptor status but independent of p53 and Ki-67 expression. Am J Pathol 153: 1597-1607.

259. Ariel I, Miao HQ, Ji XR, Schneider T, Roll D, et al. (1998) Imprinted H19 oncofetal RNA is a candidate tumour marker for hepatocellular carcinoma. Mol Pathol 51: 21-25.

260. Cui H, Onyango P, Brandenburg S, Wu Y, Hsieh CL, et al. (2002) Loss of imprinting in colorectal cancer linked to hypomethylation of H19 and IGF2. Cancer Res 62: 6442-6446.

261. Tanos V, Prus D, Ayesh S, Weinstein D, Tykocinski ML, et al. (1999) Expression of the imprinted H19 oncofetal RNA in epithelial ovarian cancer. Eur J Obstet Gynecol Reprod Biol 85: 7-11.

262. Gabory A, Ripoche MA, Yoshimizu T, Dandolo L (2006) The H19 gene: regulation and function of a non-coding RNA. Cytogenet Genome Res 113: 188-193.

263. Ariel I, Ayesh S, Perlman EJ, Pizov G, Tanos V, et al. (1997) The product of the imprinted H19 gene is an oncofetal RNA. Mol Pathol 50: 34-44.

264. Gabory A, Ripoche MA, Le Digarcher A, Watrin F, Ziyyat A, et al. (2009) H19 acts as a trans regulator of the imprinted gene network controlling growth in mice. Development 136: 3413-3421.

265. Borensztein M, Monnier P, Court F, Louault Y, Ripoche MA, et al. (2013) Myod and H19-Igf2 locus interactions are required for diaphragm formation in the mouse. Development 140: 1231-1239.

266. Ayesh S, Matouk I, Schneider T, Ohana P, Laster M, et al. (2002) Possible physiological role of H19 RNA. Mol Carcinog 35: 63-74.

267. Keniry A, Oxley D, Monnier P, Kyba M, Dandolo L, et al. (2012) The H19 lincRNA is a developmental reservoir of miR-675 that suppresses growth and Igf1r. Nat Cell Biol 14: 659-665.

268. Tsang WP, Ng EK, Ng SS, Jin H, Yu J, et al. (2010) Oncofetal H19-derived miR-675 regulates tumor suppressor RB in human colorectal cancer. Carcinogenesis 31: 350-358.

269. Cai X, Cullen BR (2007) The imprinted H19 noncoding RNA is a primary microRNA precursor. RNA 13: 313-316.

270. Berteaux N, Aptel N, Cathala G, Genton C, Coll J, et al. (2008) A novel H19 antisense RNA overexpressed in breast cancer contributes to paternal IGF2 expression. Mol Cell Biol 28: 6731-6745.

271. Onyango P, Feinberg AP (2011) A nucleolar protein, H19 opposite tumor suppressor (HOTS), is a tumor growth inhibitor encoded by a human imprinted H19 antisense transcript. Proc Natl Acad Sci U S A 108: 16759-16764.

272. Sasaki H, Ishihara K, Kato R (2000) Mechanisms of Igf2/H19 imprinting: DNA methylation, chromatin and long-distance gene regulation. J Biochem 127: 711-715.

273. Gabory A, Jammes H, Dandolo L (2010) The H19 locus: role of an imprinted non-coding RNA in growth and development. Bioessays 32: 473-480.

274. Medrzycki M, Zhang Y, McDonald JF, Fan Y (2012) Profiling of linker histone variants in ovarian cancer. Front Biosci 17: 396-406.

275. Medrzycki M, Zhang Y, Cao K, Fan Y (2012) Expression analysis of mammalian linker-histone subtypes. J Vis Exp.

276. Franken NA, Rodermond HM, Stap J, Haveman J, van Bree C (2006) Clonogenic assay of cells in vitro. Nat Protoc 1: 2315-2319.

277. Gao WL, Liu M, Yang Y, Yang H, Liao Q, et al. (2012) The imprinted H19 gene regulates human placental trophoblast cell proliferation via encoding miR-675 that targets Nodal Modulator 1 (NOMO1). RNA Biol 9: 1002-1010.

278. Yang Y, Hu JF, Ulaner GA, Li T, Yao X, et al. (2003) Epigenetic regulation of Igf2/H19 imprinting at CTCF insulator binding sites. J Cell Biochem 90: 1038-1055.

279. Hark AT, Schoenherr CJ, Katz DJ, Ingram RS, Levorse JM, et al. (2000) CTCF mediates methylation-sensitive enhancer-blocking activity at the H19/Igf2 locus. Nature 405: 486-489.

280. Bell AC, Felsenfeld G (2000) Methylation of a CTCF-dependent boundary controls imprinted expression of the Igf2 gene. Nature 405: 482-485.

281. Dammann RH, Kirsch S, Schagdarsurengin U, Dansranjavin T, Gradhand E, et al. (2010) Frequent aberrant methylation of the imprinted IGF2/H19 locus and LINE1 hypomethylation in ovarian carcinoma. Int J Oncol 36: 171-179.

282. Berteaux N, Lottin S, Monte D, Pinte S, Quatannens B, et al. (2005) H19 mRNA-like noncoding RNA promotes breast cancer cell proliferation through positive control by E2F1. J Biol Chem 280: 29625-29636.

283. Lottin S, Adriaenssens E, Dupressoir T, Berteaux N, Montpellier C, et al. (2002) Overexpression of an ectopic H19 gene enhances the tumorigenic properties of breast cancer cells. Carcinogenesis 23: 1885-1895.

284. Matouk IJ, DeGroot N, Mezan S, Ayesh S, Abu-lail R, et al. (2007) The H19 non-coding RNA is essential for human tumor growth. PLoS One 2: e845.

285. Yang F, Bi J, Xue X, Zheng L, Zhi K, et al. (2012) Up-regulated long non-coding RNA H19 contributes to proliferation of gastric cancer cells. FEBS J 279: 3159-3165.

286. Luo M, Li Z, Wang W, Zeng Y, Liu Z, et al. (2013) Long non-coding RNA H19 increases bladder cancer metastasis by associating with EZH2 and inhibiting E-cadherin expression. Cancer Lett.

287. Barsyte-Lovejoy D, Lau SK, Boutros PC, Khosravi F, Jurisica I, et al. (2006) The c-Myc oncogene directly induces the H19 noncoding RNA by allele-specific binding to potentiate tumorigenesis. Cancer Res 66: 5330-5337.

288. Li Y, Meng G, Guo QN (2008) Changes in genomic imprinting and gene expression associated with transformation in a model of human osteosarcoma. Exp Mol Pathol 84: 234-239.

289. Hao Y, Crenshaw T, Moulton T, Newcomb E, Tycko B (1993) Tumour-suppressor activity of H19 RNA. Nature 365: 764-767.

290. Yoshimizu T, Miroglio A, Ripoche MA, Gabory A, Vernucci M, et al. (2008) The H19 locus acts in vivo as a tumor suppressor. Proc Natl Acad Sci U S A 105: 12417-12422.

291. Giambra V, Volpi S, Emelyanov AV, Pflugh D, Bothwell AL, et al. (2008) Pax5 and linker histone H1 coordinate DNA methylation and histone modifications in the 3' regulatory region of the immunoglobulin heavy chain locus. Mol Cell Biol 28: 6123-6133.

292. Maclean JA, Bettegowda A, Kim BJ, Lou CH, Yang SM, et al. (2011) The rhox homeobox gene cluster is imprinted and selectively targeted for regulation by histone h1 and DNA methylation. Mol Cell Biol 31: 1275-1287.

293. Hill DA, Imbalzano AN (2000) Human SWI/SNF nucleosome remodeling activity is partially inhibited by linker histone H1. Biochemistry 39: 11649-11656.

294. Simon JA, Lange CA (2008) Roles of the EZH2 histone methyltransferase in cancer epigenetics. Mutat Res 647: 21-29.

295. Brown DT, Sittman DB (1993) Identification through overexpression and tagging of the variant type of the mouse H1e and H1c genes. J Biol Chem 268: 713-718.

296. Heid CA, Stevens J, Livak KJ, Williams PM (1996) Real time quantitative PCR. Genome Res 6: 986-994.

297. Zhang L, Volinia S, Bonome T, Calin GA, Greshock J, et al. (2008) Genomic and epigenetic alterations deregulate microRNA expression in human epithelial ovarian cancer. Proc Natl Acad Sci U S A 105: 7004-7009.

298. Kwon MJ, Shin YK (2011) Epigenetic regulation of cancer-associated genes in ovarian cancer. Int J Mol Sci 12: 983-1008.

299. Moore JM, Rabaia NA, Smith LE, Fagerlie S, Gurley K, et al. (2012) Loss of maternal CTCF is associated with peri-implantation lethality of Ctcf null embryos. PLoS One 7: e34915.

300. Qi CF, Martensson A, Mattioli M, Dalla-Favera R, Lobanenkov VV, et al. (2003) CTCF functions as a critical regulator of cell-cycle arrest and death after ligation of the B cell receptor on immature B cells. Proc Natl Acad Sci U S A 100: 633-638.